In Vivo Tracking of Skin-Derived Immune Cells in Murine Models of Psoriasis Using Dendra2 Photoconversion

Dissertation

Zur Erlangung des Grades

Doktor der Naturwissenschaften

Am Fachbereich Biologie

Der Johannes Gutenberg-Universität Mainz

Vorgelegt von

Theresa Franziska Schaller

Geboren am 24. September 1993 in Regensburg, Deutschland

Mainz, 2026

Dekan: Prof. Dr. Eckhard Thines
1. Berichterstatter:
2. Berichterstatter:
Tag der mündlichen Prüfung: 21.04.2026

TABLE OF CONTENTS

ABBREVIATIONS

Abbreviation	Full name
°C	Temperature in degrees Celsius
ab	Antibody
ACK	Ammonium chloride potassium bicarbonate
ADAMTSL5	ADAMTS-like protein 5
AIRE	Autoimmune regulator
aLN	Axillary lymph node(s)
AMP	Antimicrobial peptide(s)
ANOVA	Analysis of variance
APC	Antigen-presenting cells
BAFFR	B-cell activating factor receptor
bLN	Brachial lymph node(s)
bp	Base pair
CCL	CC chemokine ligand
Cd	Choline-deficient
CD	Cluster of differentiation
cIAP	Cellular inhibitor of apoptosis
cLN	Cervical lymph node(s)
CVD	Cardiovascular disease
CXCL	CXC chemokine ligand
D2	Dendra2
DC	Dendritic cell(s)
DPBS	Dulbecco's phosphate-buffered saline
DTT	Dithiothreitol
EDTA	Ethylene-diaminetetraacetic acid
EtOH	Ethanol
FACS	Fluorescence activated cell sorting
FCS	Fetal calf serum
fl	Floxed
FSC	Forward scatter
g	Gram
GM-CSF	Granulocyte-macrophage colony-stimulating factor

Abbreviation	Full name
HBSS	Gibco® Hank's buffered saline solution
HEPES	4-(2-hydroxyethyl)-1-piperazineethanesulfonic acid
HFD	High-fat diet
IBD	Inflammatory bowel disease
ICAM	Intercellular adhesion molecule
IFN	Interferon
IKK	IκB kinase
ILC	Innate lymphoid cell(s)
iLN	Inguinal lymph node
IMQ	Imiquimod
ind	Inducible
IVM	Intravital microscopy
IκB	Inhibitor of κB
K	Keratin
KC	Keratinocyte(s)
L	Liter
LC	Langerhans cell(s)
LN	Lymph node
loxP	Recognition sequence for Cre (locus of X-over P1 of coliphage P1)
LTβR	Lymphotoxinβ receptor
Ly6C	Lymphocyte antigen 6 C
Ly6G	Lymphocyte antigen 6 G
M	Molar
MAC	Membrane attack complex
MAIT	Mucosal-associated invariant T cell(s)
MCSF	Macrophage colony-stimulating factor
MCSFR	Macrophage colony-stimulating factor receptor
min	Minute
mL	Milliliter
mM	Millimolar
MMP	Matrix metalloproteinase
MPO	Myeloperoxidase

Abbreviation	Full name
mTEC	Medullary thymic epithelial cell
MyD88	Myeloid differentiation primary-response protein 88
NaCl	Sodium chloride
NAFLD	Non-alcoholic fatty liver disease
NEAA	Non-essential amino acids
NET	Neutrophil extracellular trap
NF-κB	Nuclear factor kappa-light-chain-enhancer of activated B-cells
NIK	NF-κB-inducing kinase
NK	Natural killer
NLR	NOD-like receptor
ON	Overnight
PASI	Psoriasis activity and severity index
PB	Pacific Blue
PBS	Phosphate-buffered saline
PCR	Polymerase chain reaction
pDC	Plasmacytoid dendritic cell
PE	Phycoerythrine
PerCP	Peridinin-chlorophyll-protein complex
PFA	Paraformaldehyde
PhAM	Photo-activatable mitochondria
PMA	Phorbol Myristate Acetate
P/S	Penicillin/streptomycin
RNA	Ribonucleic acid
rpm	Revolutions per minute
RPMI	Roswell Park Memorial Institute medium
RT	Room temperature
RT-PCR	Reverse transcription PCR
SDS	Sodium dodecyl sulfate
SEM	Standard error of the mean
SN	Supernatant
SSC	Side scatter
TAE	Tris-acetic acid-EDTA buffer

Abbreviation	Full name
Tc	T cytotoxic cell(s)
TCR	T cell receptor
TEC	Thymic epithelial cell(s)
TENS	Tail lysis buffer (TRIS- EDTA-NaCl-SDS)
TFH	T follicular helper cell(s)
TG	Transgene
Th	T helper cell(s)
TLR	Toll-like receptor
TNF	Tumor necrosis factor
TNFR	TNF receptor
TRAF	TNFR-associated factor
TRIS	Tris(hydroxymethyl)aminomethane
Treg	Regulatory T cell(s)
TRM	Resident memory T cell(s)
UV	Ultraviolet
VEGF	Vascular endothelial growth factor
v/v	Volume per volume
w/v	Weight per volume
µL	Microliter
µM	Micromolar

SUMMARY

Psoriasis is a chronic, systemic and inflammatory skin disease with comorbidities including cardiovascular disease, inflammatory bowel disease and non-alcoholic fatty liver disease. However, whether skin-derived immune cells contribute directly to systemic pathology remains unclear. In this study, I established and validated Dendra2-based photoconversion as a robust *in vivo* platform for quantitative tracking of skin-derived immune cell trafficking across lymphoid and non-lymphoid organs in murine psoriasis models, providing direct mechanistic insight into how psoriatic inflammation influences systemic immunity.

The method was first optimized in the acute IMQ-induced psoriasis model. Photoconversion of inflamed skin was feasible, non-invasive and did not alter disease progression. The red Dendra2 signal remained stable during tissue processing and flow cytometry, enabling sensitive detection of skin-derived immune cells. Analyses revealed that immune cells from the skin migrate primarily to draining lymph nodes and the spleen, with no detectable trafficking to distant organs such as the aorta or bone marrow.

Application of the method to the chronic K14-IL-17A$^{ind/+}$ model, which mimics sustained IL-17A-driven systemic inflammation originating from the skin, confirmed efficient labeling of immune cells in the skin. Dendra2-red^{+} cells were detectable in lymphoid organs and, at extremely low frequency, in the liver. Migratory populations in lymphoid organs were predominantly CD11b^{+} myeloid cells and T cells, whose proportions were largely unchanged during psoriatic inflammation. Even under chronic systemic inflammation, migration to distant organs, including the aorta, colon and liver, remained absent or minimal, demonstrating that organ inflammation is driven primarily by systemic cytokine-mediated immune activation and bone marrow-derived myeloid cell mobilization, rather than direct skin-to-organ immune cell trafficking.

Overall, this work establishes Dendra2 photoconversion as a powerful and reliable tool for *in vivo* tracking of skin-derived immune cells and provides strong evidence that systemic IL-17A-driven inflammation, rather than immune cell egress from the skin, drives vascular, intestinal and hepatic pathology in psoriasis. These findings highlight the importance of targeting systemic IL-17A-driven inflammation to prevent psoriasis-associated comorbidities and establish a versatile platform for studying organ-organ immune cell crosstalk in chronic inflammatory disease.

ZUSAMMENFASSUNG

Psoriasis ist eine chronische, systemische und entzündliche Hauterkrankung, die mit Begleiterkrankungen wie Herz-Kreislauf-Erkrankungen, entzündlichen Darmerkrankungen und nicht-alkoholischer Fettleber assoziiert ist. Ob Immunzellen aus der Haut direkt zur systemischen Pathologie beitragen, ist bislang unklar. In dieser Studie wurde die Dendra2-basierte Photokonversion als robuste *in vivo* Plattform etabliert und validiert, um die Wanderung von Immunzellen aus der Haut in lymphoide und nicht-lymphoide Organe in Psoriasis Mausmodellen quantitativ zu verfolgen.

Die Methode wurde zunächst im akuten IMQ-induzierten Psoriasis-Modell optimiert. Photokonversion entzündeter Haut war realisierbar, nicht-invasiv und veränderte den Krankheitsverlauf nicht. Das rote Dendra2-Signal blieb stabil während Gewebeaufbereitung und Durchflusszytometrie, wodurch Immunzellen kommend aus der Haut nachweisbar waren. Analysen zeigten, dass Immunzellen aus der Haut primär in drainierende Lymphknoten und die Milz migrieren, während keine Wanderung in entfernte Organe wie Aorta oder Knochenmark nachweisbar war.

Anwendung auf das chronische, psoriatische K14-IL-17A$^{ind/+}$ Modell, das anhaltende IL-17A-getriebene systemische Entzündung aus der Haut nachahmt, bestätigte effiziente Markierung von Haut-residenten Immunzellen. Dendra2-rot^{+} Immunzellen wurden in lymphoiden Organen und in sehr geringer Häufigkeit in der Leber nachgewiesen. Die migrierenden Populationen in den lymphoiden Organen bestanden überwiegend aus CD11b^{+} myeloiden Zellen und T-Zellen, deren relative Anteile während psoriatischer Entzündung weitgehend unverändert blieben. Selbst unter chronischer, systemischer Entzündung blieb die Migration in entfernte Organe wie der Aorta and dem Kolon absent, was darauf hinweist, dass Organentzündung primär durch systemische Zytokin-vermittelte Immunaktivierung und Mobilisierung myeloider Zellen aus dem Knochenmark, nicht durch direkte Wanderung von Haut-infiltrierenden Immunzellen, getrieben wird.

Diese Arbeit etabliert Dendra2-Photokonversion als leistungsfähiges Werkzeug zur *in vivo* Verfolgung von Immunzellen aus der Haut und liefert starke Evidenz, dass IL-17A-getriebene systemische Entzündung und nicht Auswanderung von Haut-residierenden Immunzellen, vaskuläre, intestinale und hepatische Pathologie bei Psoriasis verursacht. Die Ergebnisse betonen die Bedeutung der gezielten Therapie von systemischer IL-17A-getriebener Entzündung zur Prävention Psoriasis-assoziierter Komorbiditäten und bieten eine vielseitige Plattform zur Untersuchung von Organ-zu-Organ Immunzellen *Crosstalk* bei chronischen Entzündungserkrankungen.

1 INTRODUCTION

1.1 The skin

The skin, the body's largest organ, is a complex and highly specialized interface that serves as a critical interface between the internal and external environments. Its primary function is to act as a physical barrier, protecting underlying tissues from external insults such as mechanical trauma, harmful microorganisms and environmental pollutants (Agrawal, Hu and Bollag 2023). In addition, the skin maintains fluid balance and prevents dehydration by forming a selective barrier to water and electrolytes (Madison 2003, Proksch, Brandner and Jensen 2008).

Beyond its barrier function, the skin plays a central role in thermoregulation through mechanisms such as sweat production and vasodilation and enables sensory perception by detecting stimuli including touch, pressure, temperature and pain (Romanovsky 2014, Filingeri 2015). The skin also contributes to metabolic homeostasis, most notably through the synthesis of vitamin D upon exposure to ultraviolet radiation, which is essential for calcium regulation and bone health (Fleet 2017).

Importantly, the skin is continuously exposed to environmental antigens and microbial challenges and therefore functions not only as a passive barrier but also as an active immunological organ (Zhang, Merana et al. 2022). This dual role requires tight coordination between structural integrity and immune regulation to maintain tissue homeostasis and prevent pathological inflammation, a balance that is disrupted in chronic inflammatory skin diseases such as psoriasis.

1.1.1 Architecture

The skin is a highly organized organ, stratified into distinct layers, each with specialized structural and functional roles (Figure 1.1). The epidermis, the outermost layer of the skin, is primarily composed of keratinocytes (KCs) that originate in the stratum basale. These cells undergo a tightly regulated program of differentiation, progressing through the stratum spinosum and stratum granulosum, then losing their nuclei as they transition into the stratum corneum. This outermost layer, termed the cornified layer, also harbors also multiple lipid-rich sheets that form a water-impermeable, mechanically resilient barrier that is continuously renewed to maintain tissue integrity and protect against environmental insults (Proksch, Brandner and Jensen 2008). The epidermis also contains melanocytes, which regulate pigmentation and provide ultraviolet protection, and Merkel cells, which mediate sensory perception (Kobayashi,

Nakagawa et al. 1998, Yamaguchi and Hearing 2009, Clayton, Vallejo et al. 2017, Bataille, Le Gall et al. 2022). At the microanatomical level, tight junctions in the stratum granulosum reinforce barrier function, while interspersed immune populations, including Langerhans cells (LCs), γδ T cells and resident memory T (T_{RM}) cells, provide a first line of defense and continuous immunological surveillance (Kabashima, Honda et al. 2019).

Beneath the epidermis lies the dermis, comprising the papillary and reticular layers. The papillary dermis contains loose connective tissue and a dense capillary network that sustains epidermal metabolism and waste clearance, while dermal papillae interdigitate with the epidermis to enhance mechanical stability. The reticular dermis, the thicker dermal compartment, consists of dense irregular connective tissue rich in collagen and elastin fibers, providing tensile strength and elasticity. Embedded within this layer are blood and lymphatic vessels, peripheral nerves, and skin appendages, including hair follicles, sebaceous glands, and sweat glands, which collectively contribute to thermoregulation, lubrication and excretion (Rippa, Kalabusheva and Vorotelyak 2019). Critically, the dermal vasculature and lymphatics enable immune cell trafficking between the skin, regional lymph nodes (LN) and systemic circulation, integrating local and systemic immunity.

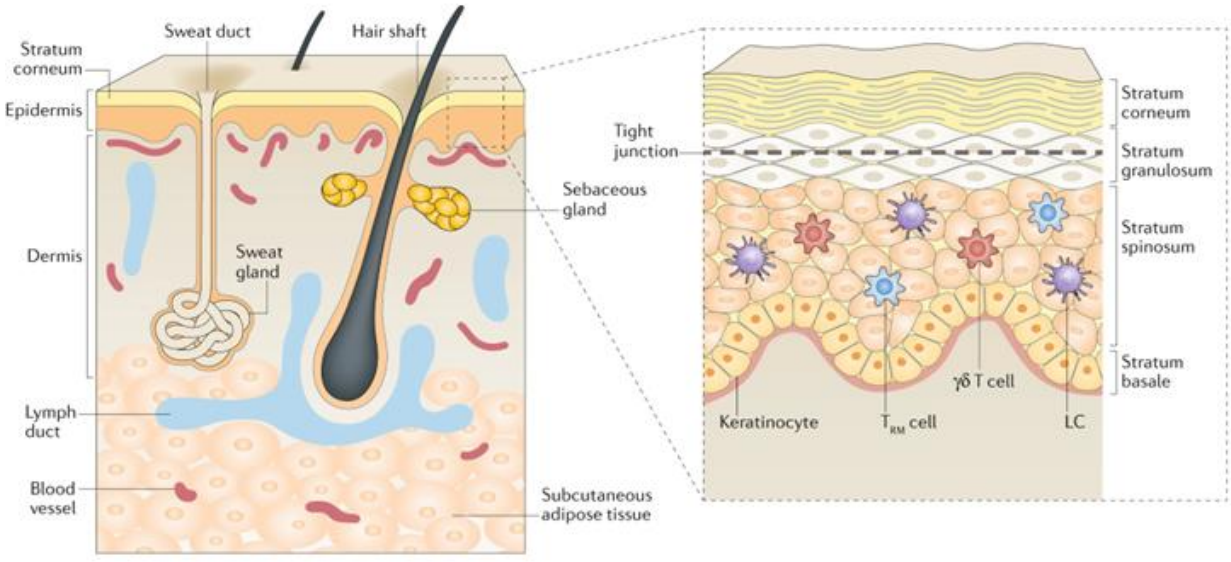

Figure 1.1: Structure of the skin (Kabashima, Honda et al. 2019)

The skin is composed of three major layers: the epidermis, dermis and subcutaneous adipose tissue (left). The dermis contains blood and lymphatic vessels, hair follicles, sebaceous glands and sweat glands, supporting skin homeostasis, thermoregulation and excretory functions. The epidermis is organized into the stratum basale, stratum spinosum, stratum granulosum and stratum corneum (right). Within the epidermis, tight junctions in the stratum granulosum reinforce the barrier beneath the stratum corneum. Three immune cell populations - Langerhans cells (LCs), γδ T cells and resident memory T (TRM) cells - interspersed among KCs provide continuous epidermal immune surveillance. Figure is adapted from Kabashima, Honda et al. 2019.

The hypodermis, or subcutaneous layer, lies beneath the dermis and consists primarily of loose connective tissue and adipose tissue. It functions as a mechanical cushion, thermal insulator, and energy reservoir, while housing larger blood vessels and nerves that support both local skin metabolism and systemic physiological connectivity (Proksch, Brandner and Jensen 2008, Baroni, Buommino et al. 2012).

While human and murine skin differ in thickness, hair follicle density and epidermal organization, the fundamental architecture of epidermal, dermal and hypodermal layers, alongside conserved immune and vascular structures, underscores the translational value of mouse models for investigating skin immunity and inflammatory diseases (Pasparakis, Haase and Nestle 2014).

1.1.2 Immune function

The skin is not merely a physical barrier but a dynamic immunological organ, hosting a diverse array of immune cells that maintain tissue homeostasis, provide continuous surveillance and respond rapidly to injury or infection (Figure 1.2) (Kabashima, Honda et al. 2019).

The epidermis contains LCs, embryonically seeded dendritic cells (DC) that capture antigens and migrate to draining LNs, initiating adaptive immune responses (Clayton, Vallejo et al. 2017, Rajesh, Wise and Hibma 2019, Zhu, Yao and Li 2024). Under homeostasis, LCs self-renew, but bone marrow (BM)-derived monocytes can supplement the LC niche during inflammation (Doebel, Voisin and Nagao 2017). KCs constitutively synthesize the CC chemokine ligand (CCL)27 that attracts $CCR10^+$ T cells into normal skin for immune surveillance (Morales, Homey et al. 1999, Homey, Alenius et al. 2002). KCs themselves act as sentinel cells, expressing pattern recognition receptors, including Toll-like receptors (TLRs) and NOD-like receptors (NLRs), which detect microbial components and host-derived nucleic acids. Upon activation, these cells produce antimicrobial peptides (AMP, e.g. β-defensins, cathelicidins like LL37, S100A7-9) pro-inflammatory cytokines (e.g. interleukin (IL)-1β, IL-6, IL-17, interferon (IFN)-α, tumor necrosis factor (TNF)-α, CCL20), and chemokines (e.g. CXC chemokine ligand (CXCL)1), thereby shaping the local immune microenvironment and recruiting additional immune cells (Krutzik, Tan et al. 2005, Sun, Liu and Zhang 2019, Wang and Lai 2024). These responses are largely mediated through Nuclear factor kappa-light-chain-enhancer of activated B-cells (NF-κB)-dependent signaling pathways, positioning KCs as central regulators of cutaneous inflammation (Van Nuffel, Schmitt et al. 2017, Wang and Lai 2024).

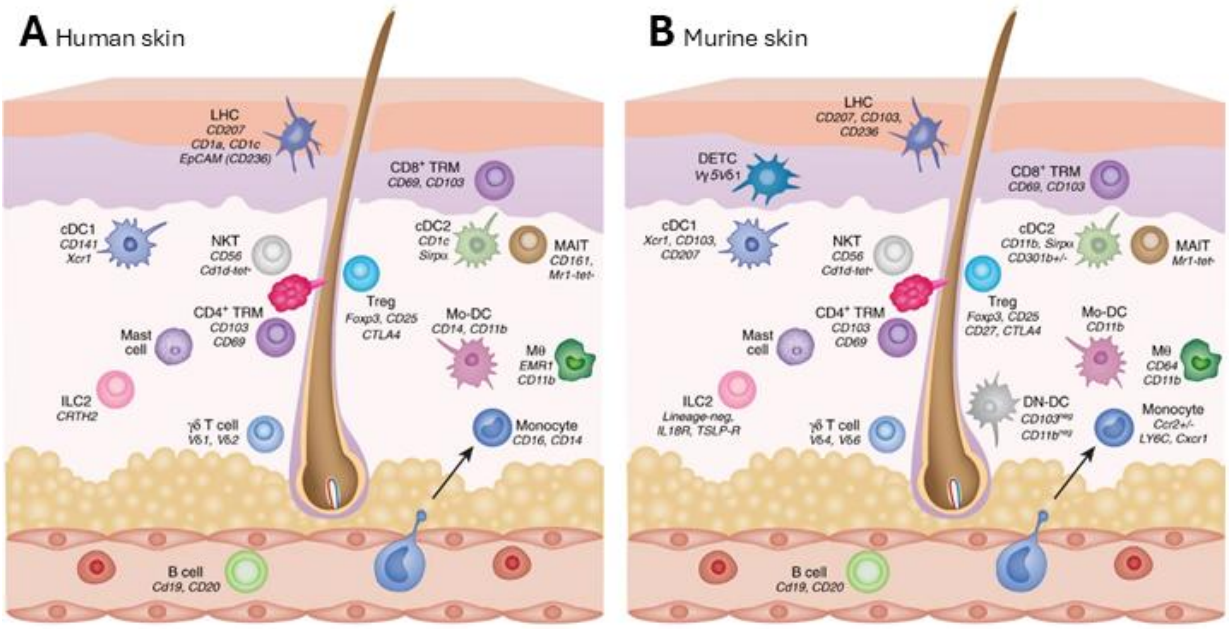

Figure 1.2: Immune cells in human and murine skin (Zhang, Merana et al. 2022)

Overview of major immune cell types present in **(A)** human and **(B)** murine skin, including epidermal and dermal compartments, together with commonly used surface markers identifiable by flow cytometry. Shown populations include Langerhans cells (LC), dendritic epidermal T cells (DETC),cluster of differentiation (CD)8^+ and $CD4^+$ resident memory T cells (TRM), conventional/ monocyte-derived/ double negative dendritic cells (cDC1/2, Mo-DC and DN-DC), type 2 innate lymphoid cells (ILC2), mucosal-associated invariant T cells (MAIT), macrophages (Mθ), natural killer T cells (NKT), regulatory T cells (Treg). Figure is adapted from Zhang, Merana et al. 2022.

Within the dermis the innate immune compartment comprises conventional DCs (cDCs), monocyte-derived DCs (moDCs), macrophages, mast cells, Natural Killer T (NKT) cells and innate lymphoid cells (ILC1–3, predominantly ILC2) (Di Nardo, Yamasaki et al. 2008, Tamoutounour, Guilliams et al. 2013, Haniffa, Gunawan and Jardine 2015, Galli, Gaudenzio and Tsai 2020, Kobayashi, Ricardo-Gonzalez and Moro 2020). Similar to LCs, dermal DCs migrate *via* lymphatic vessels to draining LNs, where they prime naïve T cells. In addition, dermal DCs actively shape local immune responses through the production of pro-inflammatory cytokines and chemokines (Guttman-Yassky, Lowes et al. 2007). During inflammation, the resident populations expand and inflammatory cells, including neutrophils and eosinophils, are recruited, accompanied by activation-induced changes in surface marker expression (Kim, Siracusa et al. 2013, Haniffa, Gunawan and Jardine 2015, Ricardo-Gonzalez, Van Dyken et al. 2018).

In adaptive immunity, skin T cells constitute a substantial fraction of the cutaneous immune system, with many cells adopting a cutaneous lymphocyte antigen $(CLA)^+$ resident memory phenotype (TRM). The skin migratory receptor CLA mediates the binding to E-selectin which is expressed on cutaneous blood vessels (Clark, Chong et al. 2006, Watanabe, Gehad et al.

2015). In murine epidermis, Vγ5Vδ1 dendritic epidermal T cells (DETCs) interact with LCs to promote KC homeostasis and wound healing (Thelen and Witherden 2020). The human epidermis lacks DETCs but is enriched in cluster of differentiation (CD)8^+ $CD103^+$ αβ T cells with analogous functions (Watanabe, Gehad et al. 2015, Ho and Kupper 2019). Across both species, $CD4^+$ αβ T cells dominate in the dermis and regulatory T cells (Tregs) with a resident memory phenotype comprise 10-30% of cutaneous $CD4^+$ populations in humans and 20-60% in mice (Clark, Chong et al. 2006, Sanchez Rodriguez, Pauli et al. 2014, Ho and Kupper 2019, Boothby, Kinet et al. 2021). The signals driving high Tregs frequencies remain incompletely defined and may include tissue-specific cues such as ultraviolet (UV) exposure (Yamazaki, Nishioka et al. 2014).

The dermis also harbors unconventional lymphocyte populations, including dermal γδ T cells and mucosa-associated invariant T (MAIT) cells, which together with $CD4^+$ T helper (Th)17 cells represent the major sources of IL-17A and IL-22 (Cruz, Diamond et al. 2018, Legoux, Bellet et al. 2019). The abundance and function of these cells are strongly influenced by commensal microbiota, highlighting the importance of the skin-microbe interface in immune calibration (Belkaid and Harrison 2017).

The subcutaneous layer also contributes to the cutaneous immune environment and is composed of adipocytes, fibroblasts and other stromal cell populations. Adipocytes actively participate in innate immune defense through the production of AMPs, while fibroblasts express cytokines and receptors that enable dynamic interactions with neighboring immune cells and help shape local inflammatory responses (Zhang, Chen et al. 2019, Boothby, Kinet et al. 2021).

The dynamic interplay of epidermal and dermal immune populations, coupled with AMP, cytokine and chemokine microenvironments and microbial cues, underlies both homeostasis and the pathogenesis of inflammatory disorders. Importantly, these cutaneous immune processes may extend beyond the skin, contributing to systemic inflammation and comorbid organ involvement observed in chronic inflammatory diseases such as psoriasis.

1.2 Psoriasis

1.2.1 Clinical spectrum, epidemiology and pathological hallmarks of psoriasis

Psoriasis is a chronic, immune-mediated and inflammatory skin disease characterized by recurrent episodes of cutaneous inflammation and the formation of erythematous, scaly plaques (Figure 1.3) (Lowes, Suarez-Farinas and Krueger 2014). Clinically visible lesions reflect profound alterations in epidermal architecture, driven by sustained KC hyperproliferation and aberrant

differentiation, resulting in epidermal thickening, impaired barrier integrity and excessive scaling (Figure 1.4) (Boehncke and Schön 2015). The relapsing–remitting disease course underscores the persistence of pathogenic immune responses within the skin.

Globally, psoriasis affects approximately 60 million individuals, with prevalence varying substantially by geographic region, ranging from below 0.2% in parts of Eastern Sub-Saharan Africa to nearly 3.7% in Australasia (Parisi, Iskandar et al. 2020). Disease onset follows a bimodal distribution, peaking in early adulthood and later life, and occurs slightly earlier in females (Raharja, Mahil and Barker 2021). Genetic susceptibility is particularly pronounced in early-onset disease, with genome-wide association studies identifying more than 60 risk loci. These loci converge on pathways involved in antigen presentation, NF-κB signaling, type I IFN responses, the IL-23/Th17 axis, and epidermal barrier regulation, highlighting the central role of immune-epithelial interactions in disease initiation and persistence (Dand, Mahil et al. 2020).

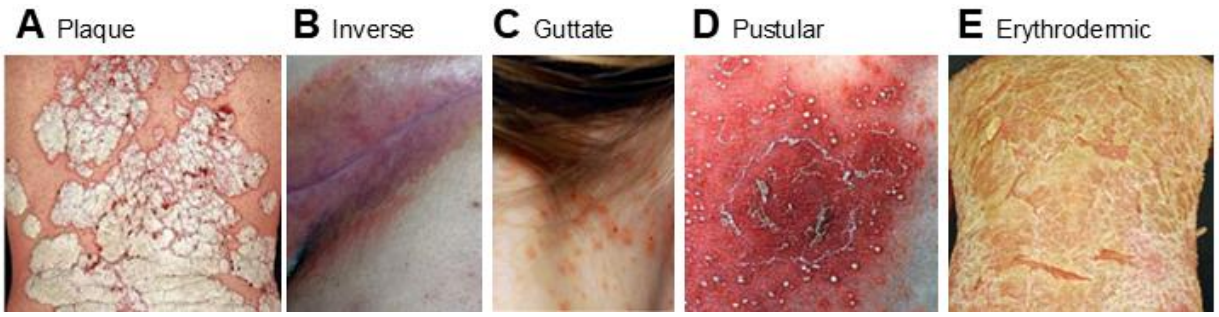

Figure 1.3: Clinical manifestations of psoriasis (Boehncke and Schön 2015)

Exemplary pictures of **(A)** plaque, **(B)** inverse, **(C)** guttate, **(D)** pustular and **(E)** erythrodermic psoriasis. Figure is adapted from Boehncke and Schön 2015.

Clinically, psoriasis encompasses a spectrum of phenotypic variants (Figure 1.3) (Rendon and Schakel 2019). Plaque psoriasis is the most prevalent form, accounting for approximately 90% of cases, and is characterized by sharply demarcated, erythematous plaques covered by silvery-white scales, most commonly affecting the trunk, extensor surfaces and scalp (Di Meglio, Villanova and Nestle 2014). Other variants include inverse psoriasis affecting intertriginous areas; guttate psoriasis, an acute presentation often triggered by streptococcal infection in children and adolescents; pustular psoriasis, which may be localized or generalized and is defined by sterile pustule formation; and erythrodermic psoriasis, a rare but life-threatening manifestation involving diffuse erythema over most of the body surface. In the clinic, patient's disease severity is scored *via* the Psoriasis Area and Severity Index (PASI) ranking erythema (redness), induration (thickness) and desquamation (scaling) of the plaques in different body areas (Boehncke and Schön 2015, Rendon and Schakel 2019). Despite their clinical

heterogeneity, these forms share common immunopathological mechanisms driven by dysregulated cytokine networks and immune cell-KC cross-talk (Lowes, Suarez-Farinas and Krueger 2014).

Histopathologically, psoriatic lesions exhibit characteristic epidermal and dermal changes These include marked thickened epidermis (acanthosis), thickened cornified layer (hyperkeratosis) and retention of cell nuclei in the cornified layer (parakeratosis), along with elongation of rete ridges (downward extensions of epidermis into the dermis) (Figure 1.4) (Boehncke and Schön 2015). The dermis exhibits dilated and tortuous capillaries into the dermis and dense immune infiltrates composed of T cells, macrophages, DCs, mast cells and neutrophils, the latter forming characteristic Munro's microabscesses within the stratum corneum and Kogoj's pustules deeper in the viable epidermis (Figure 1.4B) (Lowes, Suarez-Farinas and Krueger 2014, Boehncke and Schön 2015). These features reflect sustained inflammatory signaling within the skin and provide a morphological correlate to disease activity.

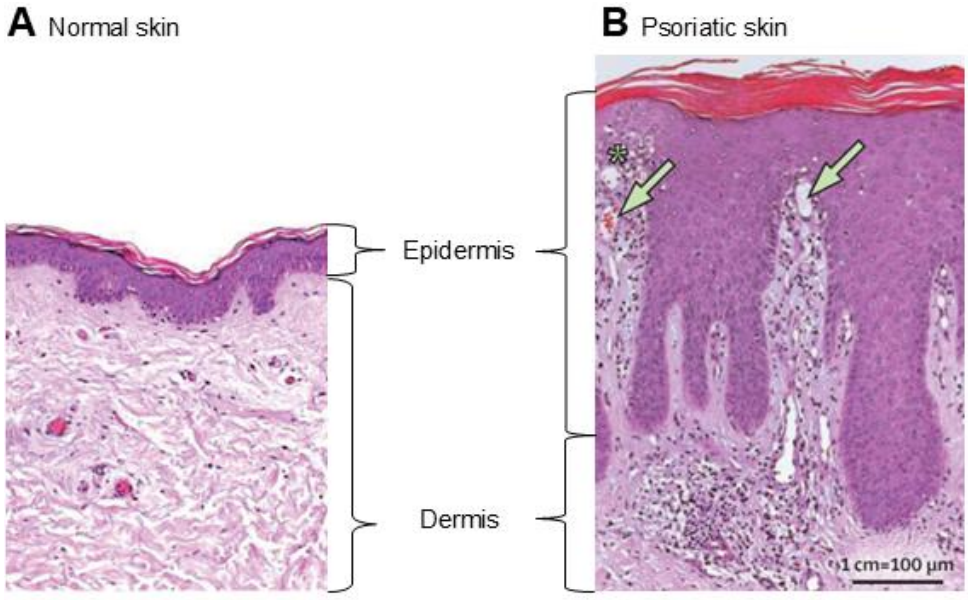

Figure 1.4: Histological hallmarks of psoriasis (Boehncke and Schön 2015)

Hematoxylin and Eosin histology stain of **(A)** normal and **(B)** psoriatic skin. Psoriatic epidermis shows epidermal acanthosis, hyperkeratosis and elongation of rete ridges. Dilated and contorted dermal blood vessels reach into the tips of the dermal papillae (arrows at **(B)**). A mixed inflammatory infiltrate with neutrophils accumulating within the epidermis is noted (asterix at **(B)**). Figure is adapted from Boehncke and Schön 2015.

The clinical manifestations and pathological hallmarks of psoriasis reflect persistent activation, differentiation and trafficking of immune cells within and beyond the skin, necessitating a detailed examination of the immunopathogenic mechanisms that drive disease initiation and maintenance.

1.2.2 Immunopathogenesis of Psoriasis

Psoriasis develops in genetically predisposed individuals and can be triggered or exacerbated by environmental and systemic factors. Mechanical skin injury (Koebner phenomenon), infections, certain medications (e.g. β-blockers, lithium, antimalarials, non-steroidal anti-inflammatory (NSAID) drugs, imiquimod (IMQ)) and autoantigens such as ADAMTS-like protein 5 (ADAMTSL5), a melanocyte-derived antigen, have all been implicated in disease initiation and flares (Fry and Baker 2007, Basavaraj, Ashok et al. 2010, Arakawa, Siewert et al. 2015). These triggers initiate complex and tightly coordinated interactions between KCs, DCs, T cells, neutrophils and stromal cells, ultimately driving chronic cutaneous inflammation.

Following mechanical injury or cellular stress, KCs undergo cell death and release damage-associated molecular patterns (DAMPs), including self-DNA and self-RNA, while simultaneously producing the AMP LL37 (Figure 1.5)(Vanbervliet, Bendriss-Vermare et al. 2003, Lande, Botti et al. 2014). Complexes formed between LL37 and self-nucleic acids activate plasmacytoid DCs (pDCs) through endosomal TLR7. Although pDCs primarily reside in blood and lymphoid organs under steady-state conditions, they rapidly infiltrate inflamed skin, where they produce large amounts of type I IFNs (IFN-α and IFN-β) (Nestle, Conrad et al. 2005, Lande, Gregorio et al. 2007, Zhang, Sen et al. 2016). In psoriatic lesions, pDC recruitment is facilitated by chemerin, which is secreted by fibroblasts, mast cells and endothelial cells (Albanesi, Scarponi et al. 2009). In parallel, myeloid DCs are activated by LL37-nucleic acid complexes via TLR8 as well as by type I IFNs, amplifying early innate immune responses. LCs also contribute during disease initiation. Upon, activation by KC-derived stimuli, they produce IL-6 and IL-23 and migrate to draining LNs, where they promote expansion of γδ T cells (Yoshiki, Kabashima et al. 2014, Zheng, Zhao et al. 2018).

Although activated dermal DCs are capable of priming naïve T cells in draining LN, psoriasis is predominantly maintained by activation, retention and local expansion of skin-resident T cell populations (Bos, Hagenaars et al. 1989). During antigen presentation, DC-derived cytokines determine T cell differentiation, with IL-12 promoting Th1 responses and IL-23, together with IL-6 and TNF-α, driving Th17 and Th22 differentiation (Sieminska, Pieniawska and Grzywa 2024). In psoriatic skin, activated T cells preferentially accumulate within the epidermis (Conrad, Boyman et al. 2007, Cheuk, Wiken et al. 2014). Figure 3.5 illustrates the sequence of early immunopathogenic events in psoriasis.

Stressed KCs further amplify these processes by secreting pro-inflammatory cytokines such as TNF-α, IL-1β and IL-6. IL-6 promotes Th17 differentiation, impairs Treg function and contributes

to angiogenesis, while TNF-α and IL-1β enhance DC activation and cytokine production (Jang, Lee et al. 2021, Kamata and Tada 2022, Sieminska, Pieniawska and Grzywa 2024). In contrast to healthy skin, where DCs are largely confined to the dermis, psoriatic lesions display a marked accumulation of DCs within the epidermis, further facilitating sustained local T cell activation (Terhorst, Chelbi et al. 2015, Martini, Wiken et al. 2017, Cheng, Sedgewick et al. 2018).

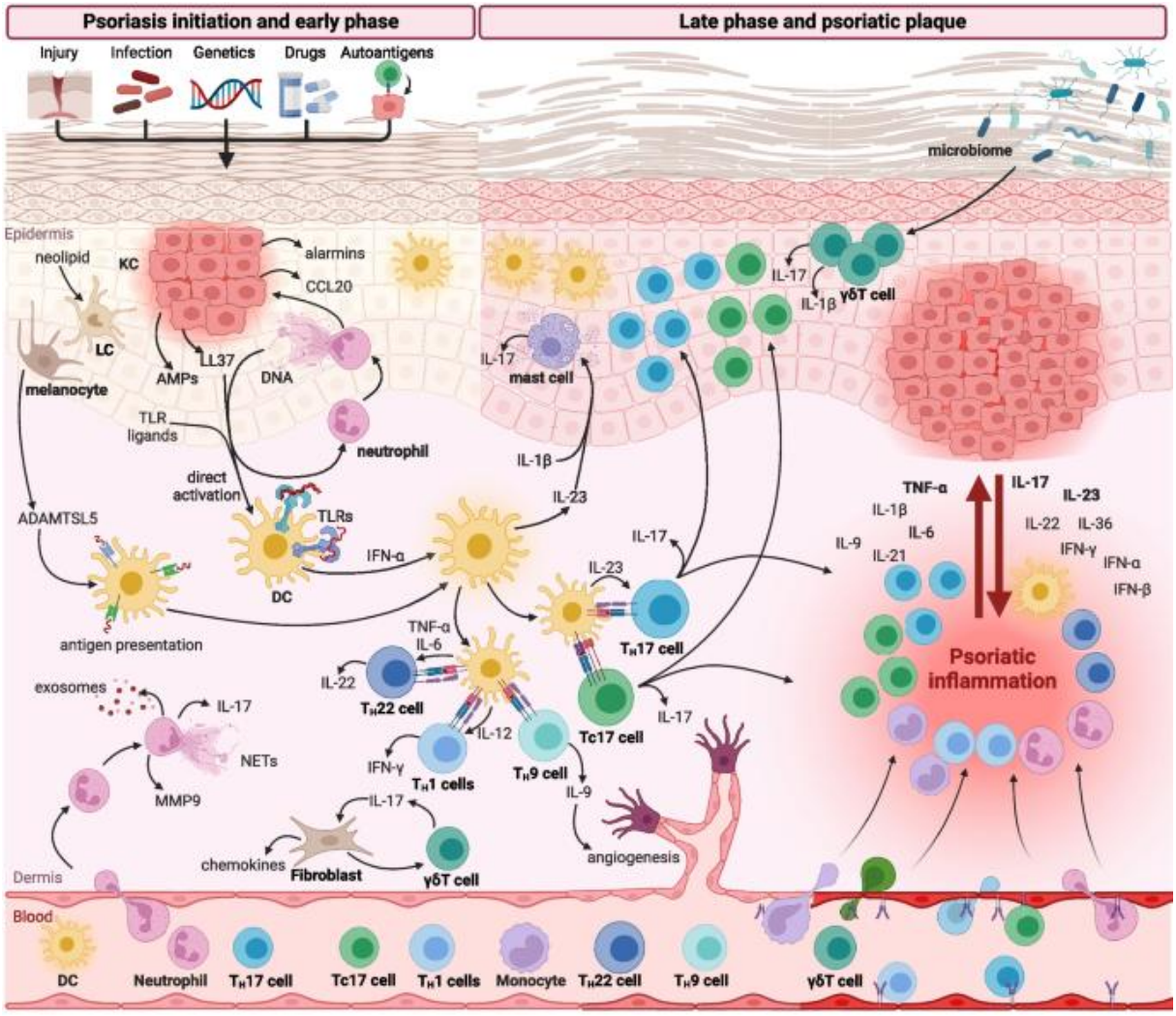

Figure 1.5: Immunopathogenesis of psoriasis (Sieminska, Pieniawska and Grzywa 2024)

Psoriasis is triggered by skin injury, infection, drugs or autoantigens in predisposed individuals. Early lesions feature neutrophil infiltration releasing neutrophil extracellular traps (NETs), matrix-metalloproteinase 9 (MMP9), IL-17 and exosomes; KC hyperproliferation and production of chemokines, AMPs and alarmins; and DC activation via TLR ligands and AMPs. DCs and LCs prime T cells, including Th17, cytotoxic T cell (Tc) 17, Th1, Th9 and Th22 subsets, while γδ T cells produce IL-17 and IL-1β in response to microbiome perturbation. Late lesions are characterized by dense immune cell infiltration, elevated cytokines and chemokines, KC hyperproliferation and angiogenesis, which together sustain chronic inflammation. Figure is taken from Sieminska, Pieniawska and Grzywa 2024.

Activated T cell subsets secrete cytokines characteristic of psoriasis, including IL-17, IL-22 and IFN-γ, which profoundly shape KC responses. In lesional skin, the IL-17 family members IL-17A, IL-17C and IL-17F are particularly strongly upregulated (Johnston, Fritz et al. 2013, Wang, Fogel et al. 2021). These cytokines induce KCs to produce chemokines, AMPs and alarmins, thereby reinforcing immune cell recruitment and activation.

Th1 cells secrete IFN-γ, which induces KC expression of CXCL9, CXCL10 and CXCL11, promoting further recruitment of Th1 cells (Austin, Ozawa et al. 1999, Krueger 2002, Nograles, Zaba et al. 2008, Kagami, Rizzo et al. 2010). Th17 cells release IL-17, driving KC production of CCL20, CXCL1, CXCL2, CXCL8/IL-8 and AMPs such as β-defensins, LL37 and S100 proteins (S100A7, S100A8, S100A9)(Liang, Tan et al. 2006, Wilson, Boniface et al. 2007, Nograles, Zaba et al. 2008, Pene, Chevalier et al. 2008). These mediators recruit $CCR6^+$ Th17 cells, $CCR6^+$ γδ T cells and neutrophils, establishing a self-amplifying inflammatory circuit (Mukaida, Harada et al. 1992, Schroder, Gregory et al. 1992, Mabuchi, Takekoshi and Hwang 2011, Kim, Jee et al. 2014, Campbell, Ebsworth et al. 2017). Th22 cells produce IL-22, which promotes KC hyperproliferation and epidermal thickening (Eyerich, Eyerich et al. 2009, Reynolds, Vegh et al. 2021). Collectively, Th1, Th17 and Th22 cells are increased in both lesional skin and peripheral blood of psoriasis patients, underscoring their contribution to disease pathology (Kagami, Rizzo et al. 2010).

$CD8^+$ cytotoxic T cells (Tc), including Tc17 cells, are enriched in the circulation of psoriasis patients and preferentially infiltrate the epidermis, where they produce IL-17, IL-22 and IFN-γ and directly contribute to epidermal inflammation (Res, Piskin et al. 2010, Hijnen, Knol et al. 2013). In addition, dermal γδ T cells, stimulated by IL-23, IL-1β and IL-17, represent a major source of IL-17 in psoriatic lesions and are essential for disease pathogenesis (Mabuchi, Takekoshi and Hwang 2011, Cai, Xue et al. 2014, Qi, Wang et al. 2021). In contrast, γδ T cells are reduced in the peripheral blood of psoriasis patients, suggesting preferential recruitment to and retention within inflamed skin (Laggner, Di Meglio et al. 2011). Other T cell subsets, including Th9, Th2, Tregs and granulocyte-macrophage colony-stimulating factor (GM-CSF) producing T cells, further modulate disease severity and chronicity (Sieminska, Pieniawska and Grzywa 2024, Fan, Xu et al. 2025).

Neutrophils are rapidly recruited into early psoriatic lesions via chemokines (CXCL1, CXCL2, CXCL8/IL-8, CCL20), leukotriene B4, IL-17E and complement-derived chemoattractants such as C5a (Katayama 2018, Senra, Mylonas et al. 2019, Metzemaekers, Gouwy and Proost 2020). Within the epidermis, neutrophils undergo respiratory burst, degranulation and formation of neutrophil extracellular traps (NETs), releasing IL-1α, IL-1β, IL-6 and IL-17A (Metzemaekers, Gouwy and Proost 2020, Rodriguez-Rosales, Langereis et al. 2021, Liu, Shi et al. 2022). NETs

contain extracellular DNA and LL37, which further activate KCs and DCs, reinforcing inflammatory signaling loops (Hu, Yu et al. 2016, Shao, Fang et al. 2019).

In psoriasis, circulating neutrophils frequently exhibit a pre-activated phenotype, including low-density granulocytes with enhanced NET-forming capacity, which correlates with disease severity (Lin, Rubin et al. 2011, Hu, Yu et al. 2016, Skrzeczynska-Moncznik, Zabieglo et al. 2020). Neutrophil-derived matrix metallopeptidase-9 (MMP-9) and extracellular vesicles activate endothelial cells, increase vascular permeability and facilitate further immune cell infiltration into the skin (Lin, Rubin et al. 2011, Liu, Shi et al. 2022).

Activated monocytes and macrophages are expanded in lesional skin and draining LN in experimental models of psoriasis (Stratis, Pasparakis et al. 2006, Wang, Peters et al. 2006). In human psoriatic skin, macrophages accumulate in both dermis and epidermis, particularly during later disease stages (Wang, Edelmayer et al. 2019). Activated by IFN-γ, macrophages produce IL-23, inducible nitric oxide synthase (iNOS) and TNF-α, thereby contributing to maintenance of the IL-23/IL-17 axis (Fuentes-Duculan, Suarez-Farinas et al. 2010). IL-17 further promotes a pro-inflammatory macrophage phenotype, while monocytes are recruited by diverse chemokines and cytokines (Erbel, Akhavanpoor et al. 2014). In addition, monocytic myeloid-derived suppressor cells (M-MDSCs) are expanded in both peripheral blood and lesional skin of psoriasis patients and correlate with disease severity, although their precise role remains unclear (Liu, Peng et al. 2021).

Beyond immune cells, stromal cells actively shape the inflammatory microenvironment. IL-17 signaling in dermal fibroblasts induces mediators that enhance IL-17 production by γδ T cells and promote KC hyperproliferation through growth factor-rich microenvironments (Saiag, Coulomb et al. 1985, Ha, Wang et al. 2014). Fibroblasts express elevated levels of cytokines and chemokines, including IL-6, CXCL8/IL-8, CXCL2 and CCL19, in some cases exceeding KC-derived production (Angiolilli, Leijten et al. 2022). Endothelial cells also play a central role, as increased dermal vascularity is a hallmark of psoriasis. Elevated levels of vascular endothelial growth factor (VEGF), angiopoietins and TNF-α drive angiogenesis, while IL-17A and IL-36γ activate endothelial cells, inducing proliferation, cytokine production and upregulation of adhesion molecules such as intercellular adhesion molecule (ICAM)-1 (Singh, Schon et al. 2013, Suzuki, Hirakawa et al. 2014, Mercurio, Failla et al. 2020). Transcriptional profiling of psoriatic endothelial cells reveals enrichment of pathways related to leukocyte adhesion, T cell activation, and IL-8 signaling, facilitating sustained immune cell trafficking into the skin (Reynolds, Vegh et al. 2021).

Collectively, psoriasis is sustained by a self-amplifying inflammatory circuit in which IL-23-producing DCs, IL-17- and IL-22-producing T cells and activated KCs mutually reinforce chronic skin inflammation (Figure 1.5). While these interactions are spatially organized within the skin, the cytokines, chemokines and activated immune cell populations that drive this process are not restricted to the cutaneous compartment. Their persistence and dissemination provide a mechanistic rationale for considering psoriasis as a systemic inflammatory disease rather than a solely skin-limited disorder.

1.2.3 Psoriasis as a systemic inflammatory disease

Building on the concept of sustained cutaneous immune activation, psoriasis is now widely recognized as a systemic inflammatory disease rather than a disorder confined to the skin. Chronic inflammation within psoriatic lesions results in persistent release of pro-inflammatory cytokines, chemokines, and activated immune cells into the circulation, thereby influencing immune responses and tissue homeostasis at distant sites. Consistent with this systemic inflammatory state, psoriasis is associated with a broad spectrum of comorbidities that substantially increase disease burden and impair quality of life, including psoriatic arthritis, cardiovascular disease (CVD), metabolic syndrome, non-alcoholic fatty liver disease (NAFLD), inflammatory bowel disease (IBD) and neuropsychiatric disorders (Vlachos, Gaitanis et al. 2016, Yamazaki 2021, Mrowietz, Lauffer et al. 2024, Lada 2025). These associations support the concept that immunopathogenic mechanisms initiated in the skin extend beyond the cutaneous compartment.

Systemic immune activation in psoriasis is reflected by elevated serum levels of multiple pro-inflammatory cytokines, including TNF-α, IFN-γ, IL-6, IL-12, IL-17, and IL-22, which correlate with disease severity in patients with moderate-to-severe disease (Arican, Aral et al. 2005, Suarez-Farinas, Li et al. 2012, Yilmaz, Cicek et al. 2012, de Oliveira, Cardoso et al. 2015, Fotiadou, Lazaridou et al. 2015). In parallel, psoriasis is associated with quantitative and qualitative alterations in circulating immune cell populations, including increased frequencies of activated Th1, Th17, and Th22 cells, pre-activated neutrophils and inflammatory monocytes, consistent with sustained immune priming and mobilization (Kagami, Rizzo et al. 2010, Golden, Groft et al. 2015, Hu, Yu et al. 2016, Skrzeczynska-Moncznik, Zabieglo et al. 2020, Liu, Peng et al. 2021). Systemic inflammation is further accompanied by endothelial activation, characterized by increased expression of adhesion molecules, altered vascular permeability, and a pro-inflammatory vascular phenotype conducive to leukocyte recruitment and tissue damage (Singh,

Schon et al. 2013, Suzuki, Hirakawa et al. 2014, Mercurio, Failla et al. 2020, Reynolds, Vegh et al. 2021, Chen, Ruan et al. 2022).

IL-17A is a central mediator of systemic pathology in psoriasis. Beyond its canonical roles in KCs, immune cells and endothelium, IL-17A acts directly on vascular smooth muscle, hepatocytes and intestinal epithelium, mechanistically linking skin inflammation to multi-organ comorbidities (Pietrowski, Bender et al. 2011, Tang, Bian et al. 2011). While psoriasis-associated comorbidities are often attributed to circulating inflammatory mediators, whether direct migration of immune cells from the skin to peripheral organs remains incompletely resolved.

CVD represents the most extensively studied and clinically significant systemic comorbidity of psoriasis. Patients with severe disease exhibit increased cardiovascular morbidity and mortality, accompanied by widespread vascular inflammation and increased non-calcified coronary plaque burden, which correlates with skin disease severity (Mehta, Azfar et al. 2010, Vena, Vestita and Cassano 2010, Mehta, Yu et al. 2011). Therapeutic targeting of key psoriatic cytokines, including TNF-α, IL-12/23 and IL-17, reduces coronary inflammation, supporting shared immunopathogenic pathways between psoriasis and CVD (Elnabawi, Dey et al. 2019, Elnabawi, Oikonomou et al. 2019). Mechanistically, chronic systemic inflammation promotes endothelial dysfunction and atherosclerosis, with IL-17A enhancing endothelial activation, immune cell recruitment and vascular inflammation (von Stebut, Boehncke et al. 2019). Experimental studies in mouse models corroborate these findings, demonstrating IL-17A-dependent neutrophil accumulation, oxidative stress, and endothelial dysfunction within the aorta (Karbach, Croxford et al. 2014, Karbach, Wenzel et al. 2014, Schüler, Brand et al. 2019). Skin barrier dysfunction itself has emerged as an additional systemic stressor capable of inducing cardiovascular consequences, including arterial hypertension (Wild, Jung et al. 2021). Platelet hyperactivation and oxidative stress further amplify both cutaneous and vascular inflammation, reinforcing psoriasis-associated cardiovascular risk (Forstermann and Munzel 2006, Hot, Lenief et al. 2010, Maione, Cicala et al. 2011, Mizuguchi, Gotoh et al. 2021, Orlando, Molon et al. 2022, Jiang, Jiang et al. 2023).

Beyond the vasculature, psoriasis is associated with inflammatory manifestations in multiple organ systems. Psoriatic arthritis represents a prototypic extracutaneous extension of disease, sharing dysregulated IL-23/IL-17 and TNF-α signaling pathways with psoriasis, as illustrated by the clinical efficacy of cytokine-targeting therapies, including JAK inhibitors (Neurath, Sticherling et al. 2024). Increasing evidence also supports immunological crosstalk between barrier tissues, particularly the skin and gut. Shared cytokine networks, overlapping homing receptor expression and microbiome alterations suggest bidirectional communication between these organs (Oyoshi,

Elkhal et al. 2011, Salem, Ramser et al. 2018, Chen, Li et al. 2020, De Pessemier, Grine et al. 2021). Consistent with this concept, psoriasis is associated with an increased risk of IBD, although IL-17A plays divergent, context-dependent roles in intestinal immunity, as reflected by the paradoxical effects of IL-17 inhibition in psoriasis (Lolli, Saraceno et al. 2015, Deng, Wang et al. 2023, Bezzio, Cavalli et al. 2024, Alsakarneh, Al Ta'ani et al. 2025). Psoriasis is also strongly linked to metabolic syndrome and non-alcoholic fatty liver disease (NAFLD), driven by shared inflammatory and immune-metabolic pathways involving IL-17A, TNF-α, IL-6, oxidative stress and insulin resistance (Gelfand and Yeung 2012, Zindanci, Albayrak et al. 2012, Xu, Su et al. 2017, Balak, Piaserico and Kasujee 2021, Heitmann, Frings et al. 2021). In addition, patients with psoriasis exhibit increased prevalence of depression and anxiety, reflecting combined effects of chronic systemic inflammation and psychosocial burden (Lada 2025).

Collectively, these findings establish psoriasis as a systemic inflammatory disease with multi-organ involvement. However, whether inflammation in peripheral tissues arises primarily cytokine-driven systemic immune activation or also from direct migration of skin-derived immune cells remains unclear. Addressing this unresolved question is essential for understanding the mechanistic basis of psoriasis-associated comorbidities. These observations underscore the need for mechanistic models that can distinguish between cytokine-driven systemic inflammation and direct immune cell migration from the skin to other organs, a central aim of this thesis.

1.2.4 Therapeutic implications

The therapeutic management of psoriasis aims to suppress chronic inflammation, prevent disease flares and improve long-term patient outcomes. Conventional treatments, including topical agents such as corticosteroids and vitamin D_3 analogues, as well as phototherapy, remain effective for mild to moderate disease. In patients with moderate to severe psoriasis, systemic immunosuppressants such as methotrexate and cyclosporine are frequently employed but are limited by cumulative toxicity and adverse effects (Pardasani, Feldman and Clark 2000, Zhu, Jing et al. 2022). However, the identification of psoriasis as a cytokine-driven immune-mediated disorder has revolutionized therapy, particularly with biologics targeting IL-12/23, TNF-α, IL-17 and IL-23 (Pardasani, Feldman and Clark 2000, Kerdel and Zaiac 2015, Zhu, Jing et al. 2022).

Among these, IL-17 pathway inhibitors demonstrate particularly robust efficacy in moderate-to-severe disease, providing strong clinical validation of IL-17-driven pathology (Waisman 2012, Kurschus and Moos 2017, Erichsen, Jensen and Kofoed 2020, Ten Bergen, Petrovic et al.

2020). Importantly, therapeutic benefit extends beyond improvement of skin lesions, indicating that systemic inflammatory circuits are responsive to targeted cytokine blockade (Elnabawi, Dey et al. 2019).

Despite these advances, a substantial proportion of patients exhibit incomplete responses, secondary loss of efficacy or adverse effects. Moreover, clinical observations reveal tissue-specific consequences of cytokine modulation: IL-17 inhibition trigger or exacerbate IBD, while TNF inhibition may induce psoriasis (Conrad, Di Domizio et al. 2018, Mylonas and Conrad 2018, Xie, Xiao et al. 2022, Deng, Wang et al. 2023, Alsakarneh, Al Ta'ani et al. 2025). These paradoxical outcomes highlight that therapeutic efficacy depends not only on cytokine neutralization but also on context-dependent immune regulation across tissues.

A central unresolved question is how skin-directed therapies exert systemic effects. Specifically, it remains unclear whether improvement in extracutaneous manifestations primarily reflects suppression of circulating inflammatory mediators or altered immune cell trafficking from inflamed skin. Dissecting these mechanisms is essential for refining therapeutic strategies and for understanding psoriasis-associated comorbidities. Addressing this gap requires experimental systems that allow mechanistic dissection of systemic immune consequences arising from defined cutaneous inflammation, which is achieved using complementary mouse models described below.

1.3 Mouse models of psoriasis

Mouse models have been instrumental in elucidating immunopathogenic mechanisms in psoriasis and enabling preclinical evaluation of targeted therapies. Although no single model fully recapitulates the genetic complexity, chronicity or immunological heterogeneity of human psoriasis, complementary approaches allow dissection of distinct processes, including cytokine-driven inflammation, KC-immune cell interactions and systemic immune consequences.

Early models arose from spontaneously occurring mutations producing psoriasiform skin phenotypes, though many lacked robust T cell infiltration. Xenograft models, in which human psoriatic skin is transplanted onto immunodeficient mice, provide translational insight but are limited by technical complexity and patient-derived tissue availability (Nickoloff, Kunkel et al. 1995, Gudjonsson, Johnston et al. 2007, Lowes, Suarez-Farinas and Krueger 2014).

Genetic engineering has generated numerous psoriasis-associated strains, facilitated mechanistic dissection of individual genes and signaling pathways. Global gain- or loss-of-function approaches are informative but can disrupt endogenous regulation, yield non-physiological expression and obscure tissue-specific contributions to systemic comorbidities

(Lowes, Suarez-Farinas and Krueger 2014, Gangwar, Gudjonsson and Ward 2022). Cell type-specific models using lineage-restricted promoters, particularly KC-specific promoters (K5, K6, K10, K14, involucrin, loricrin), enable precise manipulation of cytokines, growth factors and signaling molecules, while immune cell-specific models refine mechanistic insight (Hafner, Wenk et al. 2004, Gangwar, Gudjonsson and Ward 2022). Inducible systems, such as tetracycline- or tamoxifen-responsive models, allow temporal control of gene expression in fully developed animals, avoiding developmental artefacts (Gangwar, Gudjonsson and Ward 2022).

Acute and inducible models, including intradermal IL-23 or topical TLR7 agonist IMQ, are technically straightforward, cost-effective and combinable with genetic modifications. Their acute, self-resolving nature limits modelling of chronic disease and long-term systemic effects (Chan, Blumenschein et al. 2006, van der Fits, Mourits et al. 2009).

In this thesis, two complementary models were selected to interrogate IL-17A-driven inflammation: the acute IMQ-induced psoriasis model and the chronic KC-specific IL-17A overexpression model (K14-IL17A$^{ind/+}$).

1.3.1 Imiquimod-induced psoriasis

The IMQ-induced mouse model is widely used for studying acute psoriasiform skin inflammation (van der Fits, Mourits et al. 2009). Imiquimod, a TLR7 agonist formulated in Aldara™ cream, is clinically approved for HPV-associated warts, actinic keratosis and non-melanoma skin cancers, but can induce or exacerbate psoriatic lesions, providing the rationale for its experimental use (Beutner, Tyring et al. 1998, Geisse, Rich et al. 2002, Gilliet, Conrad et al. 2004, Szeimies, Gerritsen et al. 2004, Wu, Siller and Strutton 2004, Fanti, Dika et al. 2006, Rajan and Langtry 2006, Tillman and Carroll 2007).

Topical application of 5% IMQ to mouse ear or dorsal skin induces erythema, scaling and epidermal thickening, accompanied by KC hyperproliferation, parakeratosis and immune cell infiltration (van der Fits, Mourits et al. 2009). Disease severity varies with genetic background, whereas C57BL/6 mice best recapitulate human psoriasis (Swindell, Michaels et al. 2017).

IMQ activates TLR7, recruiting myeloid differentiation primary-response protein 88 (MyD88) and triggering NF-κB-dependent expression of pro-inflammatory cytokines, AMP and chemokines (Akira, Takeda and Kaisho 2001, Kawasaki and Kawai 2014). MyD88 deficiency protects against IMQ-induced disease (Wohn, Ober-Blobaum et al. 2013). IMQ also activates inflammasomes, eliciting inflammation in non-TLR7-expressing cells and vehicle components can independently drive inflammatory responses (Flutter and Nestle 2013, Walter, Schafer et al. 2013).

IMQ strongly engages the IL-23/IL-17 axis, expanding Th17 and γδ T cells and upregulating IL-17A, IL-22 and TNF-α (Cai, Shen et al. 2011, El Malki, Karbach et al. 2013). KC-specific IL-17 receptor deletion reduces dermatitis, selectively impairing neutrophil recruitment while leaving monocyte infiltration intact, highlighting KCs as key mediators of IL-17A-driven neutrophil attraction (Moos, Mohebiany et al. 2019). Both innate and adaptive components contribute, making this model valuable for early inflammatory cascade studies.
While reflecting acute TLR-driven inflammation rather than chronic disease, the IMQ model provides a robust platform for mechanistic studies.

1.3.2 Keratinocyte-specific IL-17A overexpression (K14-IL-17A$^{ind/+}$)

KC-restricted IL-17A overexpression allows the mechanistic study of chronic skin inflammation and systemic comorbidities. The K14-IL-17A$^{ind/+}$ mouse, generated by crossing an inducible IL-17A (IL-17A$^{ind/ind}$) knock-in allele with K14-Cre recombinase, expresses IL-17A in KCs (Hafner, Wenk et al. 2004, Haak, Croxford et al. 2009, Croxford, Karbach et al. 2014, Karbach, Croxford et al. 2014).
Epidermal IL-17A alone induces a spontaneous, severe psoriasis-like phenotype, with hyperplasia, hyperkeratosis, parakeratosis, dermal immune infiltration, neutrophilic microabscesses, scaling, erythema and skin thickening, independent of elevated IL-23. Epidermal T-cell composition shifts towards T cell receptor (TCR)β$^+$ αβ T cells, with γδ T cells absent (Croxford, Karbach et al. 2014). Systemic IL-17A elevation correlates with disease severity, accompanied by increased granulopoiesis, mobilization of inflammatory neutrophils and monocytes and elevated circulating ROS (Croxford, Karbach et al. 2014, Karbach, Croxford et al. 2014).
Sustained IL-17A expression drives vascular inflammation and dysfunction, including endothelial dysfunction and hypertension, mediated by infiltrating myeloperoxidase (MPO)$^+$ CD11b$^+$ Gr-1$^+$ granulocytes (Karbach, Croxford et al. 2014). Additional comorbidities, such as arthritis and uveitis, recapitulate patient disease (Croxford, Karbach et al. 2014). Comparative analyses with IMQ and DC-specific IL-17A models show systemic disease severity correlates with circulating IL-17A and neutrophil infiltration, underscoring organ-organ crosstalk (Schüler, Brand et al. 2019).
K14-IL-17A$^{ind/+}$ mice respond poorly to IL-17A neutralization but show attenuation with TNF-α or IL-6 blockade, highlighting context-dependent therapeutic vulnerabilities (Croxford, Karbach et al. 2014, Karbach, Croxford et al. 2014, Schüler, Brand et al. 2019).

Together, the IMQ and K14-IL-17A$^{ind/+}$ models offer complementary platforms to study acute versus chronic IL-17A-driven inflammation and its systemic consequences. Determining whether peripheral organ inflammation arises from circulating mediators or direct skin-activated immune cell migration requires direct immune cell-tracking approaches, which are the focus of the following chapter.

1.4 Skin-to-organ immune cell trafficking

Understanding whether psoriasis-associated systemic pathology arises from circulating mediators or skin-derived immune cells requires direct *in vivo* tracking of cutaneous immune populations. Although elevated circulating cytokines, particularly IL-17A, correlate with disease severity and comorbidities, cytokine measurements alone cannot distinguish humoral-driven systemic inflammation from dissemination of immune cells activated within inflamed skin (Mrowietz, Lauffer et al. 2024, Sultana, Monir et al. 2024).

Immune cells in psoriatic lesions acquire migratory phenotypes and access lymphatic and vascular routes, raising the possibility that skin-derived immune cells directly contribute to organ-specific pathology (Sieminska, Pieniawska and Grzywa 2024). Conventional approaches, including blood immune profiling, cytokine neutralization or endpoint tissue analysis, remain correlative and cannot resolve immune cell origin, migration pathways or temporal dynamics.

Direct immune cell tracking is therefore essential. Photoconvertible fluorescent proteins provide a powerful strategy by enabling spatially and temporally restricted labelling of defined cell populations *in vivo* (Turkowyd, Balinovic et al. 2017). In this thesis, the photo-activatable mitochondria (PhAM) mouse serves as a ubiquitous fluorescent reporter, expressing mitochondrial-targeted Dendra2 in all cell types. This allows immune cells in inflamed skin to be selectively photoconverted and tracked (Pham, McCaffery and Chan 2012).

Dendra2 irreversibly switches from green to red fluorescence upon exposure to violet light, distinguishing labelled cells from unphotoconverted populations and enabling tracking in circulation and peripheral organs (Chudakov, Lukyanov and Lukyanov 2007, Adam, Nienhaus et al. 2009). Its high photostability, efficient photoconversion and minimal phototoxicity make it ideally suited for *in vivo* studies of immune cell trafficking (Turkowyd, Balinovic et al. 2017).

Photoconversion is first validated in the acute IMQ-induced model, which provides rapid, reproducible psoriasiform inflammation and then applied to the chronic K14-IL-17A$^{ind/+}$ model. This strategy directly distinguishes systemic effects driven by circulating mediators from those mediated by migrating skin-activated immune cells, establishing a mechanistic framework for skin-organ crosstalk in psoriasis.

1.5 Non-canonical NF-κB signaling in keratinocytes and its role in psoriasis

In addition to immune cell-mediated mechanisms, psoriasis pathogenesis is shaped by KC-intrinsic signaling pathways that may independently drive inflammation.

1.5.1 Molecular architecture of non-canonical NF-κB signaling

The NF-κB signaling pathway is a central regulator of immune responses, inflammation and cellular homeostasis, operating via two mechanistically distinct pathways: canonical and non-canonical. It comprises five transcription factors, NF-κB 1 (p50), NF-κB 2 (p52), RELA (p65), RELB and c-REL, that are retained in an inactive cytosolic state through association with inhibitors of κB (IκBs), including IκBα and the precursor proteins p105 and p100. Proteasomal processing of p105 and p100 generates the transcriptionally active p50 and p52 subunits, respectively (Figure 1.6) (Hayden and Ghosh 2008, Sun 2017).

Canonical NF-κB is rapidly induced by pro-inflammatory stimuli such as TNF, IL-1β or pathogen-associated molecular patterns and engages TGFβ-activated kinase 1 (TAK1) and the IκB kinase (IKK) complex (IKKα, IKKβ, IKKγ/NEMO), leading to phosphorylation, ubiquitin-mediated degradation of IκBα and p105 and nuclear translocation of p50-RELA or p50-c-REL dimers (Sun and Ley 2008, Vallabhapurapu and Karin 2009). This pathway drives rapid inflammatory gene expression, proliferation and survival.

In contrast, non-canonical NF-κB signaling selectively activates p52-RELB heterodimers and is characterized by slower kinetics and stringent regulation. In resting cells, RELB is sequestered in the cytoplasm by p100, which functions as an IκB-like inhibitor (Xiao, Harhaj and Sun 2001). Activation occurs downstream of a restricted set of TNF receptor (TNFR) superfamily members, including lymphotoxin-β receptor (LTβR), CD40 and B-cell activating factor receptor (BAFFR), as well as select non-TNFR signals (Coope, Atkinson et al. 2002, Dejardin, Droin et al. 2002, Kayagaki, Yan et al. 2002, Sun 2011).

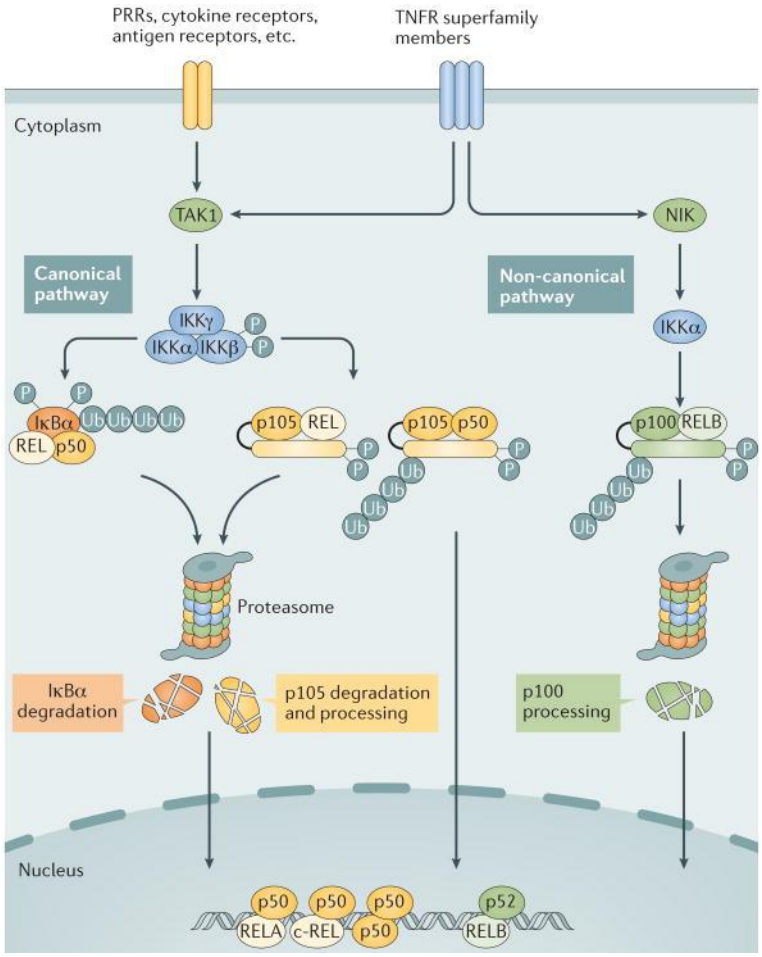

Figure 1.6: Canonical and non-canonical NF-κB signaling pathway (Sun 2017)

Canonical NF-κB signaling is initiated by various immune receptors that activate TAK1, which phosphorylates the IKK complex (IKKα, IKKβ, and IKKγ). Activated IKKβ phosphorylates IκBα and p105, leading to their ubiquitin-dependent degradation and release of NF-κB dimers (e.g., RELA-p50, c-REL-p50) for nuclear translocation and target gene activation. In contrast, non-canonical NF-κB signaling is triggered by specific TNFR superfamily members that activate NF-κB-inducing kinase (NIK). NIK activates IKKα, which phosphorylates p100, promoting selective degradation of its IκB-like C-terminus and generating p52. This enables nuclear translocation of p52-RELB dimers. Figure is adapted from Sun 2017.

A defining feature of non-canonical signaling is its dependence on NF-κB-inducing kinase (NIK). Under homeostatic conditions, NIK levels are maintained at very low by continuous ubiquitin-mediated degradation via the TRAF2-TRAF3-cIAP1/2 complex (Vallabhapurapu, Matsuzawa et al. 2008, Zarnegar, Wang et al. 2008). Engagement of non-canonical NF-κB-activating receptors induces TRAF3 degradation, allowing NIK accumulation. Stabilized NIK phosphorylates and activates IKKα, which in turn phosphorylates p100, promoting partial proteasomal processing to generate p52. The resulting p52-RELB heterodimers translocate to the nucleus and drive transcriptional programs involved in immune regulation and inflammation (Figure 3.6 and 3.7) (Sun, Ganchi et al. 1994, Liao, Zhang et al. 2004). Non-canonical signaling is further modulated by NIK degradation, TRAF3 stability, IKKα- and TBK1-dependent feedback mechanism and additional context-specific mechanisms, such as complement membrane attack

complex-dependent NIK stabilization (Jane-wit, Surovtseva et al. 2015). These regulatory layers ensure tight spatial and temporal control, preventing aberrant activation and pathological inflammation.

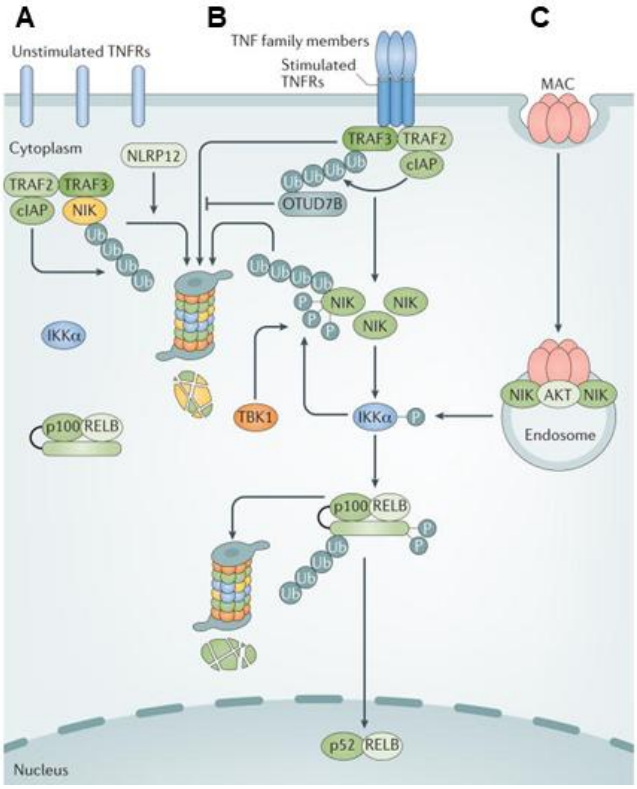

Figure 1.7: Mechanisms for activation and regulation of non-canonical NF-κB signaling (Sun 2017)

(A) In resting cells, newly synthesized NIK is bound by TRAF3 and targeted for proteasomal degradation via the cIAP-TRAF2-TRAF3 E3 ubiquitin ligase complex, preventing non-canonical NF-κB activation. **(B)** Upon ligand binding to specific TNFR superfamily receptors, TRAF3 is degraded through cIAP-mediated K48 ubiquitylation, allowing NIK accumulation and activation. This triggers p100 processing and nuclear translocation of p52-RELB. Regulation occurs via TRAF3 deubiquitylation by OTUD7B and NIK degradation by IKKα and TBK1. **(C)** The complement membrane attack complex (MAC) activates non-canonical NF-κB signaling independently of TRAFs by forming an endosomal complex with MAC, AKT and NIK. AKT activation stabilizes NIK. Figure is adapted from Sun 2017.

1.5.2 Immune functions of non-canonical NF-κB signaling

At the organismal level, non-canonical NF-κB signaling shapes the development and maintenance of the adaptive immune system. It is essential for lymphoid organogenesis, B cell maturation, DC cross-priming and thymic epithelial cell (TEC) differentiation (Miyawaki, Nakamura et al. 1994, Weih and Caamano 2003, Dejardin 2006, Katakam, Brightbill et al. 2015, Abramson and Anderson 2017).

In the thymus, this pathway regulates medullary TEC (mTEC) maturation and expression of the autoimmune regulator (AIRE), promoting central tolerance (Haljasorg, Bichele et al. 2015, Onder, Nindl et al. 2015, Abramson and Anderson 2017). In peripheral lymphoid tissues, non-

canonical NF-κB controls B cell follicle organization, germinal center formation, immunoglobulin class switching and T follicular helper (TFH) cell differentiation (Hu, Wu et al. 2011, Mesin, Ersching and Victora 2016). In T cells, it modulates effector and memory differentiation, cytokine production and regulatory T cell maintenance (Murray 2013, Rowe, Murray et al. 2013, Yu, Zhou et al. 2014). Although most studies focus on immune cells, non-canonical NF-κB signaling also regulates KC differentiation and epidermal homeostasis via IKKα-dependent pathways, highlighting its relevance beyond classical immune cells (Liu, Xia et al. 2008).

Collectively, these functions contrast with the rapid, inflammatory outputs of canonical NF-κB. Non-canonical signaling therefore acts as a fine-tuning mechanism that maintains immune architecture and homeostasis over time.

1.5.3 Keratinocyte-intrinsic non-canonical NF-κB signaling in psoriasis

KCs, the predominant cell type of the epidermis, are central drivers of psoriasis pathogenesis. Within psoriatic lesions, KCs undergo hyperproliferation, exhibit impaired terminal differentiation and produce a broad spectrum of cytokines and chemokines, including IL-1 family members, IL-36 and CXCL8. These mediators promote immune cell recruitment and activation, establishing a self-amplifying inflammatory circuit that sustains chronic skin inflammation (Lowes, Russell et al. 2013, Furue, Furue et al. 2020, Wang and Lai 2024).

Canonical NF-κB signaling is a well-established driver of psoriatic inflammation, promoting KC proliferation, survival and inflammatory gene expression, as well as IL-23 production in DCs (Goldminz, Au et al. 2013). In contrast, the contribution of non-canonical NF-κB signaling to KC-intrinsic inflammatory programs in psoriasis remains poorly defined.

Emerging evidence indicates that NIK, the central kinase of the non-canonical pathway, is a critical regulatory node. In TECs, NIK activity shapes dermal γδ T cell maturation and IL-17 production, linking non-canonical signaling to pathogenic cytokine loops (Mair, Joller et al. 2015). In DCs, the E3 ligase complex $CRL4^{DCAF2}$ promotes NIK degradation independently of TRAF3, limiting RELB activation and IL-23 production. Loss of DCAF2 or pharmacologic inhibition is leading to NIK stability and exacerbates IMQ psoriasiform (Huang, Gao et al. 2018). Similarly, ANKRD22 restrains NIK activity and IL-23 production in DCs, with deficiency exacerbating IMQ-induced skin inflammation and overexpression accelerating its resolution (Xia, Zhu et al. 2024).

KC-specific deletion of TRAF2 triggers spontaneous psoriasis-like inflammation, confirming that dysregulated non-canonical NF-κB signaling drives KC-intrinsic disease initiation (Etemadi 2015). Conversely, pharmacologic inhibition of NIK attenuates IMQ-induced skin inflammation,

supporting its functional relevance in disease pathogenesis (Zhu, Ma et al. 2020). Together, these findings suggest that similar regulatory mechanisms may operate within KCs, influencing disease initiation and progression.

Together, these findings underscore the importance of tight NIK regulation in psoriasiform inflammation and support a KC-intrinsic role for non-canonical NF-κB signaling. However, the precise contribution of this pathway to psoriasis pathogenesis remains incompletely understood, positioning it as a mechanistically distinct, skin-intrinsic axis complementary to the immune cell trafficking focus of this thesis.

1.6 Rationale of the study

Severe psoriasis is not merely a skin disorder, it is a systemic inflammatory disease with profound multi-organ implications. Patients exhibit increased risk of comorbidities including psoriatic arthritis, IBD and NAFLD and most critically, CVD (Griffiths and Barker 2007, Di Meglio, Villanova and Nestle 2014, Yamazaki 2021). Cardiovascular complications are the leading cause of mortality in this population and psoriasis itself constitutes an independent risk factor beyond traditional cardiovascular risk determinants (Mehta, Azfar et al. 2010, Vena, Vestita and Cassano 2010). These observations highlight a pressing mechanistic question: how does inflammation originating in the skin drive systemic pathology?

We hypothesized that skin-activated immune cells may act as vectors of systemic inflammation, directly linking cutaneous lesions to distant organ pathology. To investigate this, we established a severe psoriatic mouse model capable of tracking immune cell migration from the skin to peripheral tissues, including the vasculature. This was achieved by combining the K14-IL-17A$^{ind/+}$ mouse, which develops pronounced skin and vascular inflammation, with the photoconvertible Dendra2 reporter background PhAM (Pham, McCaffery and Chan 2012, Croxford, Karbach et al. 2014, Karbach, Croxford et al. 2014). This model allows spatiotemporal labelling of skin-derived immune cells, providing a direct experimental framework to dissect immune cell versus cytokine-mediated drivers of systemic disease.

Separately, emerging evidence implicates KC-intrinsic non-canonical NF-κB signaling as a central driver of psoriasis. Inhibition of NIK ameliorates skin inflammation in the IMQ-induced mouse model (Zhu, Ma et al. 2020), whereas KC-specific TRAF2 deletion triggers psoriasis-like pathology (Etemadi 2015). Building on this, we hypothesized that a KC-specific NIK knockout could attenuate skin inflammation. To test this, we generated NIK$^{fl/fl}$-K14Cre mice and characterized them in the IMQ-induced psoriasis model, establishing a mechanistic framework for therapeutic intervention in psoriasis.

2 MATERIAL AND METHODS

2.1 Chemicals and technical equipment

All the chemicals and solvents used in the frame of these projects are listed in Table 2.1.

Table 2.1: List of chemicals and their corresponding suppliers

Reagent	Supplier
β-Mercaptoethanol	Fluka Chemie GmbH, St. Louis, KS, USA
0.9% NaCl solution for infusion	Berlin-Chemie, Berlin, Germany
Acetic acid	Carl Roth, Karlsruhe, Germany
Agarose	Biozym, Hessisch Oldendorf, Germany
AldaraTM 5% cream	Meda Pharma, Solna, Sweden
Ammonium chloride (NH_4Cl)	Merck, Darmstadt, Germany
Augen- und Nasensalbe (eye salve containing 5% dexpanthenol)	Bepanthen, Bayer, Leverkusen, Germany
BD FACSFlowTM	BD Biosciences, Franklin Lakes, NJ, USA
BD FACSRinseTM Solution	BD Biosciences, Franklin Lakes, NJ, USA
BD FACSTM Shutdown Solution	BD Biosciences, Franklin Lakes, NJ, USA
Bovine Serum Albumin (BSA)	Merck, Darmstadt, Germany
Brefeldin A	Merck, Darmstadt, Germany
Chloroform	Roth, Karlsruhe, Germany
DNase I	Roche, Basel, Switzerland
Dulbecco's modified PBS (DPBS)	Merck, Darmstadt, Germany
Dithiothreitol (DTT)	Thermo Fisher Scientific, Waltham, MA, USA
Ethanol	AppliChem, Darmstadt, Germany
Ethylenediaminetetraacetic acid (EDTA)	Merck, Darmstadt, Germany
Fetal bovine serum (FBS)	Thermo Fisher Scientific, Waltham, MA, USA
GeneRulerTM 100 bp Plus DNA ladder	Thermo Fisher Scientific, Waltham, MA, USA

Reagent	Supplier
Gibco® Hank's buffered saline solution (HBSS)	Thermo Fisher Scientific, Waltham, MA, USA
Gibco® Hank's buffered saline solution (HBSS) with Ca2+ and Mg2+	Thermo Fisher Scientific, Waltham, MA, USA
Gibco® RPMI 1640	Thermo Fisher Scientific, Waltham, MA, USA
GoTaq® qPCR Master Mix	Promega, Madison, WI, USA
Hydroxyethylpiperazine thane sulfonic acid (HEPES)	Thermo Fisher Scientific, Waltham, MA, USA
Ionomycin	Merck, Darmstadt, Germany
Isoflurane	AbbVie, Wiesbaden, Germany
Isopropyl alcohol	AppliChem, Darmstadt, Germany
L-Glutamine	Thermo Fisher Scientific, Waltham, MA, USA
LiberaseTM	Roche, Basel, Switzerland
Midori Green	Nippon Genetics, Düren, Germany
MEM non-essential amino acids (NEAA)	Thermo Fisher Scientific, Waltham, MA, USA
Paraformaldehyde (PFA) 4%	Santa Cruz, Dallas, TX, USA
Penicillin/Streptomycin (P/S)	Thermo Fisher Scientific, Waltham, MA, USA
Percoll	Merck, Darmstadt, Germany
Phorbol Myristate Acetate (PMA)	Merck, Darmstadt, Germany
Proteinase K	Roche, Basel, Switzerland
REDTaq® ReadyMixTM	Merck, Darmstadt, Germany
Roti Histofix	Roth, Karlsruhe, Germany
Sodium chloride (NaCl)	Roth, Karlsruhe, Germany
Sodiumdodecylsulfate (SDS)	AppliChem, Darmstadt, Germany
Sodium pyruvate	Thermo Fisher Scientific, Waltham, MA, USA
Tris(hydroxymethyl)aminomethane (TRIS)	Merck, Darmstadt, Germany
TRIzolTM Reagent	Thermo Fisher Scientific, Waltham, MA, USA

Reagent	Supplier
Trypan blue	Thermo Fisher Scientific, Waltham, MA, USA
Veet Depilation Crème	Reckitt Benckiser, Mannheim, Germany

2.2 Antibodies and kits

Antibodies for flow cytometry were purchased from BD Biosciences (Franklin Lakes, NJ, USA), BioLegend (San Diego, California, USA) and eBioscience (San Diego, California, USA).

Table 2.2: List of antibodies used in flow cytometry studies and their corresponding suppliers

Antibody	Conjugate	Clone	Host	Dilution	Supplier
CD3	BB515	145-2C11	armenian hamster	100	BioLegend
CD4	APC	GK1.5	rat	1000	BioLegend
CD11b	PE-Cy7	M1/70	rat	500	BioLegend
CD11b	BV510	M1/70	rat	1000	BioLegend
CD11b	BV605	M1/70	rat	500	BD Bioscience
CD11c	APC	HL3	armenian hamster	200	BD Bioscience
CD11c	APC-R700	N418	armenian hamster	500	BD Bioscience
CD19	Alexa Fluor700	6D5	rat	200	BioLegend
CD19	BYG670-P	6D5	rat	800	BioLegend
CD43	PE	S7	rat	1000	BD harmigen
CD45	BV510	30-F11	rat	200	BioLegend
CD45pan	BUV805	30-F11	rat	1000	BD Bioscience
CD45.2	APC	104	mouse	200	eBioscience
CD90.2	PerCP	53-2.1	rat	1000	BioLegend
CD90.2	SB645	53-2.1	rat	100	eBioscience
CX3CR1	APC	SA011F11	mouse	300	BioLegend
F4/80	BB790-P	T45-2342	rat	200	BD Bioscience

Antibody	Conjugate	Clone	Host	Dilution	Supplier
FcεR1α	PE CF594	MAR-1	rat	500	BD Bioscience
GM-CSF	PE	MP1-22E9	rat	200	BioLegend
Gr-1	V450	RB6-8C5	rat	500	BD Bioscience
IFNγ	PE-Cy7	XMG1.2	rat	1000	eBioscience
IL-17A	eFl450	eBio17B7	rat	300	eBioscience
Ly6C	V450	AL-21	rat	200	BD Bioscience
Ly6C	BV570	HK1.4	rat	500	BioLegend
Ly6G	BV750	1A8	rat		BD Bioscience
Ly6G	PE	1A8	rat	400	BioLegend
MHCII	BV786	M5/114.15.2	rat	1000	BD Bioscience
NK1.1	APC-Cy7	PK136	mouse	1000	BioLegend
Siglec F	BUV489	E50-2440	rat	500	BD Bioscience
Sirp1α	PE-Cy7	P84	rat	500	BD Bioscience
TCRβ	Fitc	H57-597	armenian hamster	200	BioLegend
TCRγδ	PerCP-eFl710	eBio GL3	armenian hamster	200	eBioscience
XCR1	BV650	ZET	mouse	500	BioLegend

For fixation/permeabilization of cells the BD Cytofix/Cytoperm Fixation/Permeabilization Solution Kit from BD Bioscience (Franklin Lakes, NJ, USA) was used.

2.3 Instruments

Table 2.3: List of laboratory instruments and their corresponding suppliers

Instrument	Supplier
Analytical balance AEJ 120-4M	Kern & Son, Balingen, Germany
Balance SNR 49608372	Sartorius, Göttingen, Germany
Caliper C1X018	Kroeplin, Schlüchtern, Germany

Instrument	Supplier
Centrifuge Biofuge fresco, Heraeus	Thermo Fisher Scientific, Waltham, MA, USA
Centrifuge Fresco 21 centrifuge, Heraeus	Thermo Fisher Scientific, Waltham, MA, USA
Centrifuge Mutlifuge 3SR+	Thermo Fisher Scientific, Waltham, MA, USA
Centrifuge Rotana 469 RS	Hettich Zentrifugen, Tuttlingen, Germany
Collimator 10 mm beam diameter	Omicron-Laserage Laserprodukte, Rodgau-Dudendorf, Germany
Electrophoresis power supply Power Pac Basis	Bio-Rad, Hercules, CA, USA
Flow Cytometer BD FACS Canto™ II	BD Biosciences, Franklin Lakes, NJ, USA
Flow Cytometer BD FACS Symphony™	BD Biosciences, Franklin Lakes, NJ, USA
Flow Cytometer Invitrogen Attune™ NxT	Thermo Fisher Scientific, Waltham, MA, USA
Gel Imager Gel DocTM	Bio-Rad, Hercules, CA, USA
GentleMACSTM Octo Dissociator	Miltenyi Biotec, Bergisch Gladbach, Germany
Hair trimmer ECO-XS	Tondeo, Solingen, Germany
Homogenizer FastPrep®-24 MTTM	MP Biomedicals, Irvine, CA, USA
Isoflurane anesthesia device UniVet Porta	Groppler Medizintechnik, Deggendorf, Germany
Laser 405 nm Diode Laser LuxX 405-60	Omicron-Laserage Laserprodukte, Rodgau-Dudendorf, Germany
Lightcycler Step OnePlus Real-Time PCR System Thermal Cycling Block	Thermo Fisher Scientific, Waltham, MA, USA
Luna II Automated Cell Counter	BioCat GmbH, Heidelberg, Germany
Metal bead lysing matrix tubes	MP Biomedicals, Irvine, CA, USA
Multichannel Pipette Transferpette®S12 5-50µL	Brand, Wertheim, Germany
Multichannel Pipette Transferpette®S12 30-300µL	Brand, Wertheim, Germany
pH meter pH 720	WTW, Weilheim, Germany

Instrument	Supplier
Pipettes max 2, 10, 20, 100, 200 or 1000 µL	Gilson, Middleton, WI, USA
Pipettes max 10, 20, 200 or 1000 µL	Peqlab, Erlangen, Germany
Pipette controller Pipetboy 2	Integra Bioscience, Biebertal, Germany
Plate reader M200 Pro, Nano Quant Reader	Tecan, Männedorf, Switzerland
Sterile hood HeraSafe, KS15	Thermo Fisher Scientific, Waltham, MA, USA
Tabletop centrifuge Galaxy MiniStar	VWR International, Radnor, PA, USA
Thermocycler T3000	Biometra, Göttingen, Germany
Thermocycler Biometra Trio	Analytik Jena AG, Jena, Germany
Vacuum aspiration system vacusafe	Integra Biosciences, Biebertal, Germany
Vortex Mixer	VWR International, Radnor, PA, USA
Water bath WNB 7	Memmert, Schwalbach, Germany

2.4 Buffers and media

All buffers and solutions were prepared with distilled water (dH_2O) unless described differently in Table 2.4. The sterility of the T-cell medium was ensured by working under a sterile hood (HeraSafe, KS15, Thermo Fisher Scientific, Waltham, MA, USA).

Table 2.4: Buffers and media

Name	Components
0% media	1% (v/v) L-glutamine 1% (v/v) P/S 0.05% (v/v) β-Mercaptoethanol 2% (v/v) HEPES
3% media	1% (v/v) L-glutamine 1% (v/v) P/S 3% (v/v) FBS 2.5% (v/v) HEPES 1% (v/v) sodium pyruvate
ACK buffer (10 ×) pH 7.2	1.5 M NH_4Cl 100 mM $KHCO_3$

Name	Components
	10 mM EDTA-2Na NaOH/HCl for pH adjustment
FACS buffer	Phosphate-buffered saline (PBS) 2% FBS
Liver buffer I	1.25 mM HEPES 10% (v/v) FBS in RPMI
Liver buffer II	37.5% (v/v) Percoll 100 U/mL heparin in HBSS (-/-)
Shake media	1% (v/v) L-glutamine 1% (v/v) P/S 2 mM EDTA 2% (v/v) HEPES
Strip media	0.5 µM EDTA 100 µM DTT in 3% media
T-cell medium	RPMI 1640 10% FCS 100 U/mL P/S 2 mM L-Glutamine 1 % NEAA 1 mM Sodium pyruvate 1 mM HEPES 50 µM β-Mercaptoethanol
50x TRIS-acetate-EDTA (TAE) buffer (pH 8.3)	2 M TRIS 1 M acetic acid 50 mM EDTA pH 8.0
Tail lysis buffer (TENS)	10 mM Tris 5 mM EDTA (pH 8) 0.2% SDS 200 mM NaCl

2.5 Molecular Biology

2.5.1 Isolation of genomic DNA

Biopsies were taken from the ear or toe of the mouse at recommended ages, or from the tail after sacrificing. The tissue was lysed by shaking overnight (ON) at 56 °C in TENS buffer with Proteinase K (0.4 mg/mL). DNA was precipitated by mixing with an equal volume of isopropyl alcohol and pelleted by centrifugation at 13,000 × g for 5 min at room temperature (RT). The supernatant (SN) was discarded, and the DNA was washed twice with 70% (v/v) ethanol. The pellet was dried at 37 °C for 30 min and dissolved in 100-400 µL dH_2O for subsequent PCR.

2.5.2 Polymerase chain reaction (PCR)

A master mix containing 500 µL REDTaq® ReadyMix™ was supplemented with 5 µL of each primer (1 µM) and brought up to a final volume of 950 µL with dH_2O. For PCR ,19 µL of the master mix and 1 µL DNA were mixed and the reaction was performed at primer-specific annealing temperatures (Table 2.5) using one of the thermocyclers (Table 2.3).

Table 2.5: Primers used for PCR

Primer name	Primer sequence (5'-3')	Annealing temp. [°C]	Direction
β-Actin fw	TGTTACCAACTGGGACGACA	58	sense
β-Actin rev	GACATGCAAGGAGTGCAAGA	58	anti-sense
IL-17A fw	TCAGGGTCGAGAAGATGCTGG	63	sense
IL-17A rev	GTAAAGCATGTGCACCGAGG	63	anti-sense
K14 Cre fw	TTCCTCAGGAGTGTCTTCGC	58	sense
K14Cre rev	GTCCATGTCCTTCCTGAAGC	58	anti-sense
K14Cre positive control fw	CTAGGCCACAGAATTGAAAGATCT	58	sense
K14Cre positive control rev	GTAGGTGGAAATTCTAGCATCATCC	58	anti-sense
NIK fw	TATGAACTGCTCCCGTTTCG	60	sense
NIK fl rev	CCTGTGCATCACAGAGTATACTAGC	60	anti-sense

Primer name	Primer sequence (5'-3')	Annealing temp. [°C]	Direction
NIK ko rev	TTCCTGTGAACTCAAACACTCCC	60	anti-sense
Dendra-WT fw1	TCCTGGCTTCTGAGGACCGC	58	Sense
Dendra-WT fw2	TTCCCCTGCAGGACAACGCC	58	sense
Dendra-WT rev	TCAATGGGCGGGGGTCGTT	58	anti-sense
Dendra Fl-Ex fw	TACAGCTCCTGGGCAACGTGCT	58	sense
Dendra Fl-Ex rev1	TGGCAGCAGATCTAACGGCCG	58	anti-sense
Dendra Fl-Ex rev2	GTTCACGTTGCCCTCCATGT	58	anti-sense
Rosa26 F	AAAGTCGCTCTGAGTTGTTAT	60	sense
Rosa26 R	GGAGCGGGAGAAATGGATATG	60	anti-sense
Rosa26 SpliAcB	CATCAAGGAAACCCTGGACTACTG	60	anti-sense
1260.1 fw	GAGACTCTGGCTACTCAT	58	sense
1260.1 rev	CCTTCAGCAAGAGCTGGGGAC	58	anti-sense

2.5.3 Agarose gel electrophoresis

Analysis of PCR products was accomplished by agarose gel electrophoresis. 2% (w/v) agarose gels were prepared in 1 × TAE buffer and Midori green DNA stain (4 µL/100 mL). 10-18 µL of each PCR sample and 7 µL of 100 bp Plus DNA ladder were applied to each well of the gel. Gel electrophoresis was performed in 1 × TAE buffer at a constant voltage of 150 V for 25-35 min. DNA bands were visualized by UV light with the Gel Doc XR+ gel documentation system.

2.6 Cell Biology

2.6.1 Preparation of single cell suspension of different organs

Aorta: The aorta was isolated from the mouse and stored in PBS on ice for the whole procedure if not indicated otherwise. The fatty tissue was removed under the microscope. The aorta was flushed to remove any remaining blood and the length of the aorta was measured. Subsequently, the tissue was cut into small pieces by scissors and a razor blade and transferred

into 1 mL digestion mix (1 mg/mL Liberase in RPMI). The samples were incubated at 37 °C for 30 min and mixed by pipetting every 5-10 min. To stop the reaction FACS buffer was added on ice, the cells were filtered through a 70 µm cell strainer and washed with FACS buffer. The suspension was centrifuged at 300 × g for 6 min at 4 °C. The SN was discarded and the pellet was resuspended in FACS buffer for further procedures.

BM: The femur and tibia were isolated from the hind legs of the mouse. The BM was flushed out with FACS buffer by using a syringe. After centrifugation at 300 × g, 6 min at 4 °C, erythrocytes were lysed by incubating the cells for 3-5 min at RT in 1 × ACK buffer. The cells were diluted in FACS buffer, centrifuged and resuspended in FACS buffer.

Colon: The colon was isolated from the abdominal cavity of the mouse and transferred into 3% media. The colon was opened longitudinally, the feces were cleared out, and the tissue was washed twice in 3% media. 10 mL of Strip media were added and shaken at 37 °C for 20 min. The solution was passed through a sieve, and the tissue was added to 20 mL Shake media. The solution was vortexed for 30-60 sec, and the intestine was washed in fresh 3% media. The tissue was mechanically disrupted in 1 mL digestion media (0.1 mg/mL Liberase TL, 5 mg/mL DNase I in 0% media) by scissors and further 5 mL of digestion media was added. The solution was incubated at 37 °C for 30 min, passed through a 100 µm strainer and washed with 3% media. The cells were pelleted at 450 × g for 10 min at 4 °C, the SN was discarded and the pellet resuspended in 5 mL 3% media. The cells were passed through a 70 µm cell strainer and washed with 10 mL 3% media. Centrifugation was done at 450 × g for 10 min at 4 °C, the SN was discarded and the pellet resuspended in 3% media.

Ear skin: Ear samples were isolated from the mice, cleaned from remaining hair and split into dorsal and ventral parts. The samples were transferred into a 1.5 mL digestion mix (0.12 mg/mL DNase I, 0.25 mg/mL Liberase in RPMI-1640 Medium) per pair of ears. shredded into small pieces with scissors and shaken at 900 revolutions per minute (rpm) for 45-60 min at 37 °C. Subsequently, the samples were put on ice for 5 min, filtered through a 70 µm cell strainer and washed twice with FACS buffer. The cells were centrifuged at 300 × g fo 6 min at 4 °C, the SN was discarded and the cells were dissolved in FACS buffer for further use.

Kidney: The kidney was isolated from 0.9% NaCl perfused mice and added into 10 mL digestion mix (100 µg/mL DNase I and 60 mg Collagenase D in RPMI) in a C-tube. The tissue was homogenized by using the GentleMACSTM Octo Dissociator. The samples were incubated at 37 °C for 30 min. The suspensions were directly placed on ice, passed through a 70 µm cell strainer and washed with PBS. The cells were pelleted at 500 × g for 10 min at 4 °C. The SN was discarded and suspended in 3 mL Percoll (36%). The solution was transferred into a 15 mL tube and 3 mL Percoll (72%) was slowly layered beneath the cell suspension. The gradient was

centrifuged 2400 rpm for 15 min at 18 °C, with both acceleration and braking applied. The dense top layer was removed by suction and the lower layer was transferred without the pellet into a new tube. Percoll was removed by dilution with PBS and centrifugation at 300 × g for 10 min at 4 °C. The SN was then removed and the erythrocytes were lysed by incubation for 2-3 min at RT with 1 × ACK buffer. PBS was added and the cells were pelleted 300 × g for 5 min at 4 °C. Remaining leukocytes were resuspended in FACS buffer for further procedure.

Liver: The liver of 0.9% perfused mice was isolated and minced into small pieces with scissors. The disrupted tissue was passed through a 100 µm cell strainer and the strainer was washed with Liver buffer I up to 50 mL. The suspension was centrifuged at 100 × g, 1 min at RT, without braking, after which the SN was transferred to a new tube. The cells were pelleted at 500 × g for 8 min at RT with full brake and the SN was removed by suction. The pellet was resuspended in Liver buffer II. After centrifugation at 900 × g, 30 min at RT without braking, the erythrocytes were lysed in 1 × ACK buffer for 2-3 min at RT, then diluted in 10 mL FACS buffer. Leukocytes were pelleted at 500 × g for 8 min at 8 °C and resuspended in FACS buffer.

Lymphoid tissue: Spleens and LNs were pressed through a 40 µm cell strainer and washed once with FACS buffer. Erythrocytes lysis of the spleen was achieved by incubating the sample with ACK buffer for 3-5 min at RT. FACS buffer was added and the cells were pelleted at 300 × g, for 6 min at 4 °C. The SN was discarded and the pellet was resuspended in the desired buffer.

2.6.2 Cell counting

Cells were automatically counted using Luna II (BioCat) according to the manufacturer's instructions.

2.6.3 Surface staining

Single cell suspensions were incubated with anti-mouse CD16/CD32 for blocking Fc receptors in FACS buffer for 10 min at 4 °C. The cells were washed and stained with a combination of surface-binding antibodies and a viability dye (APC-ef780 eBioscience™, Thermo Fisher Scientific, Waltham, USA) in FACS buffer for 20 min at 4 °C in the dark. Samples were washed and, if no intracellular staining was planned, the cells were fixed in 2% formaldehyde in PBS for 30 min at 4 °C.

2.6.4 Intracellular staining

For intracellular cytokine staining of T cells, the cells were restimulated for 4 h with 50 ng/mL PMA, 500 ng/mL ionomycin and 1 µg/mL Brefeldin A in T-cell medium at 37 °C and 5% CO_2. Afterwards, the cell surface was stained as described in 2.6.3. For intracellular staining, the cells were fixed and permeabilized using the BD Cytofix/CytopermTM Kit according to the manufacturer's instructions.

2.6.5 Flow cytometry

Samples were acquired with a BD FACS Canto™ II, Invitrogen Attune™ NxT flow cytometer or BD FACS Symphony™. The analysis was performed by using FlowJo software version 10 (BD, Franklin Lakes, NJ, USA). In the analysis, doublets were excluded by Forward Scatter (FSC) and Side Scatter (SSC) properties.

2.7 Mouse Experiments

All mice were on a C57BL/6 background and housed in groups under pathogen-free conditions. All animal experiments were approved by the local administration (Landesuntersuchungsamt Koblenz: G17-1-076; G21-1-039 and G21-1-50) and were performed in accordance with the guidelines from the translational animal research center (TARC) of Mainz.

2.7.1 Mouse strains

PhAM mice were crossed to K14Cre mouse line (Hafner, Wenk et al. 2004, Pham, McCaffery and Chan 2012). The resulting PhAM-K14Cre mice were bred to IL-17A$^{ind/ind}$ mice to obtain the experimental PhAM-K14-IL-17A$^{ind/+}$ mice (Haak, Croxford et al. 2009). The IL-17A$^{ind/ind}$ mice were crossed to K14Cre mice to obtain the K14-IL-17A$^{ind/+}$ strain.
NIK$^{floxed/floxed}$ (NIK$^{fl/fl}$) mice were crossed to K14Cre mice to obtain NIK$^{fl/fl}$-K14Cre (Lacher, Thurm et al. 2018).

2.7.2 IMQ-induced psoriasis

For the induction of IMQ-induced psoriasis like skin inflammation, 6-10-week-old mice were used and the following procedures were conducted under isoflurane anesthesia (1.5%, Abbott) with ointment on eyes (Bepanthen). One day before treatment a 2.0 × 2.5 cm area was shaved on the dorsal side by using a hair trimmer (ECO-XS, Tondeo) and depilating with Veet hair removal

cream (Reckitt Benckiser). Mice were treated daily for 5-10 days with 50 mg Aldara™ cream (Meda Pharma) containing 5% IMQ on the back skin and 10 mg on the ears, respectively. Treatment for the control group was Sham cream (13.5% cetylstearyl alcohol, 1.5% sodium dodecyl sulfate, 12.5% paraffinum subliquidum, 22.5% white vaseline, 10% propylene glycol, 40% dH_2O) consisting out of the ingredients of the Aldara™ cream without the IMQ. Disease scoring was done as described in 4.7.3.

2.7.3 Psoriasis disease scoring

For IMQ-induced psoriasis-like disease, scoring was done daily and for the [PhAM-]K14-IL-17A$^{ind/+}$ scoring started at 5 weeks of age and was conducted weekly.
Disease severity was scored based on erythema and scaling and done according to a modified PASI system (0 = no, 1 = slight, 2 = low, 3 = medium, 4 = maximum) (Schüler, Efentakis et al. 2019). The cumulative PASI score was calculated the following way: (Erythema + Scaling) * (area/100). For IMQ-induced psoriasis the area is fixed at 45% and for the [PhAM-]K14-IL-17A$^{ind/+}$ the affected area was categorised the following: head = 10%, dorsal trunk = 35%, ventral trunk = 35%, leg = 5%. Additionally, the body weight and the skin thickness were monitored at the same frequency and calculated in percentage with the first measurement equalizing 100%.

2.7.4 Laser illumination

One day before the treatment the control mice PhAM-IL-17A$^{ind/+}$ were shaved on the upper back area by a hair trimmer (ECO-XS, Tonedo) under isoflurane anesthesia (Abbott). PhAM-K14-IL-17A$^{ind/+}$ animals were directly illuminated on the diseased skin with 0.5 cm distance. Illumination was done with a 405 nm diode laser equipped with a collimator objective for 10 mm beam diameter (LuxX 405-60, Omicron-Laserage, Rodgau-Dudendorf, Germany) at 60 mW in APC mode on scaled/shaved back skin areas and inside and outside of the ears for 4 - 5 min per area under isoflurane anesthesia (Abbott).

2.7.5 Choline-deficient high-fat diet

With the age of 4 weeks PhAM-K14-IL-17A$^{ind/+}$ and control littermates were placed on choline-deficient high-fat diet (Cd-HFD, D05010402, rodent diet with 45 kcal% fat without added choline, Research Diets, New Jersey, USA).

2.8 Bioinformatic Analysis

Statistics were performed using GraphPad Prism version 9 (GraphPad Software, San Diego, USA). Data were tested for normality. If data were normally distributed, two groups were compared using an unpaired two-tailed Student's *t*-test. For comparison of more than two groups, one-way ANOVA (analysis of variance) followed by Bonferroni post-hoc test was used. If data were not normally distributed, the Mann-Whitney test was applied. Values are represented as mean ± standard error of the mean (SEM) and p values were considered significant for * $p<0.05$, ** $p<0.01$, *** $p<0.001$ and **** $p<0.0001$.

3 RESULTS

3.1 Immune cell tracking with Dendra2 in murine psoriasis mouse models

Psoriasis is a chronic, inflammatory skin disease with systemic comorbidities, including CVD, IBD and NAFLD, which is part driven by IL-17A (de Oliveira, Cardoso et al. 2015, Wang, Zang et al. 2022, Olveira, Augustin et al. 2023, Alsakarneh, Al Ta'ani et al. 2025). In mice, conditional overexpression of IL-17A in KCs (K14-IL-17A$^{ind/+}$ mouse line) recapitulates severe psoriasis-like skin pathology accompanied by systemic inflammation and vascular dysfunction (Croxford, Karbach et al. 2014, Karbach, Croxford et al. 2014).

To determine whether skin-infiltrating immune cells migrate to distant organs - particularly the vasculature - we established a psoriasis model that allows *in vivo* tracking of immune cells using the photoconvertible fluorescent protein Dendra2. As an initial step, we optimized photoconversion in psoriatic skin using PhAM mice, which ubiquitously express Dendra2, in the IMQ-induced psoriasis model (van der Fits, Mourits et al. 2009, Pham, McCaffery and Chan 2012). While this model does not recapitulate elevated systemic IL-17A, it provides a robust and technically accessible platform for method development, enabling precise cellular tracking during the generation of the PhAM-K14-IL-17A$^{ind/+}$ mice (Schüler, Brand et al. 2019).

3.1.1 Photoconversion establishment with the IMQ-induced psoriasis

To establish a reliable photoconversion protocol in an inflammatory skin setting, PhAM mice were subjected to the IMQ-induced psoriasis model and the lesional skin was illuminated with a 405 nm laser to induce photoconversion of Dendra2 (Figure 3.1A, B).

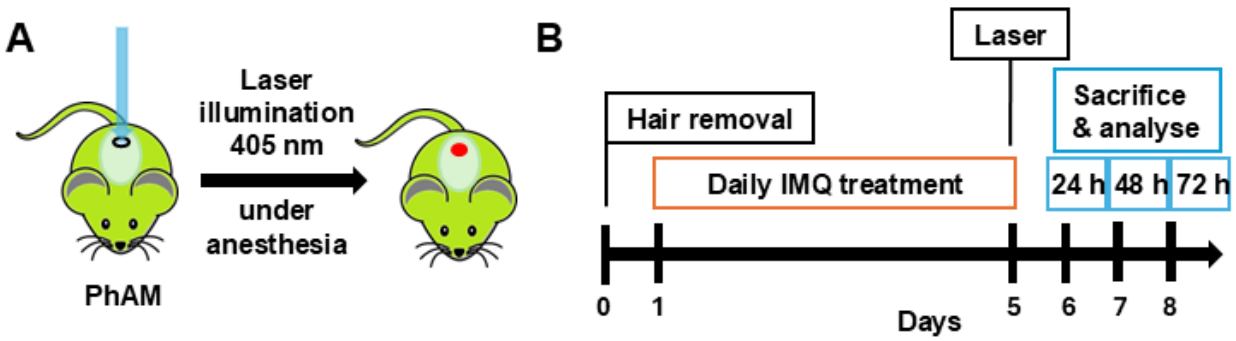

Figure 3.1: Photoconversion workflow for 24, 48 or 72 h cell migration time for IMQ-treated PhAM mice

(A) Schematic representation of the photoconversion procedure. Lesional skin of PhAM mice were illuminated with a 405 nm laser, converting green-fluorescing Dendra2 to its red-fluorescing form. **(B)** Experimental timeline for the 5-day IMQ-induced psoriasis protocol followed by laser illumination on day 5 and analysis 24, 48 or 72 h later.

Following photoconversion, mice were sacrificed at 24, 48 or 72 h to assess whether skin-resident cells labelled in the skin could be detected in distant organs. Immune cells from skin, spleen, inguinal lymph nodes (iLN), and BM were isolated and analysed by flow cytometry (Figure 3.1B and Figure 3.3). As a proof of concept, we first verified that photoconversion could be achieved in inflamed skin. IMQ treatment induced a robust psoriasiform phenotype, with maximal disease severity around day 4-5 (Figure 3.2).

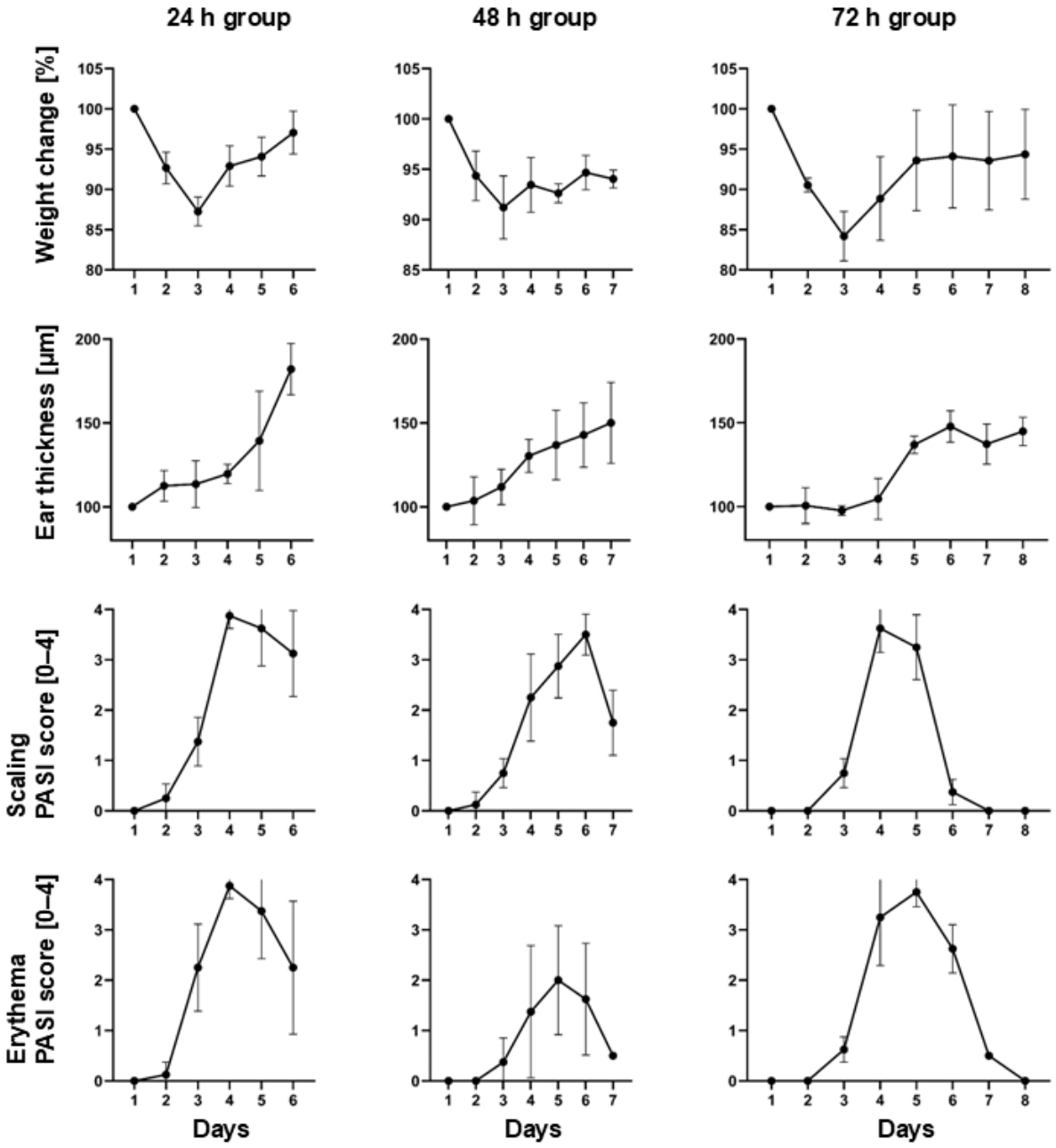

Figure 3.2: Disease scores of the IMQ-induced psoriasis model with PhAM mice and subsequent sit for 24, 48 or 72 h

Disease scores during 5-day IMQ treatment and the following sit time of PhAM mice. Shown are percentage changes in body weight, percentage increase in ear thickness and PASI-derived erythema and scaling scores for each time and group, *n* = 3 per time point. Data illustrate characteristic disease progression with peak severity around days 4-5.

Laser illumination resulted in a clear shift from green- to red-fluorescing Dendra2 in lesional skin compared with unilluminated, green fluorescing background controls (Figure 3.3). This confirmed that photoconversion was feasible under inflammatory conditions.

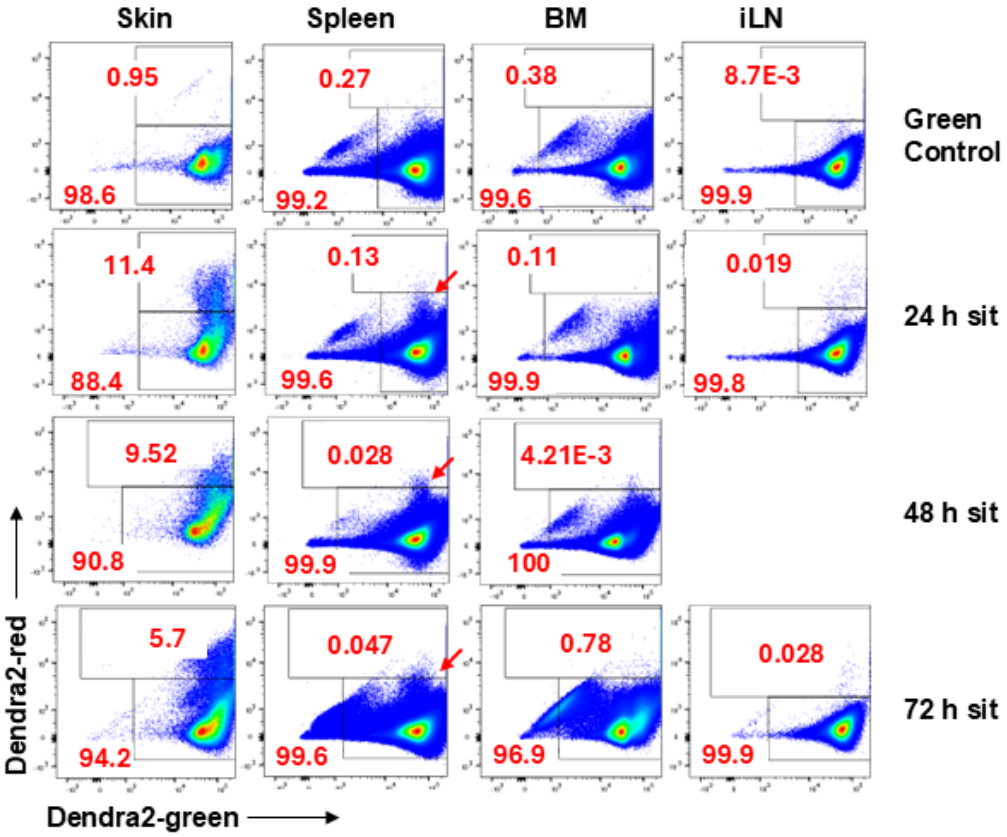

Figure 3.3: Detection of photoconverted immune cells 24, 48 or 72 h after photoconversion in the skin and lymphoid organs of 5-day IMQ-treated PhAM mice

One representative flow cytometry plot of Dendra2-red$^+$ cells pre-gated on single, live, CD45.2$^+$ per organ and group. Dendra2-red$^+$ cells of skin, spleen, BM and inguinal lymph node (iLN) of 5-day IMQ-treated PhAM mice 24, 48 or 72 h after photoconversion und and unilluminated, green fluorescing control. Percentages of gates are shown. Data was acquired with BD FACS Canto™ II flow cytometer. PhAM mice were illuminated once on both ears and one back skin area each for 10 min with 1 cm between skin and laser. Photoconversion is evident as a shift toward red fluorescence in lesional skin. Small populations of Dendra-2$^+$ cells are detectable in spleen (red arrow) and iLN, whereas no photoconverted cells were observed in BM.

Next, we considered whether photoconverted cells could be detected in secondary lymphoid organs. In both spleen and iLN samples, a small but visibly distinct population of CD45.2$^+$ Dendra2-red$^+$ cells were observed at all analysed time points, indicating that a subset of photoconverted skin-resident leukocytes could be detected in lymphoid organs (Figure 3.3). The BM showed no detectable photoconverted population.

The presence of red-fluorescing immune cells in spleen and iLN demonstrated the technical feasibility of tracking skin-derived (Dendra2-red^{+}) immune cells following IMQ-induced inflammation. To minimize signal dilution through *de novo* Dendra2 synthesis, cell proliferation or the loss of short-lived neutrophil migration events, the migration interval was set to 24 h or less for subsequent experiments.

In a second experiment, PhAM mice were subjected to IMQ-induced psoriasis for 10 consecutive days. The extended treatment period was chosen to evaluate whether prolonged skin inflammation facilitates the development of vascular immune responses. On the final treatment day, the skin was photoconverted using an expanded illumination protocol (Figure 3.4).

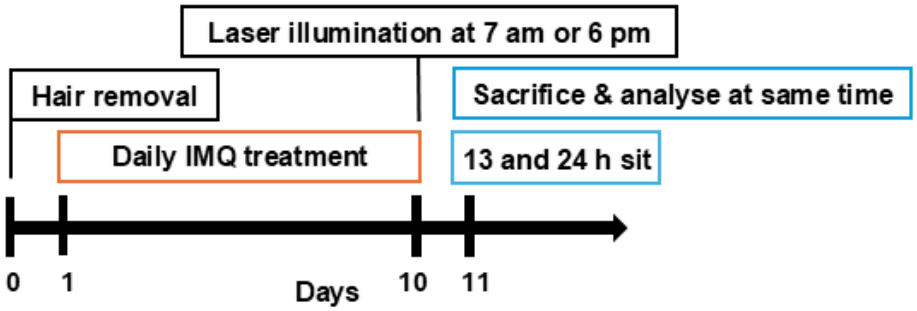

Figure 3.4: Photoconversion workflow for 13 and 24 h cell migration time in the elongated IMQ-induced psoriasis model with PhAM mice

Experimental timeline for the 10-day IMQ-induced psoriasis for PhAM mice followed by different laser illumination times on day 10 and analysis 13 or 24 h later.

Two groups of mice received photoconversion 11 hours apart and were sacrificed simultaneously, resulting in migration intervals of 13 and 24 h, respectively. Disease severity during this 10-day protocol peaked around days 4-5 (Figure 3.5).

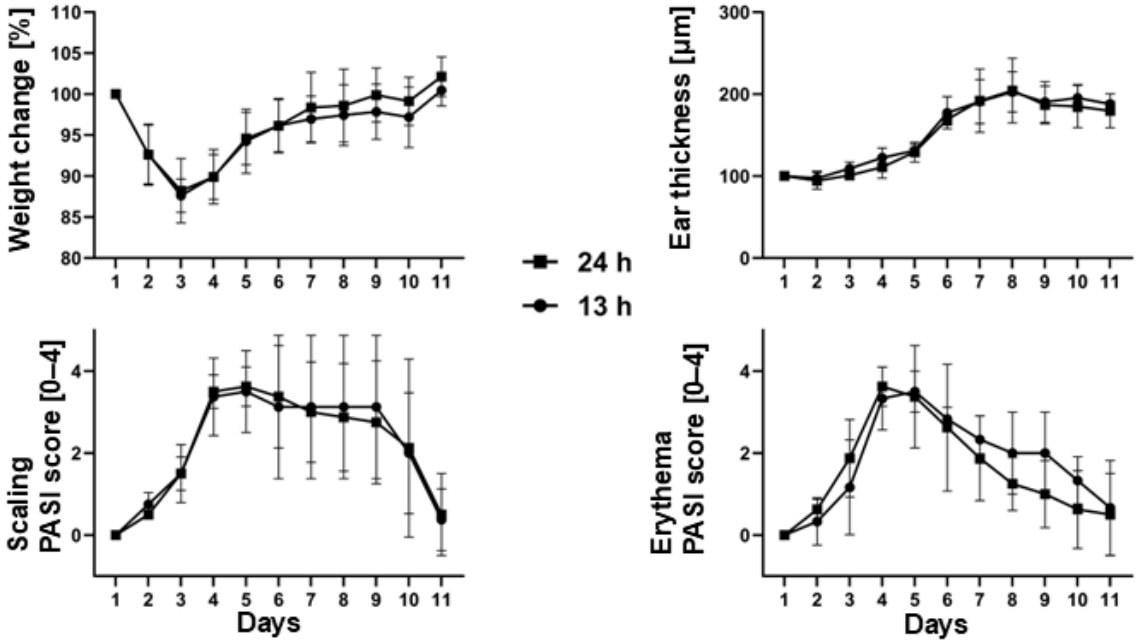

Figure 3.5: Disease scores of 10-day IMQ-treated PhAM mice

Disease scores during 10-day IMQ treatment and photoconversion on day 10 of PhAM mice. Shown are percentage changes in body weight, percentage increase in ear thickness and PASI-derived erythema and scaling scores for each time group, *n* = 3 per time point, 1 individual experiment out of 2 experiments. Data illustrate characteristic disease progression with peak severity around days 4-5.

Flow cytometric analysis of myeloid cells in the aorta of IMQ-treated and untreated PhAM mice is shown in Figure 3.6. No significant increase in $CD11b^+$ cell infiltration into the aorta was detected after 10 days of IMQ treatment (Figure 3.6B).

Flow cytometric analysis of Dendra2-green and Dendra2-red fluorescence was performed on single, viable $CD45.2^+$ cells of PhAM mice (Figure 3.7A). Photoconverted skin samples showed a pronounced Dendra2-red^+ population compared with non-illuminated controls, confirming effective *in vivo* photoconversion (Figure 3.7A, B). In the spleen, inguinal lymph nodes (iLN), and cervical LN (cLN) of illuminated PhAM mice, a small but distinct Dendra2-red^+ population was detectable, whereas these cells were largely absent in controls (Figure 3.7A, B). Signal quality for Dendra2-red^+ events in lymphoid organs improved compared to the previous experiment, although no clear differences were observed between the 13 and 24 h migration intervals.

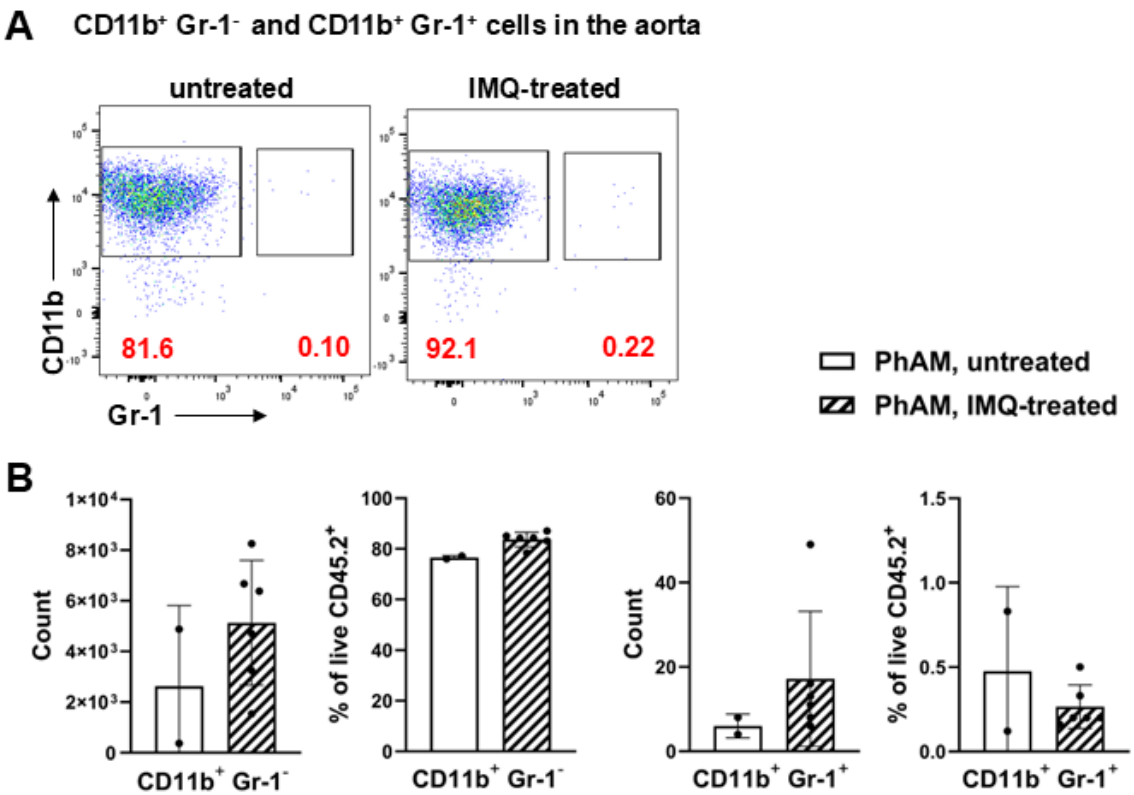

Figure 3.6: Detection of granulocytes in the aorta of 10-day IMQ-treated PhAM mice

(A) One representative flow cytometry plot of CD11b$^+$ Gr-1$^-$ or Gr-1$^+$ cells pre-gated on single, live, CD45.2$^+$, CD90.2$^-$, CD19$^-$ in aorta of 10-day IMQ-treated PhAM mice and untreated controls. Percentages of gates are shown. **(B)** Statistical analysis of absolute counts and frequencies (% of CD45.2$^+$) of CD11b$^+$ Gr-1$^-$ or Gr-1$^+$ myeloid cells in the aorta, *n* = 2-6 mice per group, 1 individual experiment out of 2 experiments, Mann-Whitney test.

In contrast, no Dendra2-red$^+$ cells were detected in the aorta (Figure 3.7A, B), consistent with the absence of increased myeloid cell infiltration in this tissue (Figure 3.6). Together, these findings indicate that IMQ-induced psoriasis in PhAM mice does not provide a suitable context for assessing vascular immune responses. Because the frequency of Dendra2-red$^+$ cells did not differ between the 13 and 24 h migration windows and both intervals fall within the reported lifespan of neutrophils. All subsequent experiments were performed using a standardized 24 h migration period to maximize the likelihood of detecting emigrating immune cells.

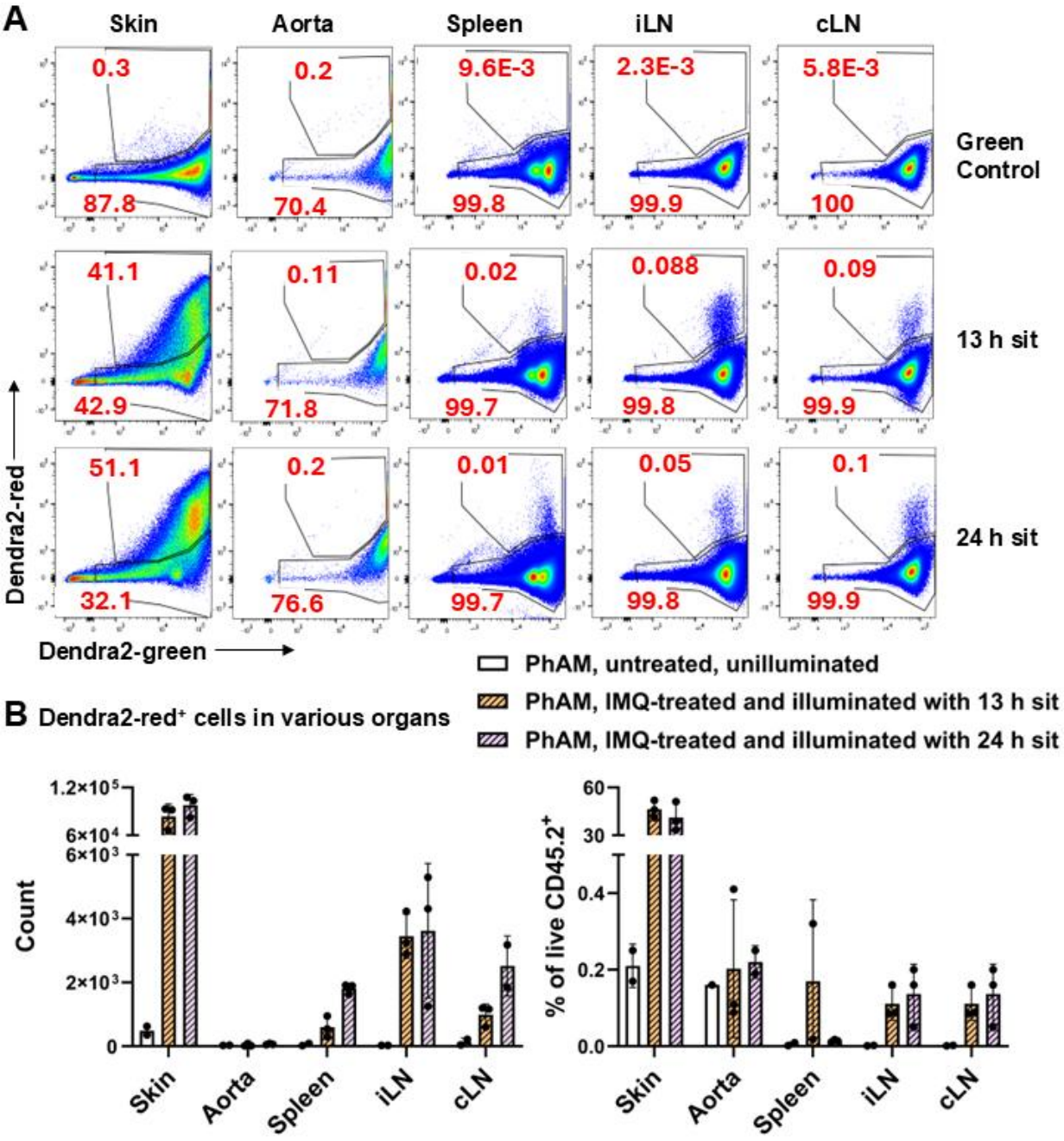

Figure 3.7: Detection of photoconverted immune cells 13 and 24 h after photoconversion in skin, aorta and lymphoid organs of 10-day IMQ-treated PhAM mice

(A) One representative flow cytometry plot of Dendra2-red$^+$ cells pre-gated on live, CD45.2$^+$ per group and organ. Dendra2-red$^+$ cells in skin, aorta, spleen, iLN and cervical LN (cLN) of 10-day IMQ-treated PhAM mice 13 or 24 h after photoconversion and an unilluminated, green fluorescing control. Percentages of gates are shown. Data was acquired with BD FACS Canto™ II flow cytometer. PhAM mice were illuminated on in- and outside of both ears and two back skin areas each for 5 min with 0.5 cm between skin and laser. This laser illumination protocol was kept for all following immune cell tracking experiments **(B)** Statistical analysis of absolute counts and frequencies (% of live CD45.2$^+$) of Dendra2-red$^+$ cells in the skin, spleen, aorta, iLN. and cLN, *n* = 2-3 mice per group, 1 individual experiment out of 2 experiments, Mann-Whitney test.

In a final IMQ-induced psoriasis experiment, PhAM mice treated with IMQ were compared to sham-treated controls. Both groups underwent photoconversion on the last day of the 6-day treatment and were sacrificed 24 h later for analysis (Figure 3.8).

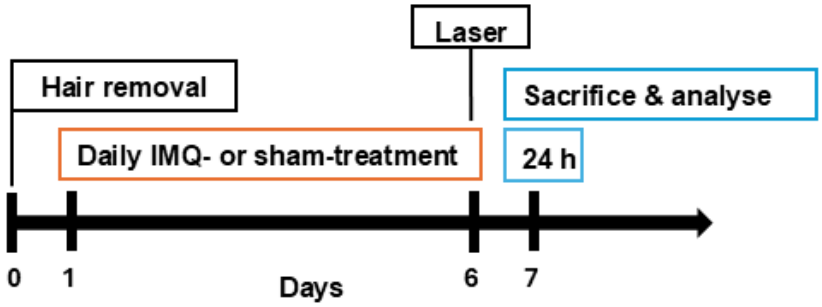

Figure 3.8: Photoconversion workflow for 24 h cell migration time of 6-day IMQ- or sham-treated PhAM mice

Experimental timeline for the 6-day IMQ- or sham-treatment of PhAM mice. On day 6, mice were photoconverted and sacrificed 24 h later.

Daily scoring confirmed robust disease induction with sham-treated controls showing no signs of inflammation (Figure 3.9).

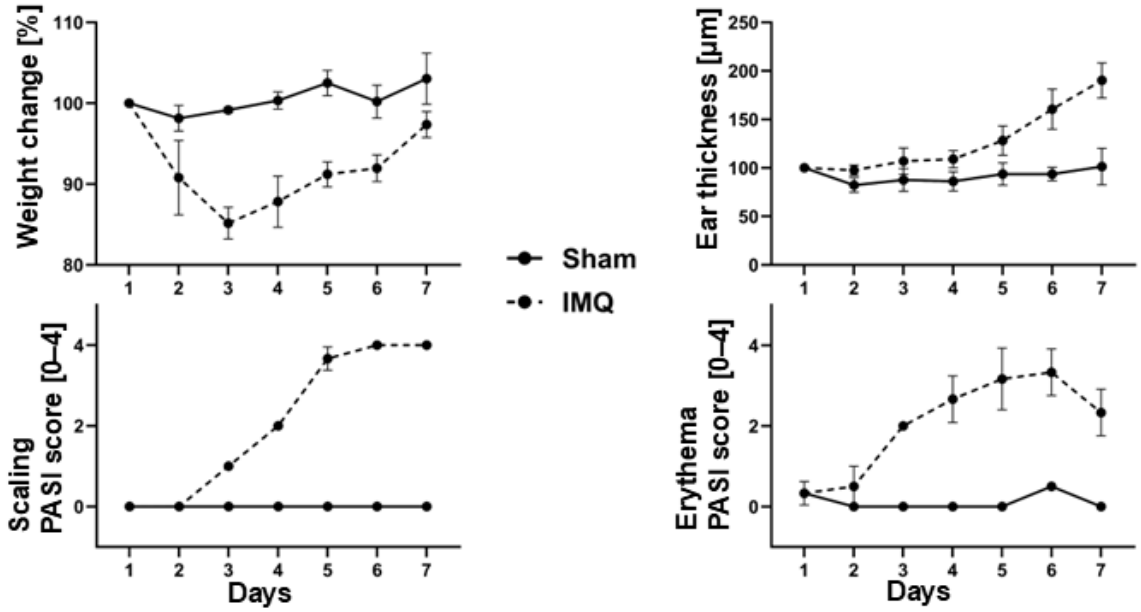

Figure 3.9: Disease scores of 6-day IMQ- or sham-treated PhAM mice

Disease scores during 6-day IMQ- or sham-treatment of PhAM mice. Disease scoring showing percentage of weight change, percentage of ear thickness and PASI scores for scaling and erythema in IMQ- or sham-treated PhAM mice, *n* = 3 per group.

Flow cytometric analysis is shown in Figure 3.10. Photoconverted cells were detected in the inguinal lymph nodes (iLN) of both IMQ-treated and sham-treated PhAM mice. Quantitative

analysis revealed no significant differences between the groups in the frequency or absolute number of Dendra2-red$^+$ cells in either the skin or the iLN (Figure 3.10B). The absence of an increased Dendra2-red$^+$ population in iLN of IMQ-treated PhAM mice indicates that acute IMQ-induced inflammation did not enhance the number of emigrating skin-derived immune cells within the tested 24 h migration window.

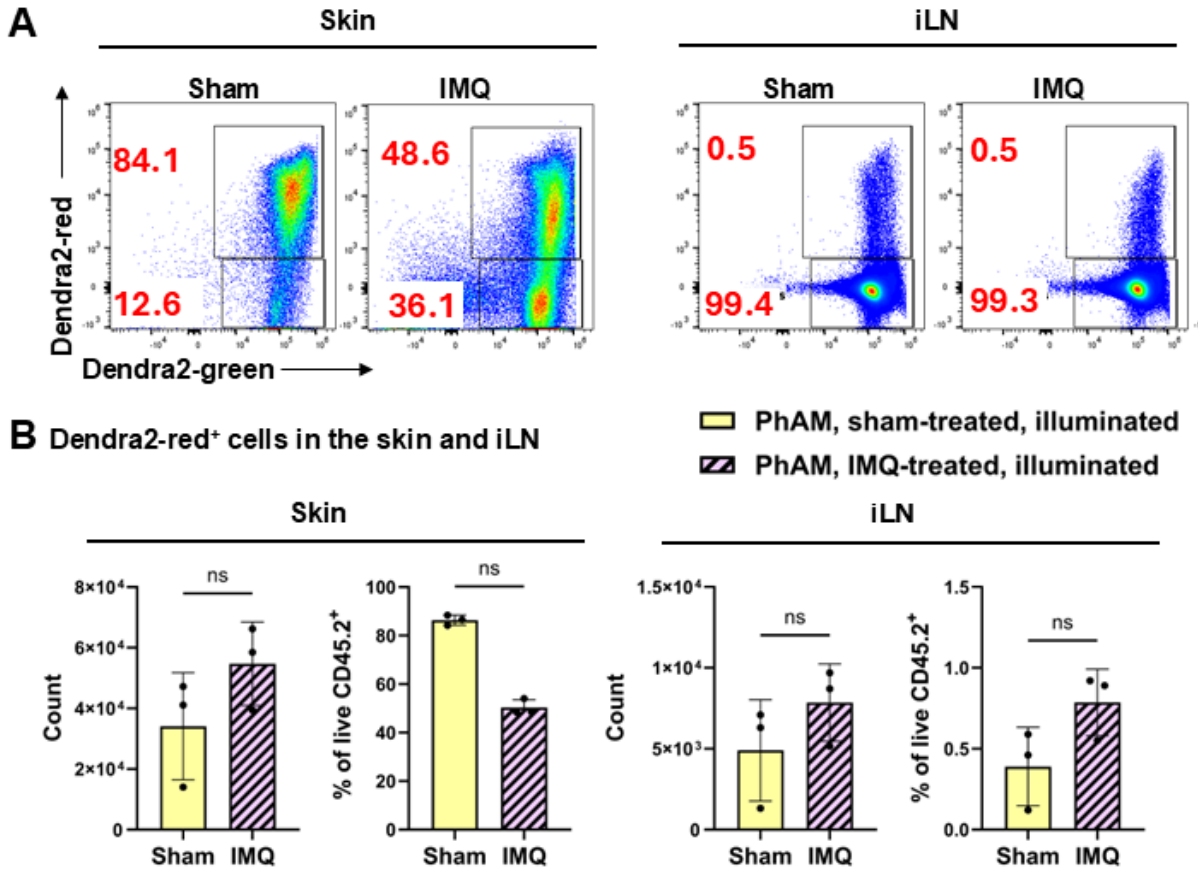

Figure 3.10: Cell tracking of skin-derived cells 24 h after photoconversion in PhAM mice with IMQ-induced psoriasis and sham controls

(A) One representative flow cytometry plot of Dendra2-red$^+$ cells pre-gated on single, live, CD45.2$^+$ per group and organ. Dendra2-red$^+$ cells in skin and iLN of 6-day IMQ- and sham-treated PhAM mice 24 h after photoconversion. Percentages of gates are shown. Data was acquired with Invitrogen Attune^{TM} NxT flow cytometer which was used for all following immune cell tracking experiments. **(B)** Statistical analysis of absolute counts and frequencies (% of live CD45.2$^+$) of Dendra2-red$^+$ cells in skin and iLN, *n* = 3 mice per group, one independent experiment, Mann-Whitney test.

In summary, the IMQ model enabled the successful establishment and refinement of the photoconversion workflow, including optimization of the illumination strategy, migration interval, and flow cytometry detection. Although this model facilitated reliable detection of skin-derived immune cells in lymphoid organs, it did not provide the inflammatory and vascular context required to assess immune cell involvement in the vasculature. With the technical parameters

fully optimized, we next implemented the approach in the PhAM-K14-IL-17A$^{ind/+}$ model, which exhibits robust skin inflammation together with a defined cardiovascular phenotype and thus enables investigation of our central biological question.

3.1.2 Skin-organ crosstalk in the PhAM-K14-IL-17A$^{ind/+}$ mice

Nine- to ten-week-old PhAM-K14-IL-17A$^{ind/+}$ mice were used, corresponding to a stage of fully developed psoriatic and cardiovascular pathology. Disease onset occurred at 4-5 weeks and progressed markedly after week 6 (Figure 3.11).

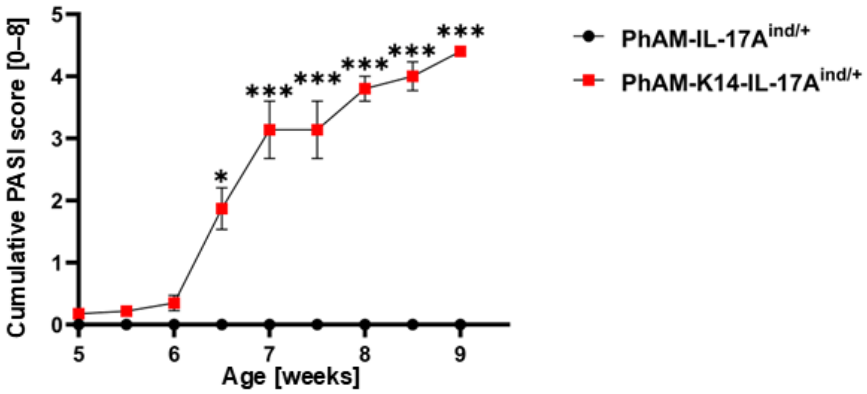

Figure 3.11: Disease scores of the PhAM-K14-IL-17A$^{ind/+}$ mice and PhAM-IL-17A$^{ind/+}$ controls

Cumulative PASI score of PhAM-K14-IL-17A$^{ind/+}$ and PhAM-IL-17A$^{ind/+}$ control mice. The sum of the erythema and scaling scores are multiplied by the affected area [%], *n* = 4 mice per group, 1 representative experiment, 2-way ANOVA with Bonferroni post-hoc test.

First, Gr-1^{+} cell infiltration was analysed in non-lymphoid and lymphoid organs (Figure 3.12 and Figure 3.13).

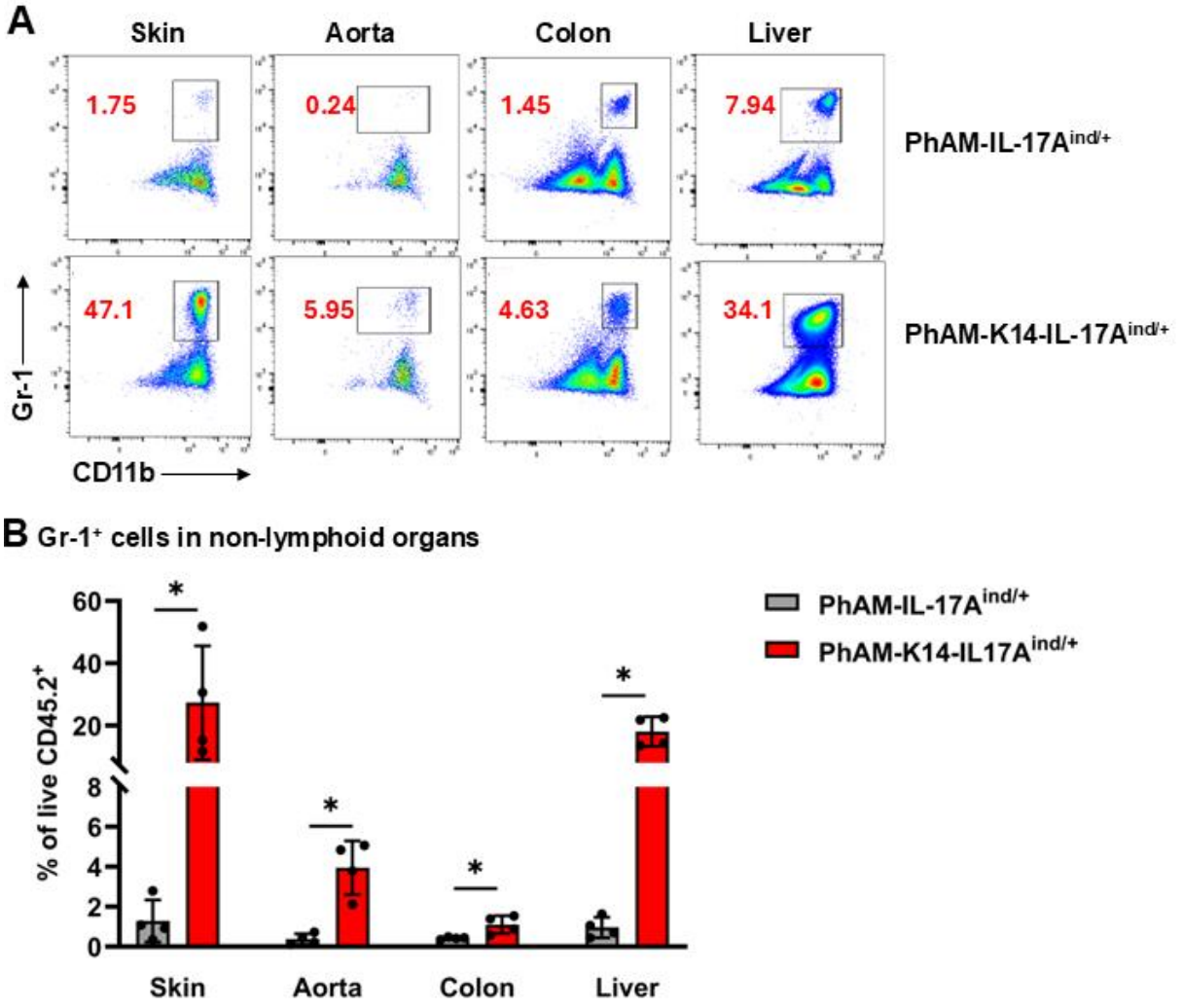

Figure 3.12: Granulocyte infiltration of the PhAM-K14-IL-17A$^{ind/+}$ mice and PhAM-IL-17A$^{ind/+}$ controls in non-lymphoid organs

(A) One representative flow cytometry plot of CD11b^{+} Gr-1^{+} cells pre-gated on single, live, CD45.2^{+}, CD90.2^{-}, CD19^{-} per organ and group. CD11b^{+} Gr-1^{+} cells in skin, aorta, colon and liver of PhAM-K14-IL-17A$^{ind/+}$ and PhAM-IL-17A$^{ind/+}$ controls. Percentages of gates are shown. **(B)** Statistical analysis of frequencies (% of live CD45.2^{+}) of CD11b^{+} Gr-1^{+} cells in the skin, aorta, colon and liver of PhAM-K14-IL-17A$^{ind/+}$ and PhAM-K14-IL-17A$^{ind/+}$ control mice. *n* = 4 mice per group, one individual experiment out of 1-9 experiments per organ, Mann-Whitney test.

Flow cytometric quantification revealed a significant increase in Gr-1^{+} cells in the skin, aorta, colon, liver, spleen, brachial lymph nodes (bLN) and mesenteric lymph nodes (mLN) indicating systemic inflammation in PhAM-K14-IL-17A$^{ind/+}$ mice (Figure 3.12 and Figure 3.13).

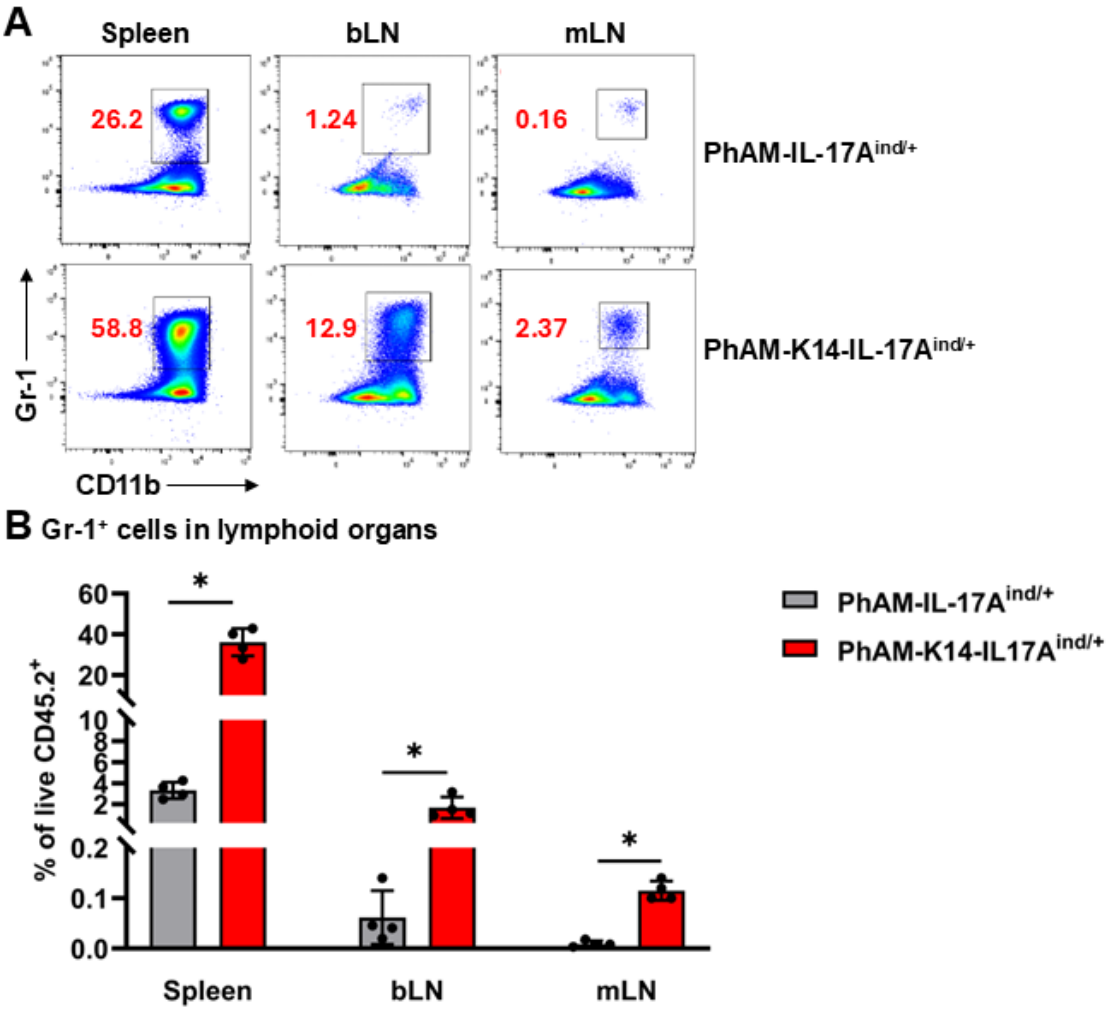

Figure 3.13: Granulocyte infiltration of the PhAM-K14-IL-17A$^{ind/+}$ mice and PhAM-IL-17A$^{ind/+}$ controls in lymphoid organs

(A) One representative flow cytometry plot of CD11b^{+} Gr-1^{+} cells pre-gated on single, live, CD45.2^{+}, CD90.2^{-}, CD19^{-} per organ and group. CD11b^{+} Gr-1^{+} cells in spleen, bLN and mLN of PhAM-K14-IL-17A$^{ind/+}$ and PhAM-IL-17A$^{ind/+}$ controls. Percentages of gates are shown. **(B)** Statistical analysis of frequencies (% of live CD45.2^{+}) of CD11b^{+} Gr-1^{+} cells^{+} in the spleen, bLN and mLN of PhAM-K14-IL-17A$^{ind/+}$ and PhAM-IL-17A$^{ind/+}$ control mice. *n* = 4 mice per group, 1 individual experiment out of 1-9 experiments per organ, Mann-Whitney test.

Skin-derived (Dendra2-red^{+}) immune cells reached lymphoid organs and liver but not aorta or colon (Figure 3.14A and Figure 3.15A). An unilluminated, green fluorescing PhAM-IL-17A$^{ind/+}$ mouse served as a background reference for Dendra2-green and Dendra2-red signal discrimination. Efficient photoconversion was confirmed in the skin of PhAM-K14-IL-17A$^{ind/+}$ mice, ensuring reliable tracking of migrated cells between organs (Figure 3.14A). Skin-derived immune cells were detected in the liver, spleen, mLN and bLN of both illuminated PhAM-K14-IL-17A$^{ind/+}$ mice and PhAM-IL-17A$^{ind/+}$ controls (Figure 3.14A, B and Figure 3.15A, B).

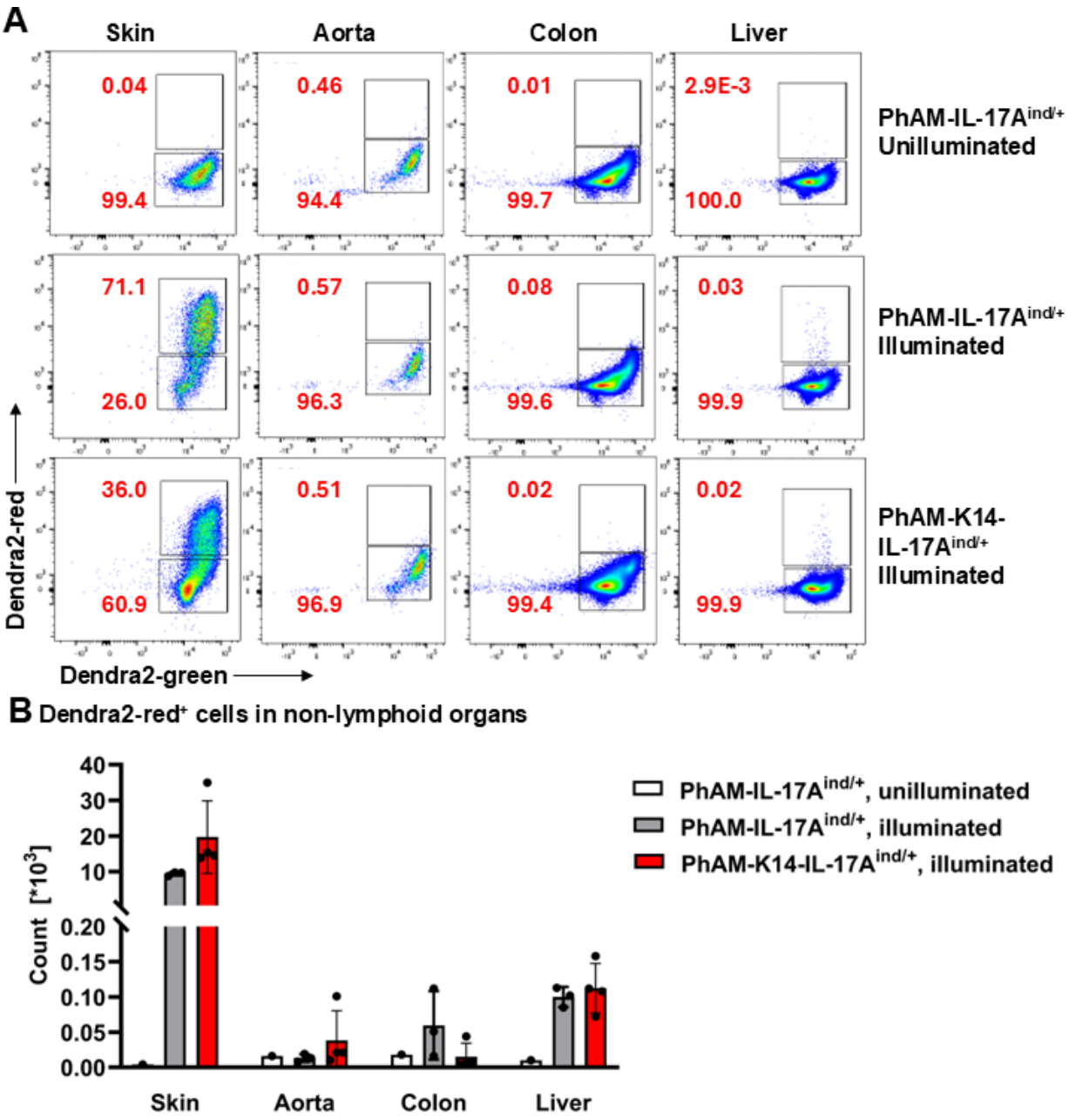

Figure 3.14: Detection of photoconverted immune cells in the skin and immune cell tracking in non-lymphoid organs 24 h after photoconversion of PhAM-K14-IL-17A$^{ind/+}$ mice and PhAM-IL-17A$^{ind/+}$ controls

(A) One representative flow cytometry plot of Dendra2-red$^+$ cells pre-gated on single, live, CD45.2$^+$ per organ and group. Dendra2-red$^+$ cells in skin, aorta, colon and liver of PhAM-K14-IL-17A$^{ind/+}$, PhAM-IL-17A$^{ind/+}$ controls and unilluminated, green fluorescing control. Percentages of gates are shown. **(B)** Statistical analysis of absolute counts of Dendra2-red$^+$ cells in skin, aorta, colon and liver. Counts of Dendra2-red$^+$ cells were calculated for the whole organ except for skin, *n* = 3-4 mice per group plus one unilluminated control, 1 representative experiment of 1-9 experiments per organ, Mann-Whitney test.

Despite robust granulocyte accumulation, no skin-derived immune cells were detected in the aorta or colon, suggesting that detectable trafficking of skin-derived immune cells to these organs does not occur within the examined 24 h migration window (Figure 3.14A, B).

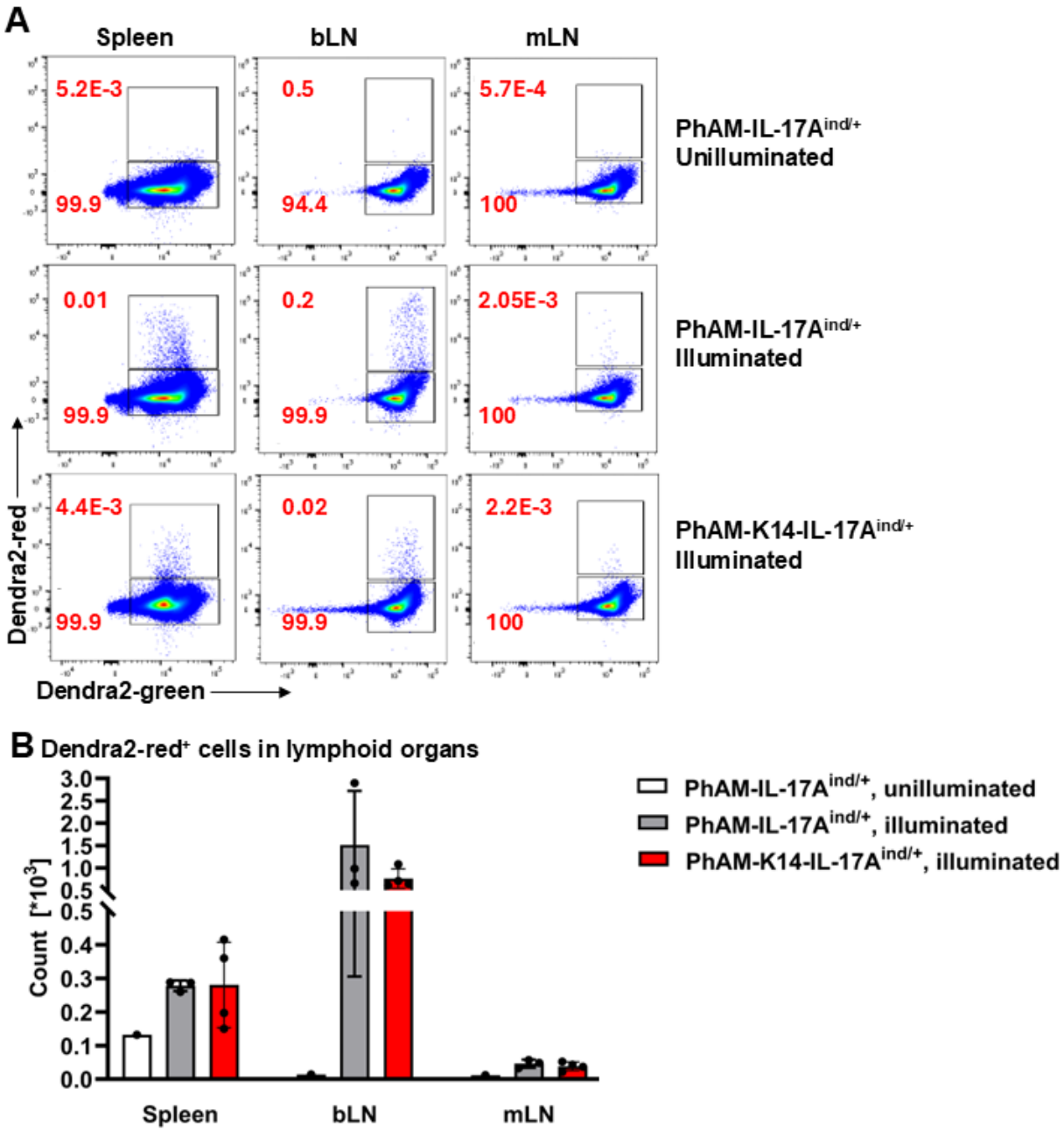

Figure 3.15: Immune cell tracking in lymphoid organs 24 h after photoconversion of PhAM-K14-IL-17A$^{ind/+}$ mice and PhAM-IL-17A$^{ind/+}$ controls

(A) One representative flow cytometry plot of Dendra2-red$^+$ cells pre-gated on live, CD45.2$^+$ per organ and group. Dendra2-red$^+$ cells in spleen, bLN and mLN of PhAM-K14-IL-17A$^{ind/+}$, PhAM-IL-17A$^{ind/+}$ controls and unilluminated green fluorescing control. Percentages of gates are shown. **(B)** Statistical analysis of absolute counts of Dendra2-red$^+$ cells in spleen, bLN and mLN. Counts of Dendra2-red$^+$ cells were calculated for the whole organ, *n* = 3-4 mice per group plus one unilluminated control, 1 representative experiment of 1-9 experiments per organ, Mann-Whitney test.

Further analysis of skin-derived immune cells was feasible only for the spleen and bLN, as Dendra2-red$^+$ cell counts in other organs were too low for reliable phenotypic resolution (Figure 3.16A, B).

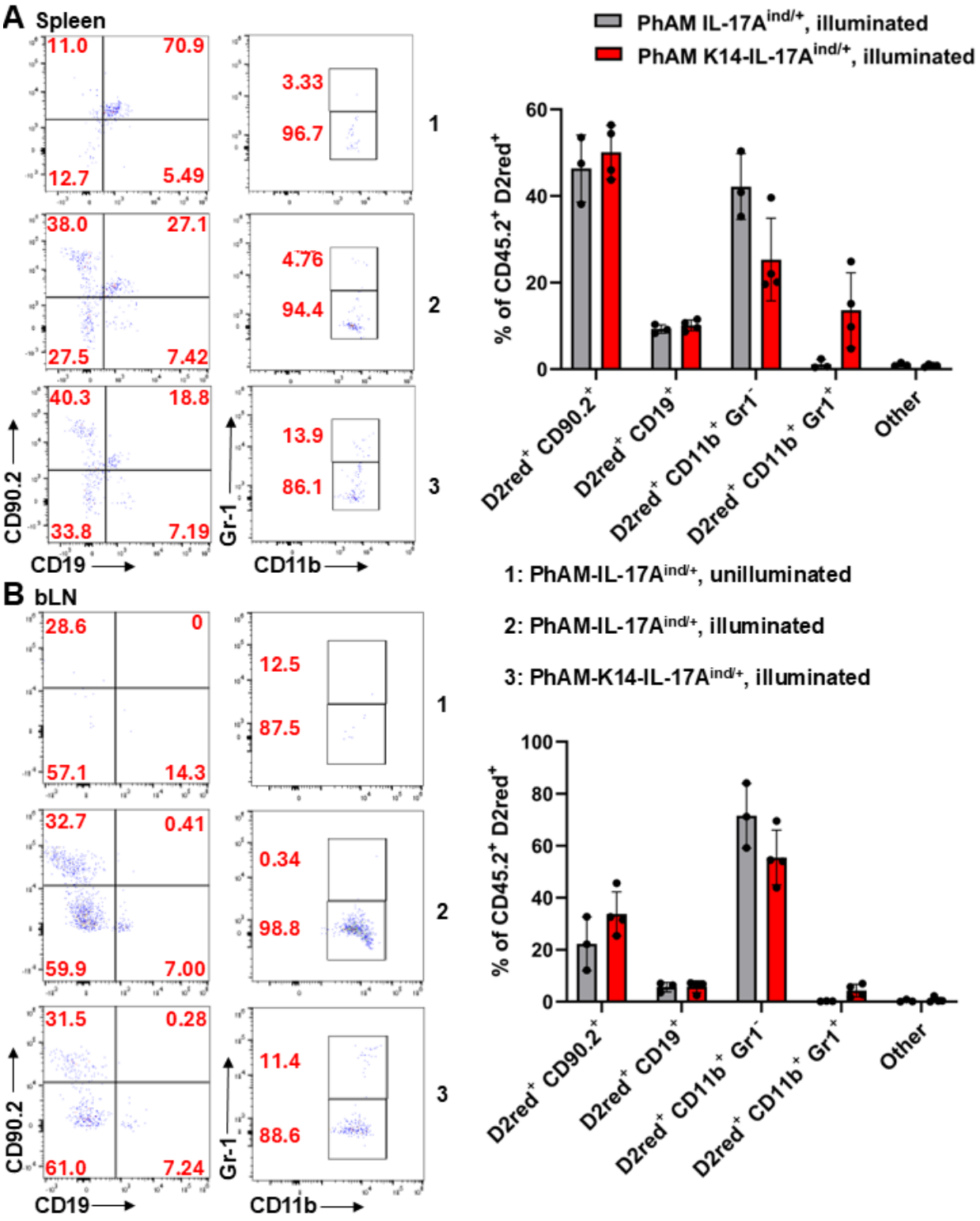

Figure 3.16: Analysis of the skin-derived immune cells in the spleen and bLN of PhAM-K14-IL-17A$^{ind/+}$ mice and PhAM-IL-17A$^{ind/+}$ controls

(A-B) One representative flow cytometry plot of skin-derived CD19$^-$ CD90.2$^+$, CD90.2$^-$ CD19$^+$, CD90.2$^-$ CD19$^-$ CD11b$^+$ Gr-1$^+$ or Gr-1$^-$ cells pre-gated on live, CD45.2$^+$, Dendra2-red$^+$ (D2red$^+$) cells per spleen **(A)** and **(B)** and group. Skin-derived immune cells of the spleen and bLN of PhAM-K14-IL-17A$^{ind/+}$, PhAM-IL-17A$^{ind/+}$ controls and unilluminated, green fluorescing control. Percentages of gates are shown. Statistical analysis of frequencies (% of CD45.2$^+$ D2red$^+$) of CD19$^-$ CD90.2$^+$, CD90.2$^-$ CD19$^+$, CD90.2$^-$ CD19$^-$ CD11b$^+$ Gr-1$^-$ or Gr-1$^+$ and other cells in the spleen and bLN in PhAM-K14-IL-17A$^{ind/+}$ and PhAM-IL-17A$^{ind/+}$ mice, *n* = 3-4 mice per group plus one unilluminated control, 1 individual experiment out of 3 experiments, Mann-Whitney test.

Among the migrating cells, CD90.2^{+} T cells and CD11b^{+} Gr-1^{-} cells constituted a large proportion of the migrating cells in both organs. In PhAM-K14-IL-17A$^{ind/+}$ mice, the relative frequency of CD11b^{+} Gr-1^{+} cells tended to be higher, whereas CD11b^{+} Gr-1^{-} cells tended to be reduced compared with PhAM-IL-17A$^{ind/+}$ controls. These differences did not reach statistical significance and should therefore be interpreted as descriptive trends rather than definitive alterations in myeloid trafficking. CD19^{+} B cell frequencies remained comparable between genotypes. In the spleen, an autofluorescent population was present in the Dendra2-red channel but was efficiently excluded during gating to avoid false-positive events.

Given that T cells represented a substantial fraction of the migrating population, a dedicated T cell panel was applied to further characterize skin-derived T cell subsets (Figure 3.17 and Figure 3.18).

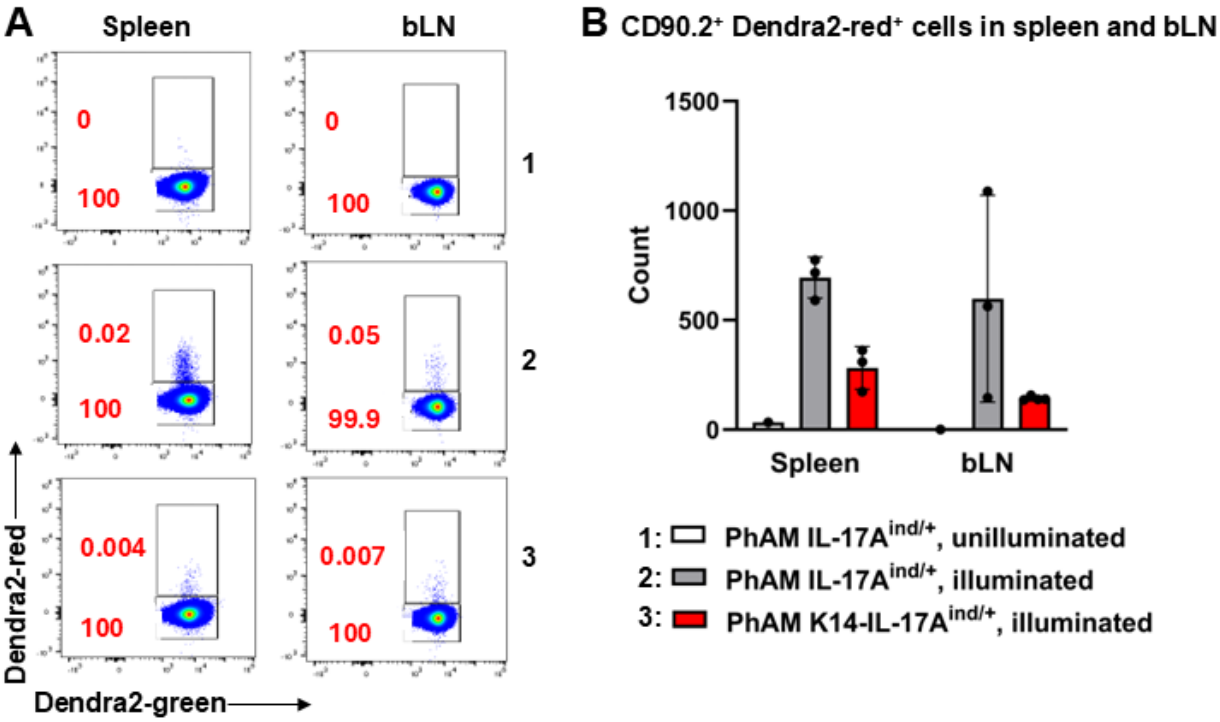

Figure 3.17: T cell tracking 24 h after photoconversion in spleen and bLN of PhAM-K14-IL-17A$^{ind/+}$ mice and PhAM-IL-17A$^{ind/+}$controls

(A) One representative flow cytometry plot of Dendra2-red^{+} cells pre-gated on live, CD90.2^{+} per organ and group. Dendra2-red^{+} cells of the spleen and bLN of PhAM-K14-IL-17A$^{ind/+}$, PhAM-IL-17A$^{ind/+}$ controls and unilluminated, green fluorescing control. Percentages of gates are shown. **(B)** Statistical analysis of absolute numbers of Dendra2-red^{+} in the spleen and bLN of PhAM-K14-IL-17A$^{ind/+}$, PhAM-IL-17A$^{ind/+}$ controls and unilluminated control. Counts were calculated for the whole organ, *n* = 3-4 mice per group plus one unilluminated control, 1 representative experiment, Mann-Whitney test.

Quantification of CD90.2^{+} Dendra2-red^{+} T cells in the spleen and bLN revealed no significant differences between genotypes, although a reduction was observed in PhAM-K14-IL-17A$^{ind/+}$

mice compared to PhAM-IL-17A$^{ind/+}$ controls (Figure 3.17B). Given the limited group size (n = 3-4 per genotype), this analysis was powered to detect only large differences.

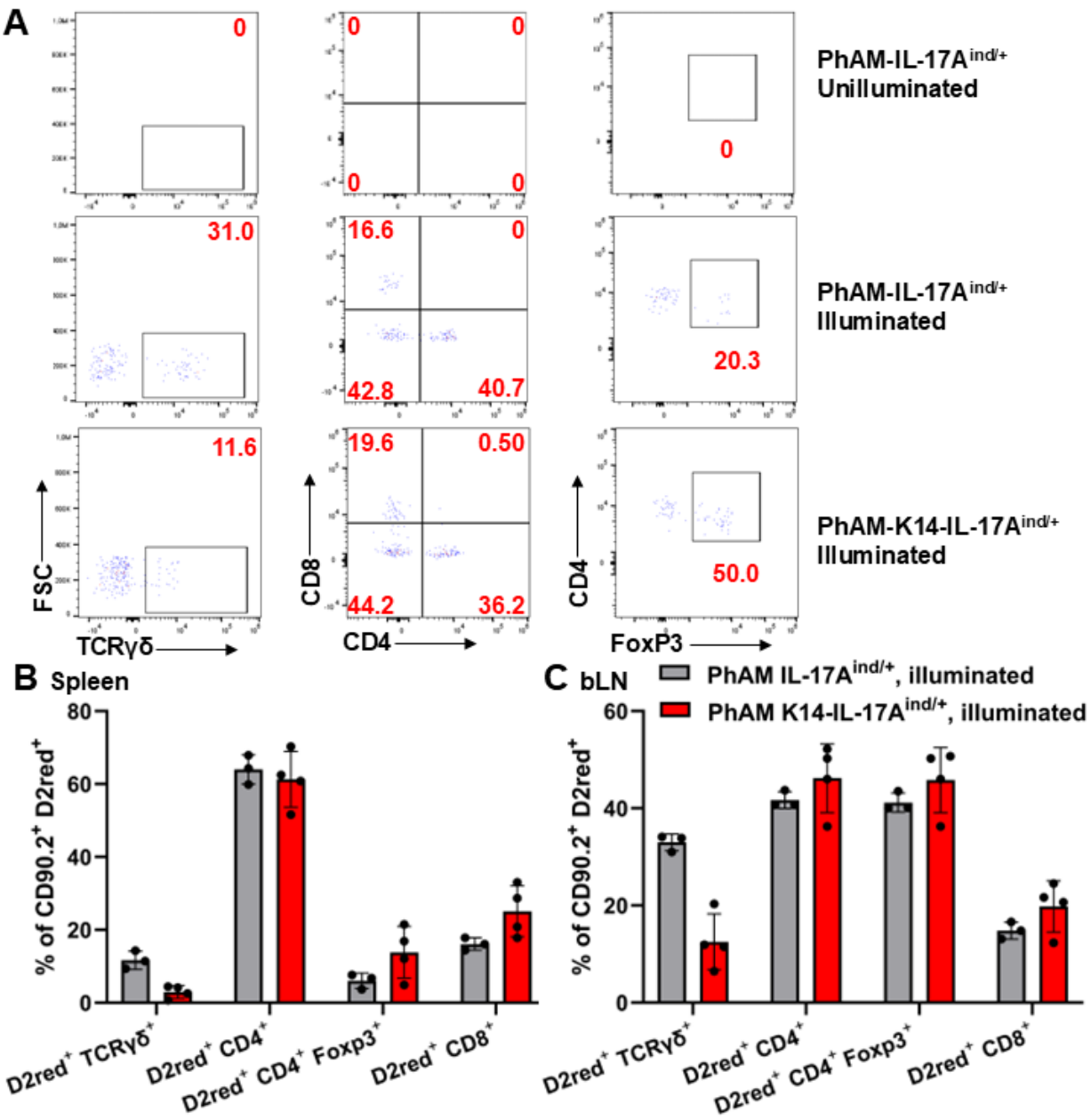

Figure 3.18: Analysis of skin-derived T cells in lymphoid organs of PhAM-K14-IL-17A$^{ind/+}$ mice and PhAM-IL-17A$^{ind/+}$ controls

(A) One representative flow cytometry plot of TCRγδ$^+$, CD8$^+$, CD4$^+$ or CD4$^+$ FoxP3$^+$ cells pre-gated on live, CD90.2$^+$, Dendra2-red$^+$ (D2red$^+$) of brachial lymph node (bLN) of PhAM-K14-IL-17A$^{ind/+}$ mice, PhAM-IL-17A$^{ind/+}$ controls and unilluminated, green fluorescing control. Percentages of the gates are shown. **(B, C)** Statistical analysis of frequencies (% of live CD90.2$^+$ D2-red$^+$) of TCRγδ$^+$, CD8$^+$, CD4$^+$ or CD4$^+$ FoxP3$^+$ cell population in the spleen **(B)** and bLN **(C)** of PhAM-K14-IL-17A$^{ind/+}$ mice and PhAM-IL-17A$^{ind/+}$ controls. Cells were gated further on TCRγδ$^+$, CD8$^+$, CD4$^+$ or CD4$^+$ FoxP3$^+$ cells, n = 3-4 mice per group, 1 individual experiment, Mann-Whitney test.

Subset analysis of skin-derived T cells showed lower frequencies of TCRγδ^{+} T cells in PhAM-K14-IL-17A$^{ind/+}$ mice compared to PhAM-IL-17A$^{ind/+}$ controls in both spleen and bLN (Figure 3.18A-C). In contrast, frequencies of conventional CD4^{+} T cells, CD4^{+} Foxp3^{+} Tregs and CD8^{+} Tc cells were comparable between genotypes. Given that K14-IL-17A$^{ind/+}$ mice are reported to exhibit a near complete loss of γδ T cells in the skin (Croxford, Karbach et al. 2014), the reduced representation of photoconverted γδ T cells in lymphoid organs likely reflects their diminished availability for photoconversion rather than altered migratory behavior.

3.1.3 Skin-liver crosstalk upon choline-deficient high-fat diet

To further investigate the Dendra2-red^{+} cell population detected in the liver of PhAM-K14-IL17A$^{ind/+}$ mice and PhAM-IL17A$^{ind/+}$ controls, animals were placed on a Cd-HFD beginning at 4 weeks of age (Figure 3.19). Cd-HFD induces steatosis and steatohepatitis within 6-8 weeks in C57BL/6 mice (Raubenheimer, Nyirenda and Walker 2006, Wolf, Adili et al. 2014). Given the rapid onset of systemic inflammation in PhAM-K14-IL-17A$^{ind/+}$ mice, a shorter feeding period (4 weeks) was expected to further amplify hepatic inflammation and potentially increase skin-derived immune cell recruitment to the liver.

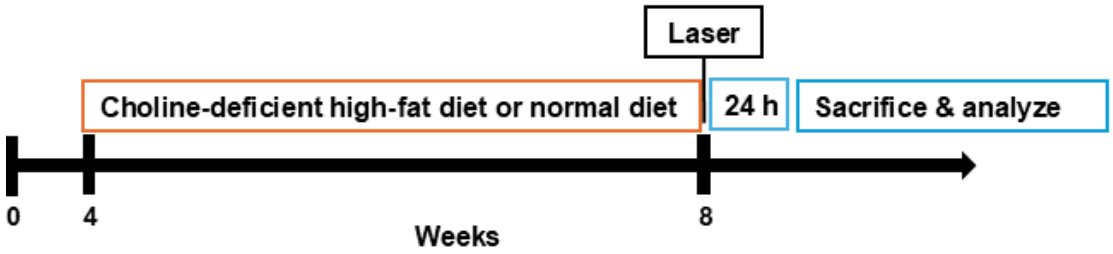

Figure 3.19: Photoconversion workflow for 24 h cell migration time of PhAM-K14-IL-17A$^{ind/+}$ mice and PhAM-IL-17A$^{ind/+}$ controls on choline-deficient high-fat diet or normal diet

Experimental timeline for PhAM-K14-IL-17A$^{ind/+}$ mice and PhAM-IL-17A$^{ind/+}$ controls on Cd-HFD or ND, followed by laser illumination on the last day of nutrition and analysis 24 h after photoconversion.

Disease severity and body weight were monitored throughout the experiment (Figure 3.20), and no differences were observed between Cd-HFD and normal diet (ND) within each genotype.

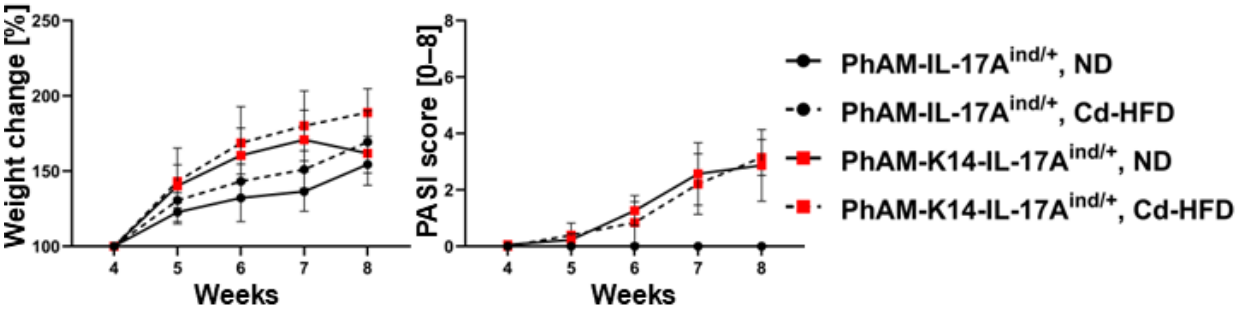

Figure 3.20: Disease scores of PhAM-K14-IL-17A$^{ind/+}$ mice and PhAM-IL-17A$^{ind/+}$ controls on choline-deficient high-fat diet or normal diet

Body weight development and cumulative PASI score of PhAM-K14-IL-17A$^{ind/+}$ mice and PhAM-IL-17A$^{ind/+}$ controls on Cd-HFD or ND. The sum of the erythema and scaling scores are multiplied by the affected area [%], *n* = 3-4 mice per group, 1 representative experiment out of 5 experiments, 2-way ANOVA with Bonferroni post-hoc test for comparing dietary effects within each genotype.

The impact of Cd-HFD on neutrophil infiltration across multiple organs and on systemic neutrophil levels was subsequently assessed (Figure 3.21 and Figure 3.22).

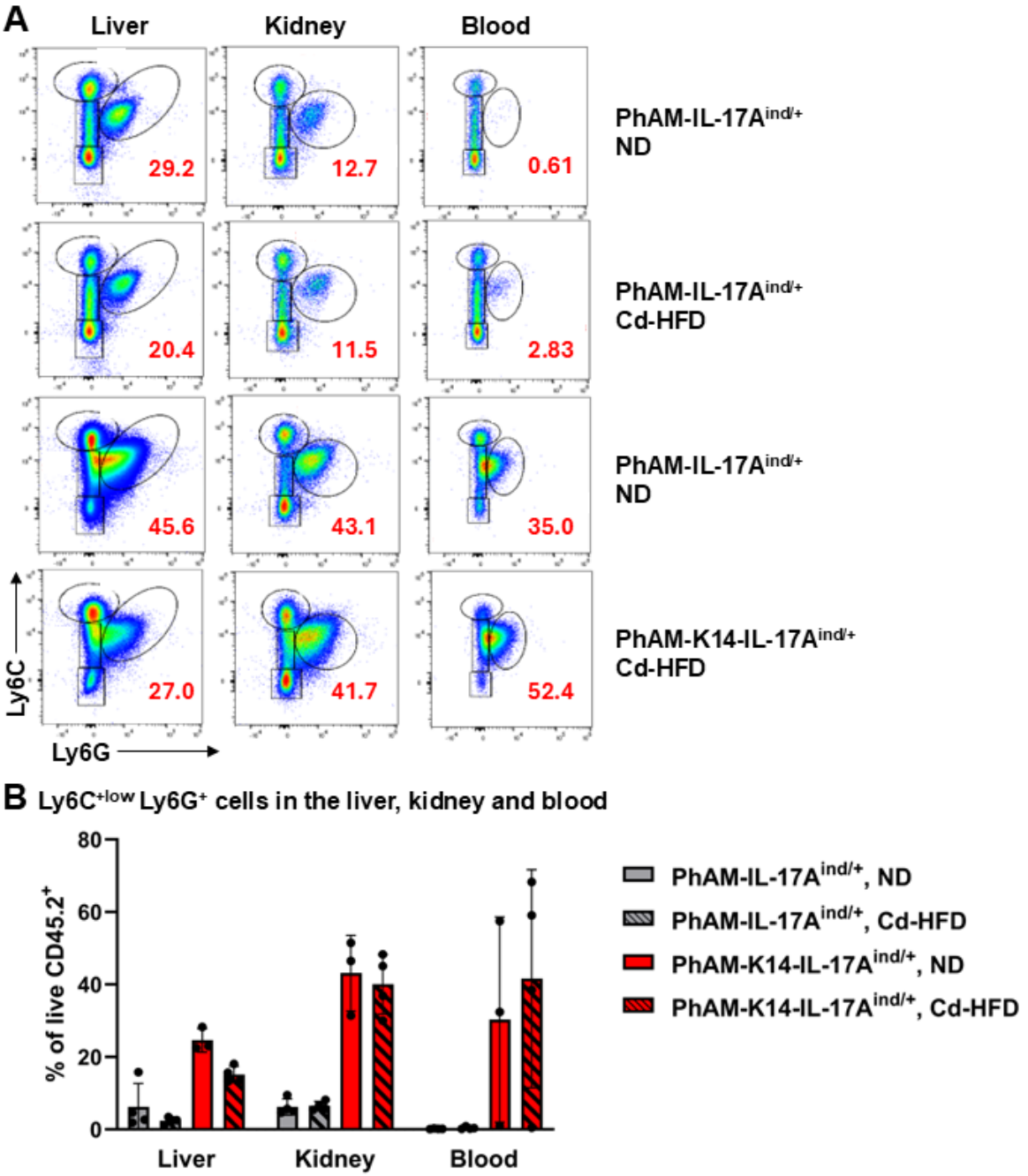

Figure 3.21: Neutrophils in the liver, kidney and peripheral blood of PhAM-K14-IL-17A$^{ind/+}$ mice and PhAM-IL-17A$^{ind/+}$ controls on choline-deficient high-fat diet or normal diet

(A) Representative flow cytometry plots of Ly6C^{+low} Ly6G^{+} cells pre-gated on live, CD45.2^{+}, CD90.2^{-}, CD11b^{+} per organ and group. Ly6C^{+low} Ly6G^{+} cells of liver, kidney and blood of PhAM-K14-IL-17A$^{ind/+}$ mice and PhAM-IL-17A$^{ind/+}$ controls on Cd-HFD or ND. Percentages of gates are shown. **(B)** Statistical analysis of frequencies (% of live CD45.2^{+}) of Ly6C^{+low} Ly6G^{+} cells in liver, kidney and blood of PhAM-K14-IL-17A$^{ind/+}$ mice and PhAM-IL-17A$^{ind/+}$ controls on Cd-HFD or ND, *n* = 3-4 mice per group, data represents one individual experiment out of 2-5 experiments per organ. Statistical comparison of ND versus Cd-HFD within each genotype was performed using the Mann-Whitney test.

Across the liver, kidney, blood, spleen, bLN and BM, frequencies of Ly6C^{+low} Ly6G^{+} neutrophils were comparable between Cd-HFD and ND groups within each genotype (PhAM-K14-IL-17A$^{ind/+}$ and littermate controls) (Figure 3.21 and Figure 3.22).

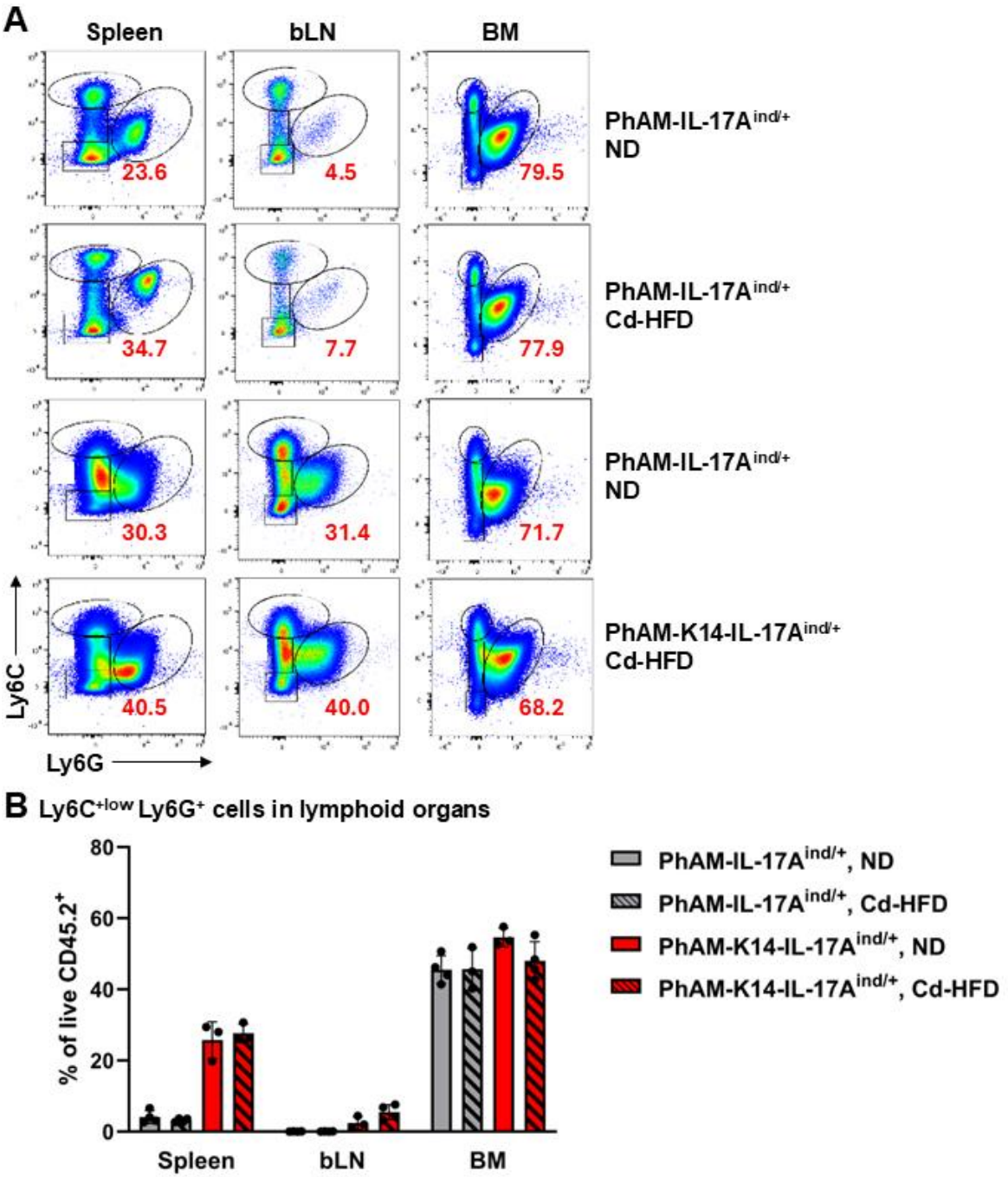

Figure 3.22: Neutrophil infiltration in lymphoid organs of PhAM-K14-IL-17A$^{ind/+}$ mice and PhAM-IL-17A$^{ind/+}$ controls on choline-deficient high-fat diet or normal diet

(A) Representative flow cytometry plots of Ly6C^{+low} Ly6G^{+} cells pre-gated on live, CD45.2^{+}, CD90.2^{-}, CD11b^{+} per organ and group. Ly6C^{+low} Ly6G^{+} cells of spleen, bLN and BM of PhAM-K14-IL-17A$^{ind/+}$ mice and PhAM-IL-17A$^{ind/+}$ controls on Cd-HFD or ND. Percentages of gates are shown. **(B)** Statistical analysis of frequencies (% of live CD45.2^{+}) of Ly6C^{+low} Ly6G^{+} cells in spleen, bLN and BM of PhAM-K14-IL-17A$^{ind/+}$ mice and PhAM-IL-17A$^{ind/+}$ controls on Cd-HFD or ND, *n* = 3-4 mice per group, data represents one individual experiment out of 2-5 experiments per organ. Statistical comparison of ND versus Cd-HFD within each genotype was performed using the Mann-Whitney test.

Skin-derived immune cells were detected in the liver, spleen and bLN of both genotypes and under both dietary conditions at similar levels indicating that Cd-HFD did not enhance liver-directed migration of skin-derived immune cells (Figure 3.23 and Figure 3.24).

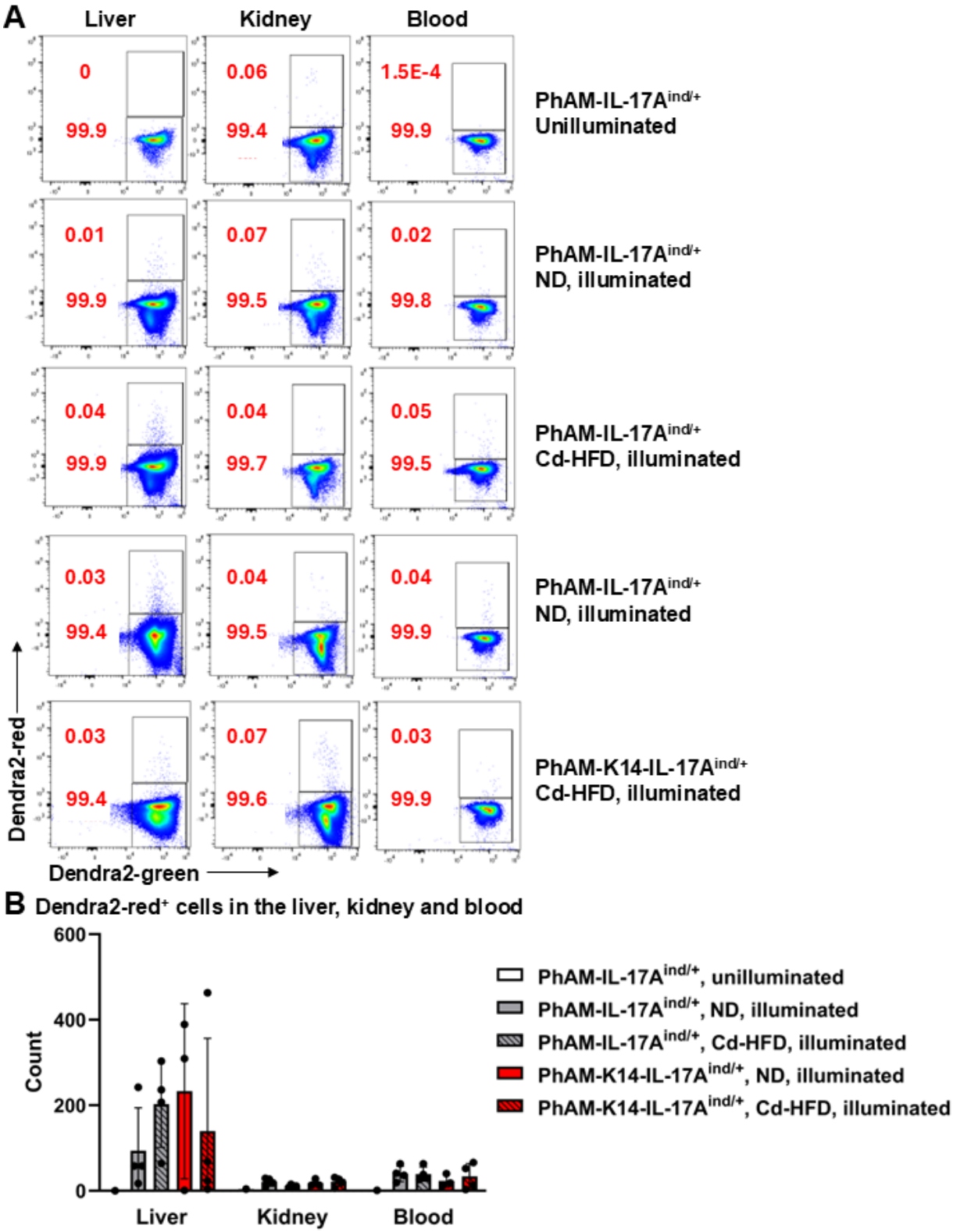

Figure 3.23: Immune cell tracking 24 h after photoconversion in liver, kidney and blood of PhAM-K14-IL-17A$^{ind/+}$ mice and PhAM-K14-IL-17A$^{ind/+}$ controls on choline-deficient high-fat diet or normal diet

(A) Representative flow cytometry plots of Dendra2-red$^+$ cells pre-gated on single, live, CD45.2$^+$ per organ and group. Dendra2-red$^+$ cells of liver, kidney and blood of PhAM-K14-IL-17A$^{ind/+}$ and PhAM-IL-17A$^{ind/+}$ control mice on Cd-HFD or ND plus unilluminated control. Percentages of gates are shown. **(B)** Statistical analysis of absolute counts of Dendra2-red$^+$ cells in liver, kidney and blood of PhAM-K14-IL-17A$^{ind/+}$ mice and PhAM-IL-17A$^{ind/+}$ controls on Cd-HFD or ND, *n* = 2-4 mice per group plus one unilluminated control, data represents one individual experiment out of 2-5 experiments per organ. Statistical comparisons of ND versus Cd-HFD within each genotype, as well as between genotypes within each diet, were performed using the Mann-Whitney test.

In contrast, almost no Dendra2-red+ immune cells were detected in the kidney and BM, likely reflecting minimal migration, and only negligible numbers were found in the blood, suggesting dilution effects (Figure 3.23A, B). The kidney thus served as a well-perfused negative reference organ, supporting that hepatic Dendra2-red+ signals represent true dermal-hepatic crosstalk rather than residual blood contamination. The near absence of Dendra2-red+ immune cells in the blood further corroborates that the liver signal is not attributable to vascular carryover (Figure 3.23A, B).

Given the limited number of tracked skin-derived immune cells in the liver, we next focused on characterizing the broader hepatic immune landscape to determine whether the K14-IL-17A$^{ind/+}$ genotype alters myeloid composition. This prompted a more comprehensive profiling of hepatic myeloid subsets.

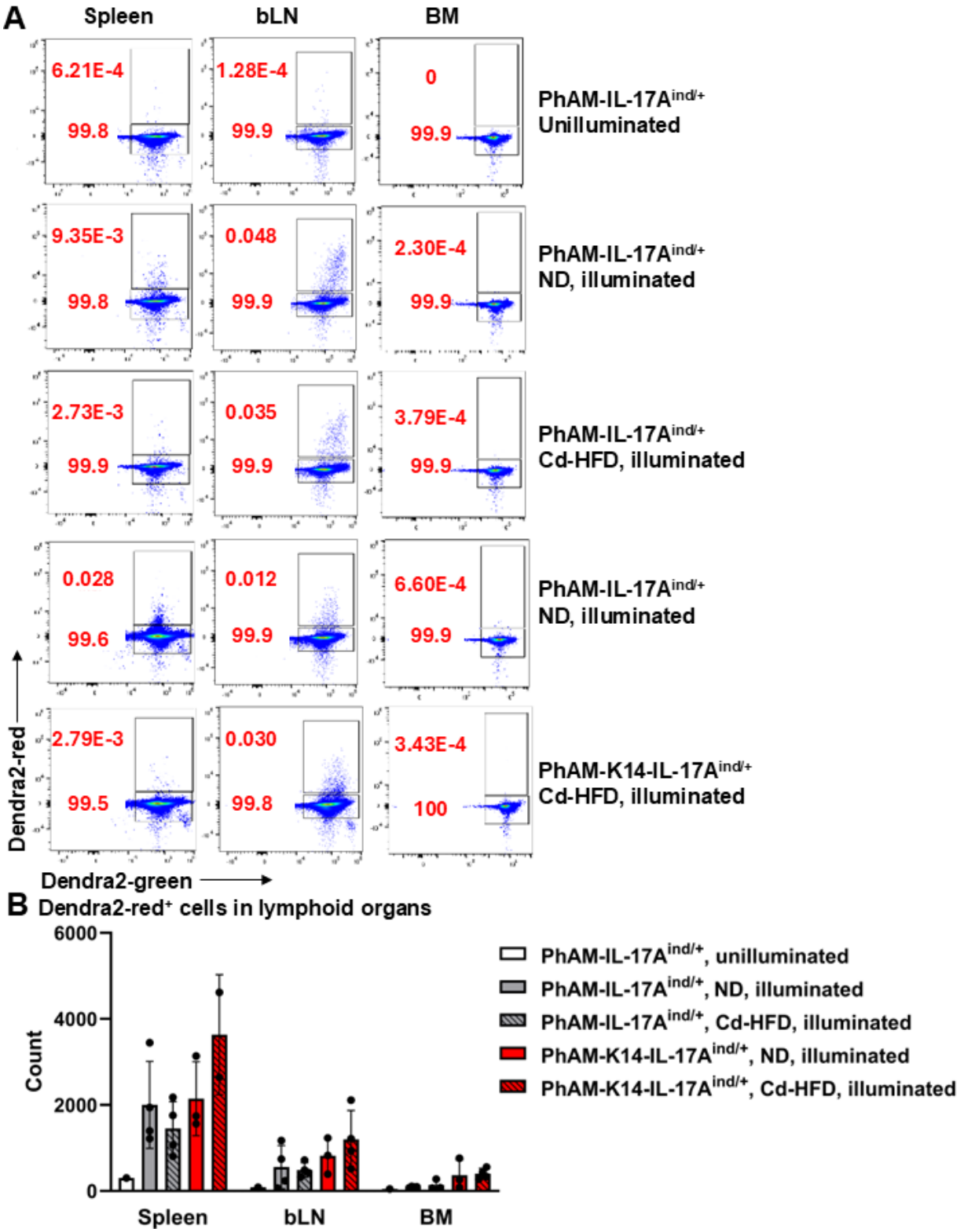

Figure 3.24: Immune cell tracking 24 h after photoconversion in lymphoid organs of PhAM-K14-IL-17A$^{ind/+}$ mice and PhAM-IL-17A$^{ind/+}$ controls on choline-deficient high-fat diet or normal diet

(A) Representative flow cytometry plots of Dendra2-red^{+} cells pre-gated on single, live, CD45.2^{+} per organ and group. Dendra2-red^{+} cells of spleen, bLN and BM of PhAM-K14-IL-17A$^{ind/+}$ mice and PhAM-IL-17A$^{ind/+}$ controls on Cd-HFD or ND plus unilluminated control. Percentages of gates are shown. **(B)** Statistical analysis of absolute counts of Dendra2-red^{+} cells in spleen, bLN and BM of PhAM-K14-IL-17A$^{ind/+}$ mice and PhAM-IL-17A$^{ind/+}$ controls on Cd-HFD or ND, counts of the whole organ were calculated except for BM, *n* = 2-4 mice per group plus one unilluminated control, data represents one individual experiment out of 2-5 experiments per organ. Statistical comparisons of ND versus Cd-HFD within each genotype, as well as between genotypes within each diet, were performed using the Mann-Whitney test.

3.2 Myeloid cell analysis of hepatic inflammation in K14-IL-7A$^{ind/+}$ mice

Our previous findings demonstrated a pronounced accumulation of myeloid cells in the livers of PhAM-K14-IL-17A$^{ind/+}$ mice compared with PhAM-IL-17A$^{ind/+}$ controls. To further characterize these infiltrating populations, immune cells were isolated from the livers of 8- to 10-week-old K14-IL-17A$^{ind/+}$ psoriatic mice and analysed using high-parameter spectral flow cytometry. After exclusion of lymphoid and NK lineages, the analysis was performed on CD45^{+} CD3^{-} CD19^{-} NK1.1^{-} cells, which were used for UMAP projection and subsequent cluster identification (Figure 3.25).

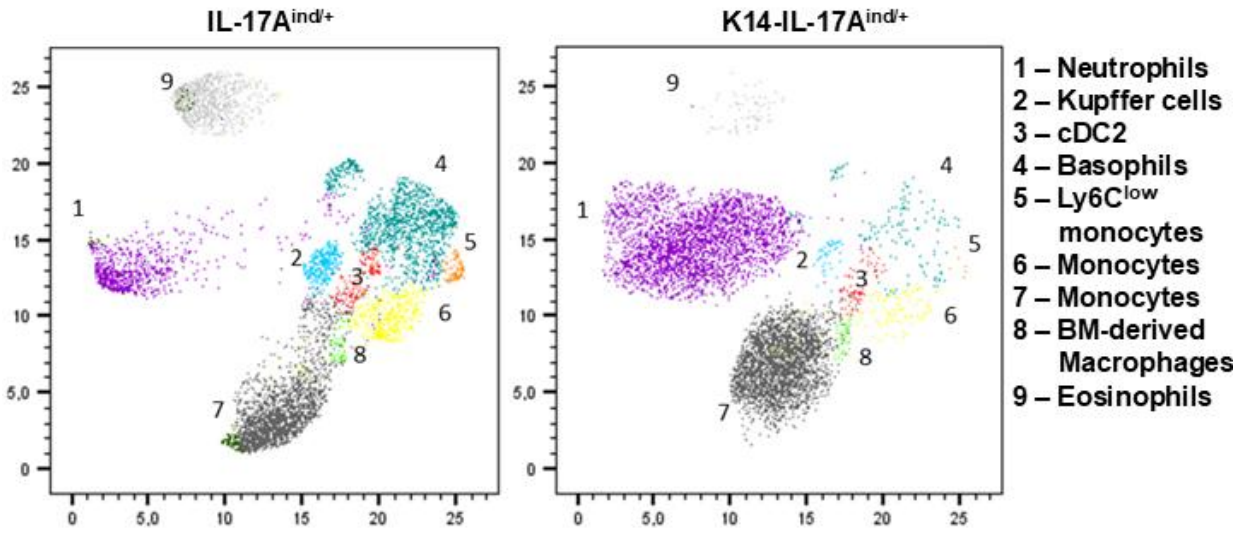

Figure 3.25: In-depth analysis of hepatic myeloid cells of K14-IL-17A$^{ind/+}$ mice and IL-17A$^{ind/+}$ controls

UMAP plots of hepatic myeloid cells isolated from K14-IL-17A$^{ind/+}$ mice and IL-17A$^{ind/+}$ controls, *n* = 4-6 mice per group, data represents one individual experiment out of 2 experiments.

The resulting UMAP landscape (Figure 3.26) revealed distinct myeloid populations and the quantitative comparison of individual clusters showed that neutrophils represented the dominant infiltrating subset in K14-IL-17A$^{ind/+}$ livers (Figure 3.26). In addition, monocytes, BM-derived macrophages and cDC2s were present at significantly increased absolute numbers in psoriatic mice compared with controls, indicating a broad remodelling of the hepatic myeloid compartment in response to chronic IL-17A-driven skin inflammation (Figure 3.26A, C).

Notably, this inflammatory profile was observed despite the very low abundance of skin-derived immune cells in the liver, suggesting that the hepatic phenotype is driven by systemic IL-17A-mediated inflammation rather than by direct trafficking of immune cells from the skin.

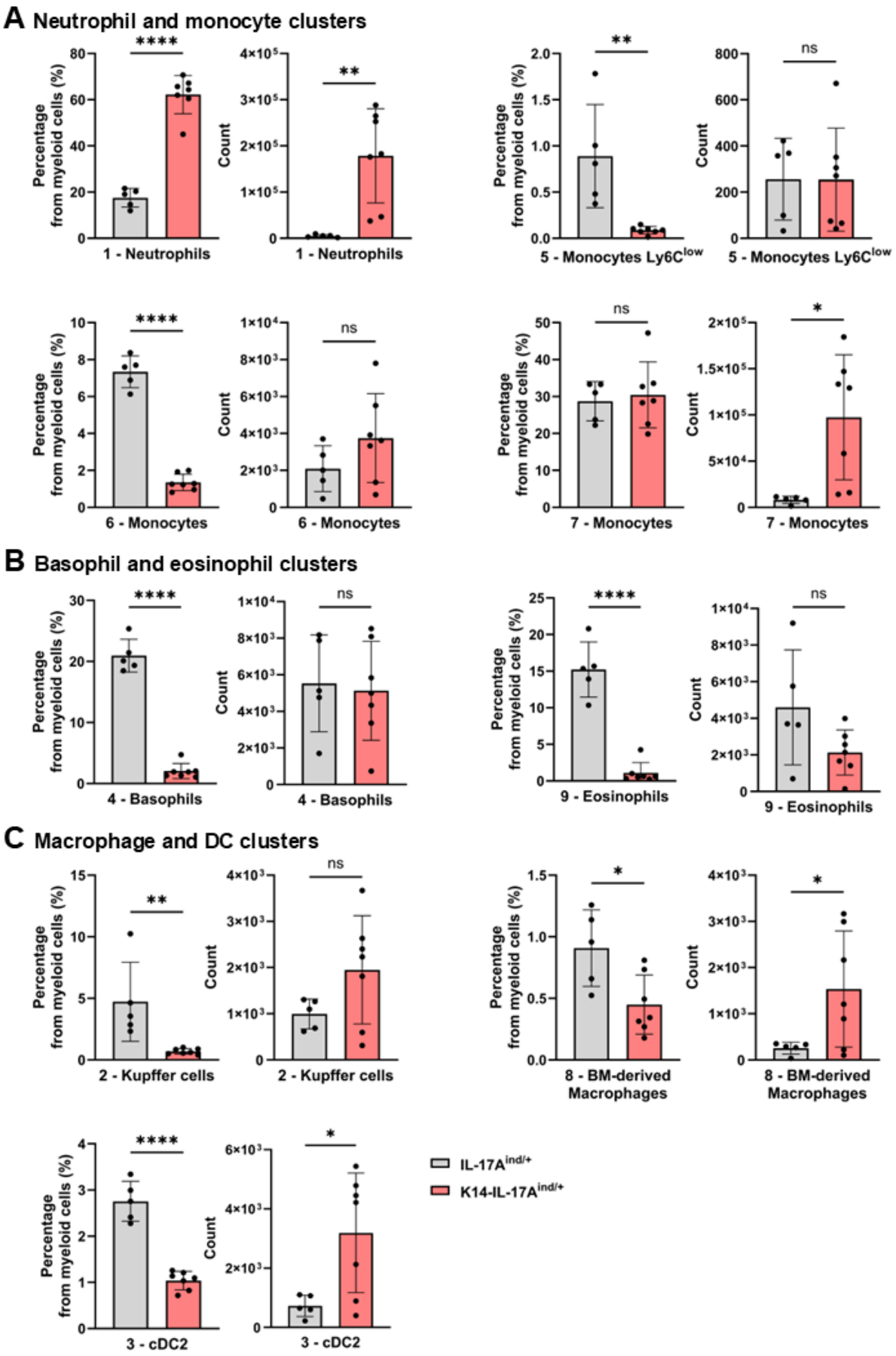

Figure 3.26: Statistical analysis of hepatic myeloid cell clusters of K14-IL-17A$^{ind/+}$ mice and IL-17A$^{ind/+}$ controls

Statistical analysis of the clusters defined by Cluster Explorer 10 of hepatic myeloid cells of K14-IL-17A$^{ind/+}$ mice and IL-17A$^{ind/+}$ controls. **(A)** shows neutrophil and monocytes clusters, **(B)** basophil and eosinophil clusters and **(C)** macrophage and conventional DC (cDC) clusters, counts of the whole organ were used, *n* = 4-6 mice per group, data represents one individual experiment out of 2 experiments, unpaired Student's *t*-test.

3.3 NIK deficiency in keratinocytes in IMQ-induced psoriasis

The role of the non-canonical NF-κB pathway in skin inflammation remains largely unexplored. Previous work demonstrated that systemic inhibition of NIK, a key regulator of this pathway, alleviates IMQ-induced psoriasis-like disease in mice (Zhu, Ma et al. 2020). However, oral administration does not reveal the specific cell types in which NIK exerts its effects. KCs are not only hyperproliferative in psoriasis but also serve as key regulators of local inflammation by producing cytokines and chemokines that shape immune cell activation. Given their central role in disease pathogenesis, we asked whether NIK activity within KCs contributes to IMQ-induced psoriasis. To address this, we generated KC-specific NIK knockout mice ($NIK^{fl/fl}$-K14Cre).

To assess the role of KC-specific NIK in psoriasis development, $NIK^{fl/fl}$-K14Cre mice and $NIK^{fl/fl}$ controls were treated with IMQ for six consecutive days. Both genotypes developed characteristic psoriasis-like features, including erythema, scaling and skin thickening (Figure 3.27). Disease severity was evaluated separately for males and females, as females displayed higher susceptibility. Male $NIK^{fl/fl}$-K14Cre mice initially exhibited slightly reduced weight loss relative to controls, but this difference disappeared by day 4. Cumulative PASI scores and skin thickening measurements were similar between genotypes in both sexes. Collectively, these clinical metrics indicate that KC-specific NIK deletion does not influence the onset or severity of IMQ-induced psoriasis.

To complement these clinical observations, we next analysed cellular infiltrates in the skin to determine whether NIK deficiency in KCs influences the composition or activation of immune cells during IMQ-induced inflammation.

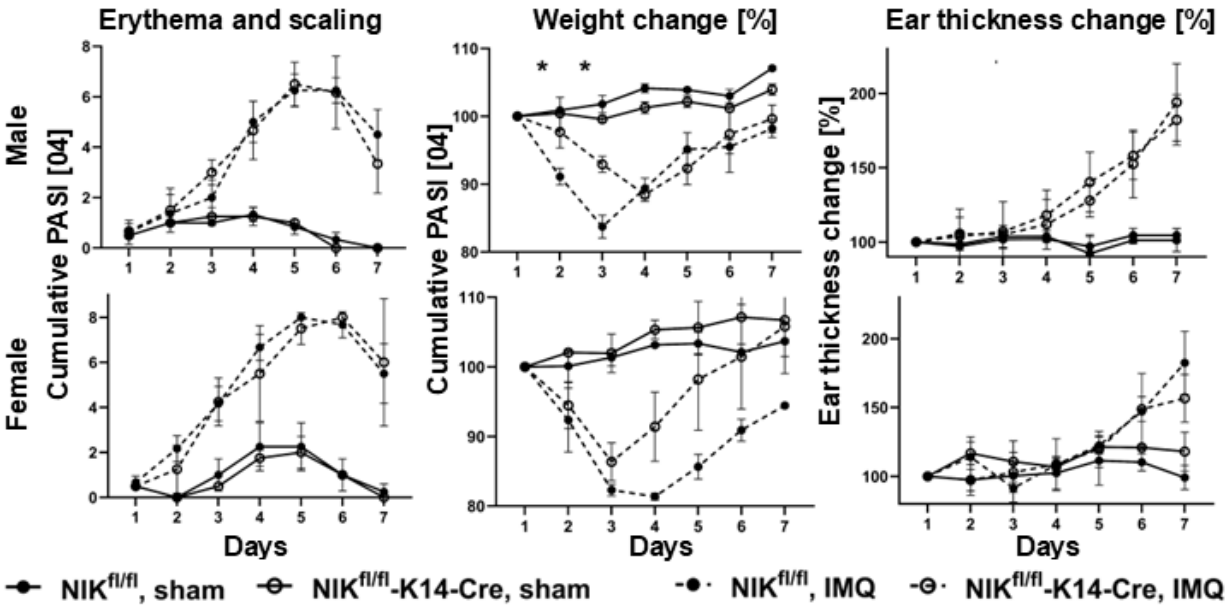

Figure 3.27: Disease scores of 6-day IMQ- or sham-treated NIK$^{fl/fl}$-K14Cre mice and NIK$^{fl/fl}$ controls

Cumulative PASI scores consisting of erythema and scaling, percentual weight and ear thickness change of 6-day IMQ- or sham-treated female and male NIK$^{fl/fl}$-K14Cre mice and NIK$^{fl/fl}$ controls, *n* = 2-4 mice per group, 2-way ANOVA with Bonferroni post-hoc test, 1 representative experiment out of 3 experiments.

Flow cytometric analysis of skin immune cells confirmed a robust increase in leukocyte infiltration following IMQ-treatment compared to sham-treated controls. The magnitude of inflammation was comparable between NIK$^{fl/fl}$-K14Cre mice and NIK$^{fl/fl}$ controls (Figure 3.28B). Subset analysis of CD11b^{+} myeloid cells revealed significant expansion of monocytes (Ly6C^{+high} Ly6G^{-}) and neutrophils (Ly6C^{+low} Ly6G^{+}) in both genotypes (Figure 3.28A, C-E), indicating that KC-specific NIK deletion does not impact the recruitment or accumulation of these myeloid populations during acute IMQ-induced inflammation.

Previous studies, including work from our lab (van der Fits, Mourits et al. 2009, El Malki, Karbach et al. 2013, Moos, Mohebiany et al. 2019) have established the critical role of the IL-23/IL-17 signaling axis in psoriasis-like disease in IMQ-induced models. Th17 cells and dermal γδ T cells are recognized as the primary sources of IL-17A (van der Fits, Mourits et al. 2009, Cai, Shen et al. 2011). To investigate whether KC-specific NIK deletion alters T cell responses, we performed flow cytometric analysis of distinct dermal T cell populations (Figure 3.29 and Figure 3.30).

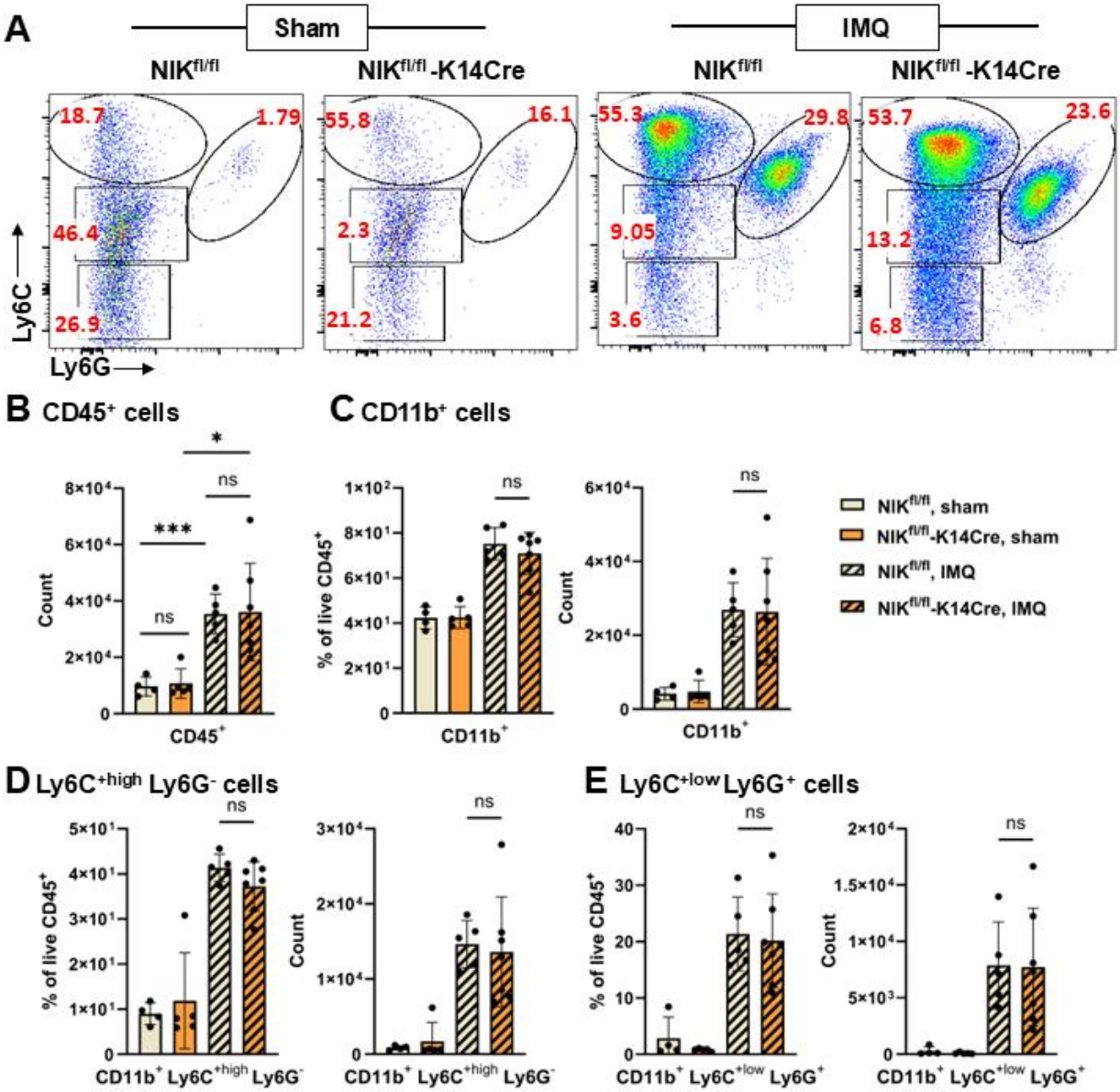

Figure 3.28: NIK$^{fl/fl}$-K14Cre mice reveal no alterations in the IMQ-induced psoriasis mouse model compared to NIK$^{fl/fl}$-controls

(A) One representative flow cytometry plot of Ly6C Ly6G gating in the skin pre-gated on single, live, CD45$^+$, CD90.2$^-$. CD11b$^+$ per group. Ly6C Ly6G cells in the skin of NIK$^{fl/fl}$-K14Cre and NIK$^{fl/fl}$ controls with IMQ- or sham-treatment. Percentages of gates are shown. Statistical analysis of **(B)** absolute counts of CD45.2$^+$ cells and absolute counts and frequencies (% of live CD45.2$^+$) of **(C)** CD11b$^+$ cells, **(D)** Ly6C^{+high} Ly6G$^-$ cells and **(E)** Ly6C^{+low} Ly6G$^+$ cells in the skin of IMQ- and sham-treated NIK$^{fl/fl}$-K14Cre mice and NIK$^{fl/fl}$ controls, *n* = 4-7 mice per group, 1 representative experiment out of 3 experiments, unpaired Student's *t* test.

As shown in Figure 3.29A, B, no significant differences were observed in the percentages of T cell populations between NIK-deficient and control mice.

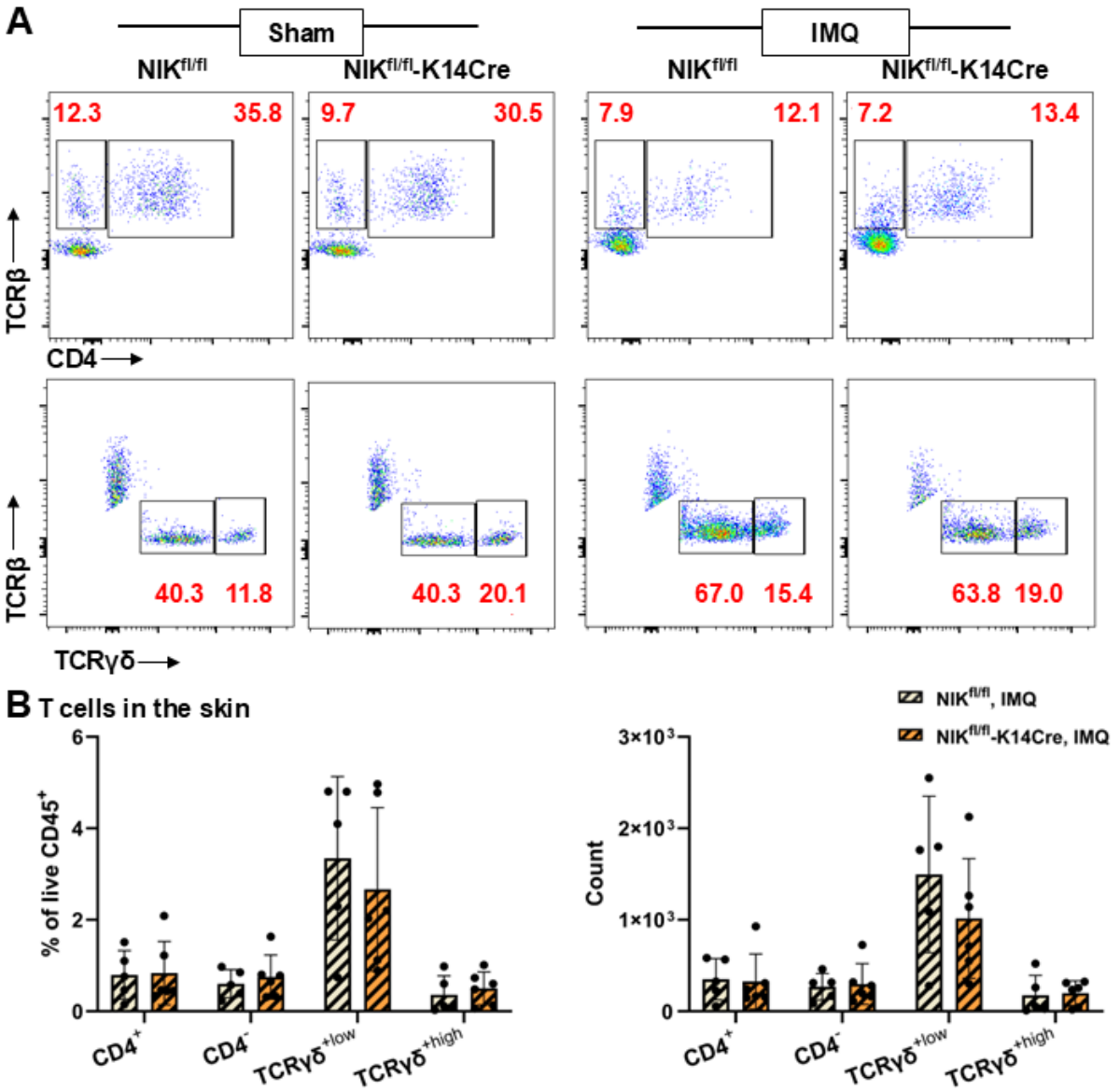

Figure 3.29: T cell subset analysis in IMQ- treated NIK$^{fl/fl}$-K14Cre mice and NIK$^{fl/fl}$ controls

(A) One representative flow cytometry plot of TCRβ CD4 and TCRγδ cells in the skin pre-gated on single, live, CD45$^+$ per group. TCRβ CD4 and TCRγδ cells in the skin of NIK$^{fl/fl}$-K14Cre and NIK$^{fl/fl}$ controls with IMQ-treatment. Percentages of gates are shown. **(B)** Statistical analysis of frequencies (% of live CD45$^+$) and absolute counts of TCRβ$^+$ CD4$^+$, TCRβ$^+$ CD4$^-$, TCRγδ^{+low} and TCRγδ^{+high} cells in the skin of IMQ-treated NIK$^{fl/fl}$-K14Cre mice and NIK$^{fl/fl}$ controls, *n* = 4-7 mice per group, 1 representative experiment, unpaired Student's *t* test.

Similarly, IL-17A production by dermal TCRγδ^{+low} cells was comparable between groups. Notably, a higher frequency of the cytotoxic TCRβ$^+$ CD4$^-$ (Tc17) population produced IL-17A than the conventional TCRβ$^+$ CD4$^+$ (Th17) cells (Figure 3.30A, B). Dermal γδ T cells (TCRγδ^{+low}) remained the predominant source of IL-17A (Figure 3.30C), whereas epidermal TCRγδ^{+high} cells did not contribute to IL-17A production but were the primary producers of IFNγ (Figure 3.30D). GM-CSF was produced by both TCRβ$^+$ and TCRγδ$^+$ populations at comparable levels between genotypes (Figure 3.30). Importantly, no significant differences in cytokine production were observed between NIK$^{fl/fl}$-K14Cre mice and NIK$^{fl/fl}$ controls.

Together with the unaltered clinical phenotype and myeloid infiltration, these data indicate that KC -intrinsic NIK is dispensable for IMQ-induced psoriasis.

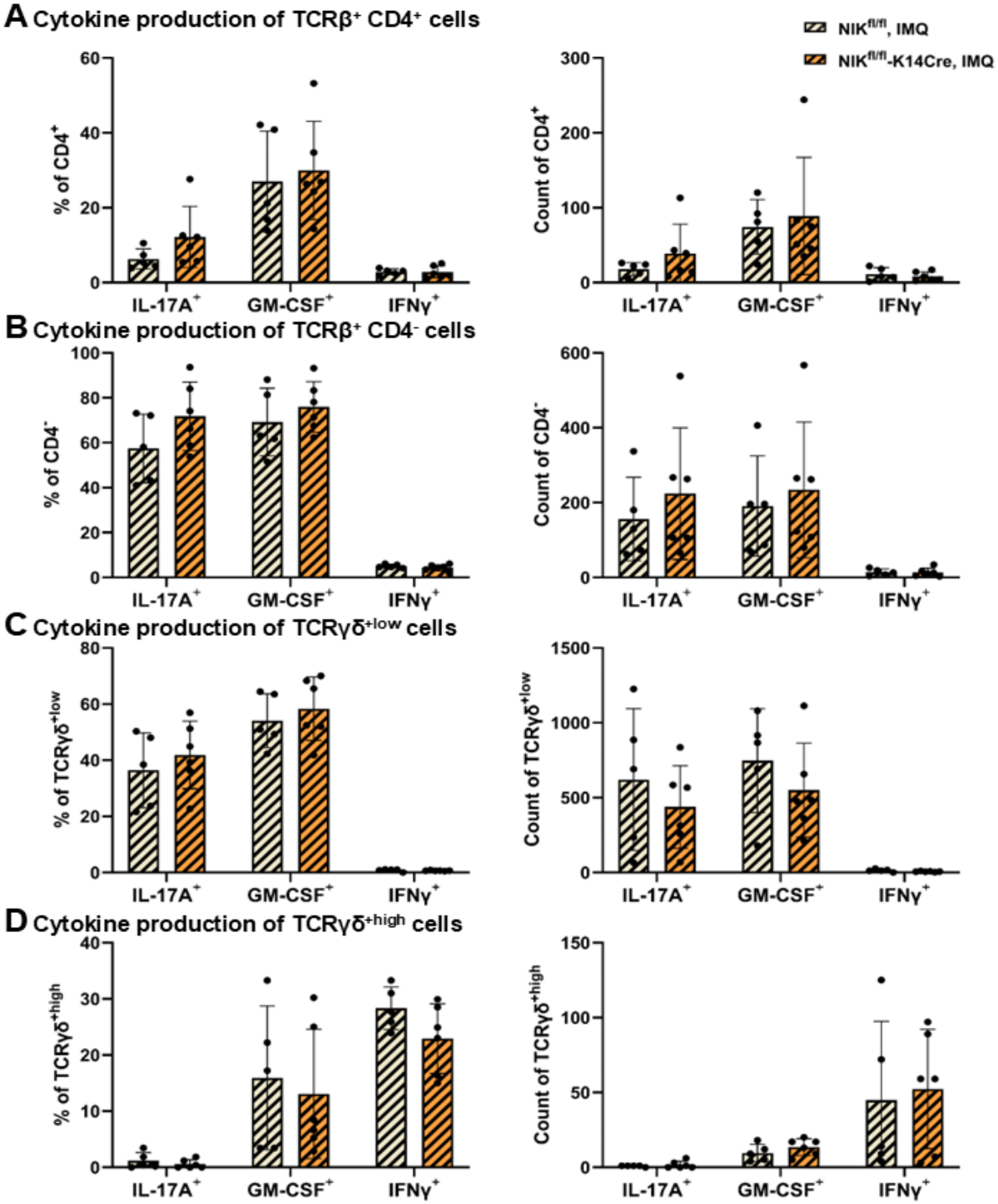

Figure 3.30: T cell cytokine analysis in IMQ-treated NIK$^{fl/fl}$-K14Cre mice and NIK$^{fl/fl}$ controls

(A-D) Statistical analysis of frequencies (% of **(A)** TCRβ^{+} CD4^{+}, **(B)** TCRβ^{+} CD4^{-}, **(C)** TCRγδ^{+}low or **(D)** TCRγδ^{+high}) and absolute cell counts of IL-17A, GM-CSF and IFNγ cytokine production in skin of IMQ-treated NIK$^{fl/fl}$-K14Cre mice and NIK$^{fl/fl}$ controls, *n* = 4-7 mice per group, 1 representative experiment, unpaired Student's *t* test.

4 DISCUSSION

4.1 Skin-organ crosstalk and immune cell trafficking in psoriatic models

Psoriasis is a systemic, inflammatory skin disease in which chronic skin inflammation drives pathology in distant organs, including the cardiovascular system, colon and liver (Mehta, Yu et al. 2011, Balak, Piaserico and Kasujee 2021, Yamazaki 2021, Orlando, Molon et al. 2022, Bezzio, Cavalli et al. 2024). However, whether this skin-organ crosstalk is mediated by direct immune cell trafficking or by circulating inflammatory signals has remained unclear. Using Dendra2-based photoconversion to fate-map immune cells emigrating from inflamed skin, this study supports the conclusion that skin-derived immune cells are largely confined to lymphoid tissue, with minimal contribution to peripheral organs. Even in the presence of robust vascular, intestinal and hepatic inflammation in the chronic K14-IL-17A$^{ind/+}$ psoriasis model, direct recruitment of skin-derived immune cells to these sites was negligible. These findings identify systemic inflammatory signaling, rather than skin-derived immune cell dissemination, as the dominant mechanism linking cutaneous inflammation to extra-cutaneous pathology in psoriasis.

4.2 Establishment and validation of the Dendra2 photoconversion for tracking skin-derived immune cells

We first established Dendra2-based photoconversion in the IMQ-induced psoriasis model, chosen for its technical simplicity, reproducibility and short disease course. Photoconversion of inflamed ear and back skin was highly feasible, non-invasive and did not alter disease progression, as PASI scores and ear thickness followed expected kinetics (van der Fits, Mourits et al. 2009, Schüler, Brand et al. 2019). The photoconverted red fluorescence remained stable during tissue isolation and flow cytometry, enabling reliable tracking of short-lived inflammatory cells such as neutrophils when using a 24 h chase period.

Under homeostatic and IMQ-driven conditions, photoconverted cells migrated primarily to draining LNs and the spleen, confirming constitutive skin-to-lymphoid trafficking. Comparable numbers of skin-derived immune cells in sham controls indicate that such migration is a physiological process, accelerated in inflammation only in terms of activation status or functional properties rather than total cell number. These results align with previous observations in photoconvertible models and classical studies of DC and T cell trafficking (Itano, McSorley et al. 2003, Tomura, Yoshida et al. 2008, Teijeira, Hunter et al. 2017).

Importantly, IMQ-induced inflammation did not support detectable dissemination of skin-derived cells to distant organs such as the BM or aorta. This likely reflects the transient nature of IMQ-driven cytokine signaling, the self-limiting inflammatory response and the limits of detecting rare or short-lived migrating cells. While absolute numbers may remain below detection thresholds, these data demonstrate that acute, innate-driven psoriasiform inflammation primarily redistributes skin-derived immune cells to local lymphoid tissues rather than systemic organs.

Together, these findings validate Dendra2 photoconversion as a robust approach for tracking dermal immune cells and establish that IMQ provides an ideal, low-impact system for method development. To assess whether chronic, sustained inflammation permits long-range trafficking, we next applied this approach to the K14-IL-17A$^{ind/+}$ model, which exhibits persistent systemic IL-17A elevation and psoriasis-associated comorbidities.

4.3 Immune cell dynamics and organ involvement in chronic IL-17A-driven psoriasis

Building on validation in the IMQ model, we applied Dendra2 photoconversion to the chronic K14-IL-17A$^{ind/+}$ model, which develops pronounced psoriasis-like skin pathology and systemic inflammation (Karbach, Croxford et al. 2014). Dendra2 expression did not alter disease course, confirming compatibility with chronic inflammation.

Photoconverted skin-derived cells were consistently detected in spleen, liver and draining LNs, demonstrating that chronic IL-17A-driven inflammation permits egress to both lymphoid and non-lymphoid organs. Detection in the liver further suggests a dermal-hepatic immune axis potentially relevant to psoriasis-associated comorbidities (Balak, Piaserico and Kasujee 2021).

Surprisingly, chronic inflammation did not increase absolute numbers of skin-derived cells in peripheral organs. This likely reflects a combination of technical limitations (reduced photoconversion efficiency in thick, heterogeneous psoriatic plaques), cell-intrinsic factors (short-lived or activated populations) and biological retention of immune cells within skin. These findings highlight that model selection in photoconvertible reporter studies should balance systemic inflammation versus uniform skin architecture, with alternative models providing complementary approaches.

CD11b^{+} myeloid cells dominated the skin-derived immune cell populations in spleen and bLN, with CD11b^{+} Gr-1^{-} cells representing a large subset regardless of inflammatory status. Chronic IL-17A-driven psoriasis showed a trend towards increased migration of CD11b^{+} Gr-1^{+} cells, reflecting expansion of inflammatory neutrophils and monocytes in the skin. Observed patterns

likely result from baseline skin composition, epidermis-biased photoconversion, short tracking window and technical detection limits, rather than selective impairment of Gr-1$^-$ cell migration. Slower-migrating immune cells like LCs and dermal DCs may require longer to be captured (Kissenpfennig, Henri et al. 2005). These data indicate that chronic IL-17A inflammation primarily reshapes local myeloid composition rather than fundamentally altering systemic trafficking.

CD90.2$^+$ T cells were the other major skin-derived immune cell population found in spleen and bLN. Total T cell frequencies among Dendra2-red$^+$ cells were similar between healthy and psoriatic mice. Subset analysis revealed reduced TCRγδ$^+$ cells in the spleen and bLN of psoriatic mice, consistent with their depletion from inflamed skin rather than altered migration (Croxford, Karbach et al. 2014). Conventional CD4$^+$, regulatory CD4$^+$ Foxp3$^+$ and CD8$^+$ T cells were unaffected.

These findings suggest that chronic IL-17A-driven psoriasis modifies local T cell composition more than systemic dissemination. As with myeloid cells, interpretation is constrained by single time-point tracking and panel limitations, which may underestimate slower or delayed trafficking.

Chronic IL-17A overexpression permits skin-derived immune cells to reach multiple organs but does not markedly enhance systemic dissemination. Immune cell redistribution is shaped primarily by local skin composition, lesion architecture and technical constraints of photoconversion. Overall, chronic psoriasis profoundly remodels the local immune landscape without dramatically increasing migration to distant tissues, emphasizing the importance of model selection and experimental design when tracking immune cell trafficking.

4.4 Systemic, not dermal, drivers of organ inflammation in psoriasis

Our photoconversion studies using PhAM-K14-IL-17A$^{ind/+}$ mice consistently demonstrate that skin-derived immune cells do not migrate directly to distant organs, including the aorta and colon, despite chronic IL-17A-driven skin inflammation. Flow cytometry and confocal imaging confirmed absence of Dendra2-red$^+$, skin-derived cells in the aorta, even under conditions of pronounced vascular inflammation (confocal microscopy data not shown). Robust photoconversion efficiency in the skin and replication across multiple mice make false negatives unlikely. These data support a model in which psoriasis-associated vascular inflammation is driven by systemic immune activation rather than cutaneous cell migration, a central finding of Schaller, Ringen et al. 2023.

Despite the lack of skin-to-aorta trafficking, K14-IL-17A$^{ind/+}$ mice develop severe aortic inflammation, characterized by neutrophil infiltration and reactive oxygen species (ROS)

production (Karbach, Croxford et al. 2014). Schaller, Ringen et al. 2023 demonstrated that circulating neutrophils in K14-IL-17A$^{ind/+}$ mice are systemically primed: they exhibit increased ROS generation and higher activity indicated by elevated expression of *Mpo*, *Prt3* and *Elane*. Additionally, expression of the genes *Cxcl2* and *S100a9* indicating enhanced neutrophil attraction are upregulated in both skin and aorta, while antioxidant responses (*Nrf2*, *Sod1-3*) remain insufficient in both organs. These findings, integrated with the absence of skin-derived immune cell migration, reveal that vascular inflammation arises from BM-derived systemic neutrophil activation (Figure 4.1).

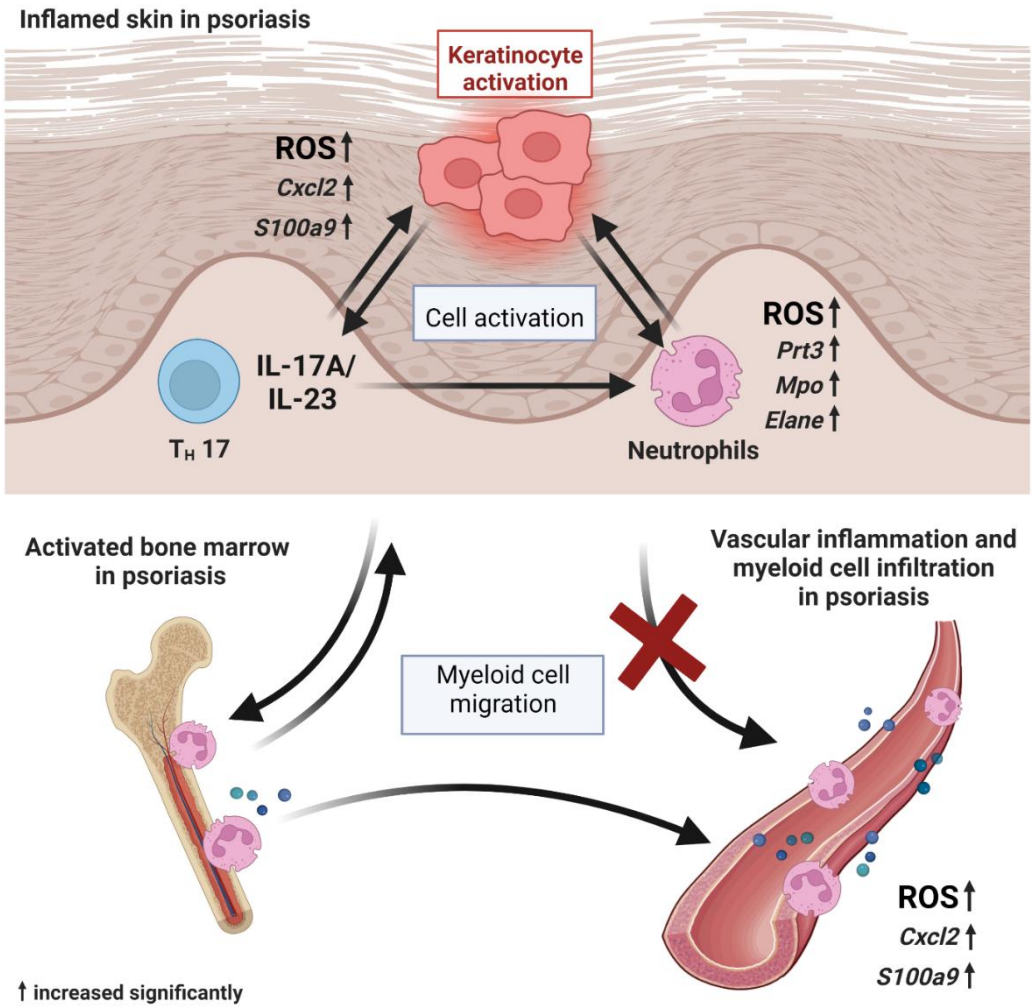

Figure 4.1: Schematic of psoriasis-driven cardiovascular inflammation in K14-IL-17A$^{ind/+}$ mice (Schaller, Ringen et al. 2023)

IL-17A overexpression in the skin induces KC activation and promotes infiltration of T cells and myeloid cell influx, resulting in robust neutrophil activation. Activated neutrophils exhibit increased production of ROS and upregulation of activation-associated genes *Mpo*, *Prt3* and *Elane*. Elevated ROS levels and inflammatory markers (*Cxcl2*, *S100a9*) indicating enhanced neutrophil attraction are detected in both skin and aorta. The absence of direct immune cell migration from the skin to the vasculature suggests that this phenotype is driven by systemic inflammatory signals that recruit BM-derived neutrophils. Graphical abstract from Schaller, Ringen et al., 2023.

Continuous KC-derived IL-17A further amplifies this process by activating endothelial and vascular smooth muscle cells, inducing TNF-α, IL-1β, CCL2 and ICAM-1 expression (Pietrowski, Bender et al. 2011, von Stebut, Boehncke et al. 2019). Beyond direct cytokine effects, IL-17A has been implicated in promoting NET formation, an emerging mechanism linking psoriatic inflammation to vascular dysfunction in CVD (Lin, Rubin et al. 2011, Hu, Yu et al. 2016, Shao, Fang et al. 2019, Doring, Libby and Soehnlein 2020, Ma, Sun et al. 2025). Additional systemic factors, including platelet hyperactivation and hypertension secondary to barrier dysfunction, synergize to exacerbate vascular pathology (Hot, Lenief et al. 2010, Maione, Cicala et al. 2011, Wild, Jung et al. 2021, Jiang, Jiang et al. 2023). Human studies corroborate these findings: psoriasis severity correlates with aortic inflammation and coronary plaque burden, both of which improve with systemic biologic therapy (Mehta, Yu et al. 2011, Elnabawi, Dey et al. 2019, Elnabawi, Oikonomou et al. 2019). Collectively, these observations establish systemic IL-17A-driven inflammation as the principal mediator of psoriasis-associated CVD.

Analogous analyses in the colon revealed no detectable skin-derived immune cells, despite chronic systemic IL-17A exposure and local inflammatory infiltrates. This indicates that granulocytic accumulation in the gut originates from BM-derived myeloid cells rather than skin-derived. The findings reflect the tissue-specific and context-dependent effects of IL-17A, consistent with clinical observations that IL-17A blockade ameliorates psoriasis but may induce or exacerbate IBD (Deng, Wang et al. 2023, Alsakarneh, Al Ta'ani et al. 2025). Thus, skin-to-gut cellular migration is not a major contributor to psoriatic comorbidity; rather, systemic cytokine signaling shapes colonic immune responses.

While small numbers of skin-derived cells were occasionally detectable in the liver, they accounted for a negligible fraction of the hepatic infiltrate in PhAM-K14-IL-17A$^{ind/+}$ mice. By contrast, neutrophils, monocytes, cDC2s and hepatic macrophages accumulated robustly in K14-IL-17A$^{ind/+}$ mice, consistent with systemic IL-17A-driven myeloid mobilization. Hepatocytes, Kupffer cells and hepatic stellate cells respond to circulating IL-17A and chemokines (CXCL1/2, G-CSF) in the liver, generating a microenvironment that recruits circulating myeloid cells independently of dermal origin (Tang, Bian et al. 2011, Meng, Wang et al. 2012, Berlanga, Guiu-Jurado et al. 2014, Cho and Szabo 2021). Short-term metabolic stress (Cd-HFD) did not alter this balance, but more severe diets or prolonged models may uncover additional contributions from systemic or skin-derived signals. Future studies combining dietary, genetic and pharmacological manipulations will help dissect the relative contributions of IL-17A-driven systemic activation versus potential low-level skin-derived cell migration.

Across multiple organs, our data converge on a unifying principle: psoriasis-associated systemic inflammation, rather than direct skin-to-organ immune cell trafficking, drives vascular, intestinal and hepatic pathology. In the aorta, this is supported by Schaller, Ringen et al. 2023, which shows that ROS-producing, activated neutrophils contribute to vascular inflammation. Colon and liver findings reinforce this paradigm, highlighting the broader systemic consequences of IL-17A overexpression. These insights underscore the importance of targeting systemic inflammatory pathways in psoriasis and monitoring cardiovascular, intestinal and hepatic comorbidities in clinical management.

4.5 Limitations of the Dendra2-based immune cell tracking approach and experimental models

While this study provides the first integrated analysis of skin-derived immune cell trafficking across acute and chronic psoriatic inflammation, several technical and biological constraints delimit the resolution and scope of the conclusions.

Chronic IL-17A-driven plaque formation in K14-IL-17A$^{ind/+}$ mice results in thick, hyperkeratotic and irregular skin in the back skin, which likely reduces and spatially heterogenizes photoconversion efficiency in this area. As a consequence, subtle quantitative differences in immune cell egress from psoriatic versus healthy skin may be underestimated, particularly in deeper dermal compartments.

Dilution of Dendra2-red fluorescence through cell proliferation and protein turnover constrains the effective chase window. Rapidly dividing or short-lived populations, such as neutrophils, may lose detectable signal before reaching distant organs, limiting sensitivity for long-range migration events. In addition, high autofluorescence in organs such as spleen and liver complicates detection of rare photoconverted cells and restricts flow cytometric panel complexity. More refined strategies, including lineage-restricted Dendra2 expression or downstream single-cell transcriptomic profiling of sorted populations, will be required to resolve subset-specific trafficking with higher sensitivity.

Photoconversion is inherently biased toward epidermal and superficial dermal layers, potentially underrepresenting deeper resident populations. Although extended illumination can mitigate this effect, complete depth-independent labeling remains challenging in chronically inflamed tissue.

Intravital microscopy (IVM) would, in principle, allow direct visualization of leukocyte egress. However, its application in chronic psoriatic skin is currently limited by impaired optical penetration, motion artifacts and the inability to track rare migratory events over the prolonged

timescales required for systemic dissemination. Thus, while conceptually complementary, IVM is not presently feasible for the longitudinal, multi-organ trafficking analyses performed here.

The IMQ model represents an acute, self-resolving inflammatory response and does not recapitulate the sustained cytokine exposure associated with psoriasis-related comorbidities such as CVD, IBD or NAFLD. In contrast, K14-IL-17A$^{ind/+}$ mice exhibit profound chronic systemic inflammation but also extreme skin pathology, which complicates standardized photoconversion and inter-genotype comparisons.

All trafficking analyses were performed at a fixed 24 h timepoint, favoring detection of rapidly migrating granulocytes while likely underestimating slower-moving populations such as DCs, macrophages and T cells (Kissenpfennig, Henri et al. 2005, Hiltensperger, Beltran et al. 2021). Comprehensive resolution of subset-specific kinetics would require extended multi-day tracking.

Finally, the absence or near-absence of skin-derived cells in organs such as aorta, colon or liver may reflect true biological exclusion. However, ultra-rare trafficking events below the detection threshold of flow cytometry cannot be fully excluded. Moreover, the K14-IL-17A$^{ind/+}$ model captures an IL-17A-dominant psoriasis endotype and may not reflect trafficking dynamics in alternative disease contexts, such as IL-36-mediated pustular psoriasis (Johnston, Xing et al. 2017).

4.6 Conclusion

Using complementary acute (IMQ) and chronic (K14-IL-17A$^{ind/+}$) psoriasis models combined with *in vivo* Dendra2 photoconversion, this study provides a comprehensive assessment of skin-derived immune cell trafficking across lymphoid and non-lymphoid organs. We show that immune cells from the skin routinely migrate to lymphoid tissues under both steady-state and inflammatory conditions, consistent with physiological immune surveillance. Neither acute nor chronic psoriatic inflammation supports substantial skin-derived immune cell trafficking to distant organs, including the aorta, colon and liver. PhAM-K14-IL-17A$^{ind/+}$ mice permits detectable but extremely sparse skin-derived migration to the liver, but this contribution is negligible relative to the large IL-17A-driven myeloid infiltrate derived from the circulation. Vascular, intestinal and hepatic inflammation arise from systemic cytokine signaling and BM-driven myelopoiesis, not from skin-derived immune cell egress. Local retention, rather than systemic emigration, characterizes the behavior of key T cell populations in chronic psoriatic skin.

Together, these data support a unifying model in which psoriasis-associated comorbidities are driven predominantly by systemic IL-17A-mediated immune activation and not by direct immune cell trafficking from skin to distant organs. This distinction has important mechanistic and

therapeutic implications: mitigating systemic IL-17A-driven myeloid activation, oxidative stress and endothelial dysfunction may be more critical for treating cardiovascular and metabolic comorbidities than targeting local skin inflammation alone.

The PhAM photoconversion approach provides a powerful framework for dissecting organ-organ immune cell communication in inflammatory diseases but also highlights the need for tailored model selection and complementary single-cell strategies to fully capture the complexity of chronic psoriatic inflammation and its systemic consequences.

4.7 Keratinocyte-specific NIK signaling is dispensable for IMQ-driven skin inflammation

The non-canonical NF-κB pathway has been implicated in inflammatory skin disease, yet its cell type-specific contribution to psoriasis remains unclear. Systemic pharmacological inhibition of NIK attenuates IMQ-induced psoriasiform inflammation, but this approach cannot distinguish effects in KCs from immune or stromal compartments (Zhu, Ma et al. 2020).

To address this, we examined IMQ-induced psoriasis in KC-specific NIK knockout mice ($NIK^{fl/fl}$-K14Cre). Across clinical parameters, including cumulative PASI score, ear thickness and body weight change, $NIK^{fl/fl}$-K14Cre mice had no altered disease onset, progression or severity in either sex. Flow cytometry confirmed comparable infiltration of leukocytes, $CD11b^{+}$ myeloid cells, inflammatory monocytes, neutrophils and T cell subsets (αβ and γδ T cells) between $NIK^{fl/fl}$-K14Cre mice and $NIK^{fl/fl}$ controls. Cytokine profiling similarly showed preserved IL-17A, GM-CSF and IFNγ production. Together, these results demonstrate that NIK in KCs does not modulate clinical or immunological features of acute IMQ-driven psoriasis.

These findings contrast with the effects of systemic NIK inhibition, suggesting that protection in IMQ-induced psoriasis arises primarily from NIK-dependent signaling in DCs, where it regulates IL-23 production, and in T cells, where it modulates effector and memory differentiation as well as cytokine production. (Murray 2013, Rowe, Murray et al. 2013, Yu, Zhou et al. 2014, Huang, Gao et al. 2018, Xia, Zhu et al. 2024).

It is important to consider model-specific limitations: IMQ induces rapid, innate-driven IL-23/IL-17 axis activation, which may render KC-specific signals functionally redundant. NIK in KCs might play a more prominent role in chronic, genetically driven models, where sustained KC-immune crosstalk occurs over longer timeframes.

In summary, these results refine our understanding of non-canonical NF-κB signaling, indicating that NIK's pathogenic effects in this model are predominantly immune cell-intrinsic rather than KC-dependent.

5 FIGURE INDEX

6 TABLE INDEX

7 LITERATURE

Abramson, J. and G. Anderson (2017). "Thymic Epithelial Cells." Annu Rev Immunol **35**: 85-118.

Adam, V., K. Nienhaus, D. Bourgeois and G. U. Nienhaus (2009). "Structural basis of enhanced photoconversion yield in green fluorescent protein-like protein Dendra2." Biochemistry **48**(22): 4905-4915.

Agrawal, R., A. Hu and W. B. Bollag (2023). "The Skin and Inflamm-Aging." Biology (Basel) **12**(11).

Akira, S., K. Takeda and T. Kaisho (2001). "Toll-like receptors: critical proteins linking innate and acquired immunity." Nat Immunol **2**(8): 675-680.

Albanesi, C., C. Scarponi, S. Pallotta, R. Daniele, D. Bosisio, S. Madonna, P. Fortugno, S. Gonzalvo-Feo, J. D. Franssen, M. Parmentier, O. De Pita, G. Girolomoni and S. Sozzani (2009). "Chemerin expression marks early psoriatic skin lesions and correlates with plasmacytoid dendritic cell recruitment." J Exp Med **206**(1): 249-258.

Alsakarneh, S., O. Al Ta'ani, R. Aburumman, I. Mikhail, J. G. Hashash and F. A. Farraye (2025). "Risk of De Novo Inflammatory Bowel Disease in Patients With Psoriasis and Psoriatic Arthritis Treated With IL-17A Inhibitors: A Population-Based Study." Aliment Pharmacol Ther **62**(1): 72-76.

Angiolilli, C., E. F. A. Leijten, C. P. J. Bekker, E. Eeftink, B. Giovannone, M. O. Nordkamp, M. van der Wal, J. L. Thijs, S. J. Vastert, F. van Wijk, T. Radstake and J. van Loosdregt (2022). "ZFP36 Family Members Regulate the Proinflammatory Features of Psoriatic Dermal Fibroblasts." J Invest Dermatol **142**(2): 402-413.

Arakawa, A., K. Siewert, J. Stohr, P. Besgen, S. M. Kim, G. Ruhl, J. Nickel, S. Vollmer, P. Thomas, S. Krebs, S. Pinkert, M. Spannagl, K. Held, C. Kammerbauer, R. Besch, K. Dornmair and J. C. Prinz (2015). "Melanocyte antigen triggers autoimmunity in human psoriasis." J Exp Med **212**(13): 2203-2212.

Arican, O., M. Aral, S. Sasmaz and P. Ciragil (2005). "Serum levels of TNF-alpha, IFN-gamma, IL-6, IL-8, IL-12, IL-17, and IL-18 in patients with active psoriasis and correlation with disease severity." Mediators Inflamm **2005**(5): 273-279.

Austin, L. M., M. Ozawa, T. Kikuchi, I. B. Walters and J. G. Krueger (1999). "The majority of epidermal T cells in Psoriasis vulgaris lesions can produce type 1 cytokines, interferon-gamma, interleukin-2, and tumor necrosis factor-alpha, defining TC1 (cytotoxic T lymphocyte) and TH1 effector populations: a type 1 differentiation bias is also measured in circulating blood T cells in psoriatic patients." J Invest Dermatol **113**(5): 752-759.

Balak, D. M. W., S. Piaserico and I. Kasujee (2021). "Non-Alcoholic Fatty Liver Disease (NAFLD) in Patients with Psoriasis: A Review of the Hepatic Effects of Systemic Therapies." Psoriasis (Auckl) **11**: 151-168.

Baroni, A., E. Buommino, V. De Gregorio, E. Ruocco, V. Ruocco and R. Wolf (2012). "Structure and function of the epidermis related to barrier properties." Clin Dermatol **30**(3): 257-262.

Basavaraj, K. H., N. M. Ashok, R. Rashmi and T. K. Praveen (2010). "The role of drugs in the induction and/or exacerbation of psoriasis." Int J Dermatol **49**(12): 1351-1361.

Bataille, A., C. Le Gall, L. Misery and M. Talagas (2022). "Merkel Cells Are Multimodal Sensory Cells: A Review of Study Methods." Cells **11**(23).

Belkaid, Y. and O. J. Harrison (2017). "Homeostatic Immunity and the Microbiota." Immunity **46**(4): 562-576.

Berlanga, A., E. Guiu-Jurado, J. A. Porras and T. Auguet (2014). "Molecular pathways in non-alcoholic fatty liver disease." Clin Exp Gastroenterol **7**: 221-239.

Beutner, K. R., S. K. Tyring, K. F. Trofatter, Jr., J. M. Douglas, Jr., S. Spruance, M. L. Owens, T. L. Fox, A. J. Hougham and K. A. Schmitt (1998). "Imiquimod, a patient-applied immune-response modifier for treatment of external genital warts." Antimicrob Agents Chemother **42**(4): 789-794.

Bezzio, C., C. A. M. Cavalli, G. Franchellucci, A. Dal Buono, R. Gabbiadini, D. Scalvini, S. Manara, A. Narcisi, A. Armuzzi and S. Saibeni (2024). "Psoriasis and inflammatory bowel disease: concomitant IMID or paradoxical therapeutic effect? A scoping review on anti-IL-12/23 and anti-IL-23 antibodies." Therap Adv Gastroenterol **17**: 17562848241299564.

Boehncke, W. H. and M. P. Schön (2015). "Psoriasis." Lancet **386**(9997): 983-994.

Boothby, I. C., M. J. Kinet, D. P. Boda, E. Y. Kwan, S. Clancy, J. N. Cohen, I. Habrylo, M. M. Lowe, M. Pauli, A. E. Yates, J. D. Chan, H. W. Harris, I. M. Neuhaus, T. H. McCalmont, A. B. Molofsky and M. D. Rosenblum (2021). "Early-life inflammation primes a T helper 2 cell-fibroblast niche in skin." Nature **599**(7886): 667-672.

Bos, J. D., C. Hagenaars, P. K. Das, S. R. Krieg, W. J. Voorn and M. L. Kapsenberg (1989). "Predominance of "memory" T cells (CD4+, CDw29+) over "naive" T cells (CD4+, CD45R+) in both normal and diseased human skin." Arch Dermatol Res **281**(1): 24-30.

Cai, Y., X. Shen, C. Ding, C. Qi, K. Li, X. Li, V. R. Jala, H. G. Zhang, T. Wang, J. Zheng and J. Yan (2011). "Pivotal role of dermal IL-17-producing gammadelta T cells in skin inflammation." Immunity **35**(4): 596-610.

Cai, Y., F. Xue, C. Fleming, J. Yang, C. Ding, Y. Ma, M. Liu, H. G. Zhang, J. Zheng, N. Xiong and J. Yan (2014). "Differential developmental requirement and peripheral regulation for dermal Vgamma4 and Vgamma6T17 cells in health and inflammation." Nat Commun **5**: 3986.

Campbell, J. J., K. Ebsworth, L. S. Ertl, J. P. McMahon, D. Newland, Y. Wang, S. Liu, Z. Miao, T. Dang, P. Zhang, I. F. Charo, R. Singh and T. J. Schall (2017). "IL-17-Secreting gammadelta T Cells Are Completely Dependent upon CCR6 for Homing to Inflamed Skin." J Immunol **199**(9): 3129-3136.

Chan, J. R., W. Blumenschein, E. Murphy, C. Diveu, M. Wiekowski, S. Abbondanzo, L. Lucian, R. Geissler, S. Brodie, A. B. Kimball, D. M. Gorman, K. Smith, R. de Waal Malefyt, R. A. Kastelein, T. K. McClanahan and E. P. Bowman (2006). "IL-23 stimulates epidermal hyperplasia via TNF and IL-20R2-dependent mechanisms with implications for psoriasis pathogenesis." J Exp Med 203(12): 2577-2587.

Chen, L., J. Li, W. Zhu, Y. Kuang, T. Liu, W. Zhang, X. Chen and C. Peng (2020). "Skin and Gut Microbiome in Psoriasis: Gaining Insight Into the Pathophysiology of It and Finding Novel Therapeutic Strategies." Front Microbiol 11: 589726.

Chen, L., G. Ruan, Y. Cheng, A. Yi, D. Chen and Y. Wei (2022). "The role of Th17 cells in inflammatory bowel disease and the research progress." Front Immunol 13: 1055914.

Cheng, J. B., A. J. Sedgewick, A. I. Finnegan, P. Harirchian, J. Lee, S. Kwon, M. S. Fassett, J. Golovato, M. Gray, R. Ghadially, W. Liao, B. E. Perez White, T. M. Mauro, T. Mully, E. A. Kim, H. Sbitany, I. M. Neuhaus, R. C. Grekin, S. S. Yu, J. W. Gray, E. Purdom, R. Paus, C. J. Vaske, S. C. Benz, J. S. Song and R. J. Cho (2018). "Transcriptional Programming of Normal and Inflamed Human Epidermis at Single-Cell Resolution." Cell Rep 25(4): 871-883.

Cheuk, S., M. Wiken, L. Blomqvist, S. Nylen, T. Talme, M. Stahle and L. Eidsmo (2014). "Epidermal Th22 and Tc17 cells form a localized disease memory in clinically healed psoriasis." J Immunol 192(7): 3111-3120.

Cho, Y. and G. Szabo (2021). "Two Faces of Neutrophils in Liver Disease Development and Progression." Hepatology 74(1): 503-512.

Chudakov, D. M., S. Lukyanov and K. A. Lukyanov (2007). "Using photoactivatable fluorescent protein Dendra2 to track protein movement." Biotechniques 42(5): 553, 555, 557 passim.

Clark, R. A., B. Chong, N. Mirchandani, N. K. Brinster, K. Yamanaka, R. K. Dowgiert and T. S. Kupper (2006). "The vast majority of CLA+ T cells are resident in normal skin." J Immunol 176(7): 4431-4439.

Clayton, K., A. F. Vallejo, J. Davies, S. Sirvent and M. E. Polak (2017). "Langerhans Cells-Programmed by the Epidermis." Front Immunol 8: 1676.

Conrad, C., O. Boyman, G. Tonel, A. Tun-Kyi, U. Laggner, A. de Fougerolles, V. Kotelianski, H. Gardner and F. O. Nestle (2007). "Alpha1beta1 integrin is crucial for accumulation of epidermal T cells and the development of psoriasis." Nat Med 13(7): 836-842.

Conrad, C., J. Di Domizio, A. Mylonas, C. Belkhodja, O. Demaria, A. A. Navarini, A. K. Lapointe, L. E. French, M. Vernez and M. Gilliet (2018). "TNF blockade induces a dysregulated type I interferon response without autoimmunity in paradoxical psoriasis." Nat Commun 9(1): 25.

Coope, H. J., P. G. Atkinson, B. Huhse, M. Belich, J. Janzen, M. J. Holman, G. G. Klaus, L. H. Johnston and S. C. Ley (2002). "CD40 regulates the processing of NF-kappaB2 p100 to p52." EMBO J 21(20): 5375-5385.

Croxford, A. L., S. Karbach, F. C. Kurschus, S. Wortge, A. Nikolaev, N. Yogev, S. Klebow, R. Schuler, S. Reissig, C. Piotrowski, E. Brylla, I. Bechmann, J. Scheller, S. Rose-John, F. Thomas Wunderlich, T. Munzel, E. von Stebut and A. Waisman (2014). "IL-6 regulates neutrophil microabscess formation in IL-17A-driven psoriasiform lesions." J Invest Dermatol **134**(3): 728-735.

Cruz, M. S., A. Diamond, A. Russell and J. M. Jameson (2018). "Human alphabeta and gammadelta T Cells in Skin Immunity and Disease." Front Immunol **9**: 1304.

Dand, N., S. K. Mahil, F. Capon, C. H. Smith, M. A. Simpson and J. N. Barker (2020). "Psoriasis and Genetics." Acta Derm Venereol **100**(3): adv00030.

de Oliveira, P. S., P. R. Cardoso, E. V. Lima, M. C. Pereira, A. L. Duarte, R. Pitta Ida, M. J. Rego and M. G. Pitta (2015). "IL-17A, IL-22, IL-6, and IL-21 Serum Levels in Plaque-Type Psoriasis in Brazilian Patients." Mediators Inflamm **2015**: 819149.

De Pessemier, B., L. Grine, M. Debaere, A. Maes, B. Paetzold and C. Callewaert (2021). "Gut-Skin Axis: Current Knowledge of the Interrelationship between Microbial Dysbiosis and Skin Conditions." Microorganisms **9**(2).

Dejardin, E. (2006). "The alternative NF-kappaB pathway from biochemistry to biology: pitfalls and promises for future drug development." Biochem Pharmacol **72**(9): 1161-1179.

Dejardin, E., N. M. Droin, M. Delhase, E. Haas, Y. Cao, C. Makris, Z. W. Li, M. Karin, C. F. Ware and D. R. Green (2002). "The lymphotoxin-beta receptor induces different patterns of gene expression via two NF-kappaB pathways." Immunity **17**(4): 525-535.

Deng, Z., S. Wang, C. Wu and C. Wang (2023). "IL-17 inhibitor-associated inflammatory bowel disease: A study based on literature and database analysis." Front Pharmacol **14**: 1124628.

Di Meglio, P., F. Villanova and F. O. Nestle (2014). "Psoriasis." Cold Spring Harb Perspect Med **4**(8).

Di Nardo, A., K. Yamasaki, R. A. Dorschner, Y. Lai and R. L. Gallo (2008). "Mast cell cathelicidin antimicrobial peptide prevents invasive group A Streptococcus infection of the skin." J Immunol **180**(11): 7565-7573.

Doebel, T., B. Voisin and K. Nagao (2017). "Langerhans Cells - The Macrophage in Dendritic Cell Clothing." Trends Immunol **38**(11): 817-828.

Doring, Y., P. Libby and O. Soehnlein (2020). "Neutrophil Extracellular Traps Participate in Cardiovascular Diseases: Recent Experimental and Clinical Insights." Circ Res **126**(9): 1228-1241.

El Malki, K., S. H. Karbach, J. Huppert, M. Zayoud, S. Reissig, R. Schuler, A. Nikolaev, K. Karram, T. Munzel, C. R. Kuhlmann, H. J. Luhmann, E. von Stebut, S. Wortge, F. C. Kurschus and A. Waisman (2013). "An alternative pathway of imiquimod-induced psoriasis-like skin

inflammation in the absence of interleukin-17 receptor a signaling." J Invest Dermatol 133(2): 441-451.

Elnabawi, Y. A., A. K. Dey, A. Goyal, J. W. Groenendyk, J. H. Chung, A. D. Belur, J. Rodante, C. L. Harrington, H. L. Teague, Y. Baumer, A. Keel, M. P. Playford, V. Sandfort, M. Y. Chen, B. Lockshin, J. M. Gelfand, D. A. Bluemke and N. N. Mehta (2019). "Coronary artery plaque characteristics and treatment with biologic therapy in severe psoriasis: results from a prospective observational study." Cardiovasc Res 115(4): 721-728.

Elnabawi, Y. A., E. K. Oikonomou, A. K. Dey, J. Mancio, J. A. Rodante, M. Aksentijevich, H. Choi, A. Keel, J. Erb-Alvarez, H. L. Teague, A. A. Joshi, M. P. Playford, B. Lockshin, A. D. Choi, J. M. Gelfand, M. Y. Chen, D. A. Bluemke, C. Shirodaria, C. Antoniades and N. N. Mehta (2019). "Association of Biologic Therapy With Coronary Inflammation in Patients With Psoriasis as Assessed by Perivascular Fat Attenuation Index." JAMA Cardiol 4(9): 885-891.

Erbel, C., M. Akhavanpoor, D. Okuyucu, S. Wangler, A. Dietz, L. Zhao, K. Stellos, K. M. Little, F. Lasitschka, A. Doesch, M. Hakimi, T. J. Dengler, T. Giese, E. Blessing, H. A. Katus and C. A. Gleissner (2014). "IL-17A influences essential functions of the monocyte/macrophage lineage and is involved in advanced murine and human atherosclerosis." J Immunol 193(9): 4344-4355.

Erichsen, C. Y., P. Jensen and K. Kofoed (2020). "Biologic therapies targeting the interleukin (IL)-23/IL-17 immune axis for the treatment of moderate-to-severe plaque psoriasis: a systematic review and meta-analysis." J Eur Acad Dermatol Venereol 34(1): 30-38.

Etemadi, N. (2015). "TRAF2 regulates TNF and NF-kB signalling to suppress apoptosis and skin inflammation independently of Sphingosine kinase 1." Elife.

Eyerich, S., K. Eyerich, D. Pennino, T. Carbone, F. Nasorri, S. Pallotta, F. Cianfarani, T. Odorisio, C. Traidl-Hoffmann, H. Behrendt, S. R. Durham, C. B. Schmidt-Weber and A. Cavani (2009). "Th22 cells represent a distinct human T cell subset involved in epidermal immunity and remodeling." J Clin Invest 119(12): 3573-3585.

Fan, S. S., X. Xu, Y. B. Luo, X. Y. Meng and Y. Liu (2025). "GM-CSF(+) Th: a central player in autoimmunity." Theranostics 15(18): 9944-9968.

Fanti, P. A., E. Dika, S. Vaccari, C. Miscial and C. Varotti (2006). "Generalized psoriasis induced by topical treatment of actinic keratosis with imiquimod." Int J Dermatol 45(12): 1464-1465.

Filingeri, H. (2015). "Human skin wetness perception: psychophysical and neurophysiological bases." Temperature 2(1): 86-104.

Fleet, J. C. (2017). "The role of vitamin D in the endocrinology controlling calcium homeostasis." Mol Cell Endocrinol 453: 36-45.

Flutter, B. and F. O. Nestle (2013). "TLRs to cytokines: mechanistic insights from the imiquimod mouse model of psoriasis." Eur J Immunol 43(12): 3138-3146.

Forstermann, U. and T. Munzel (2006). "Endothelial nitric oxide synthase in vascular disease: from marvel to menace." Circulation 113(13): 1708-1714.

Fotiadou, C., E. Lazaridou, E. Sotiriou, S. Gerou, A. Kyrgidis, E. Vakirlis and D. Ioannides (2015). "IL-17A, IL-22, and IL-23 as Markers of Psoriasis Activity: A Cross-sectional, Hospital-based Study." J Cutan Med Surg 19(6): 555-560.

Fowell, D. J. and M. Kim (2021). "The spatio-temporal control of effector T cell migration." Nat Rev Immunol 21(9): 582-596.

Fry, L. and B. S. Baker (2007). "Triggering psoriasis: the role of infections and medications." Clin Dermatol 25(6): 606-615.

Fuentes-Duculan, J., M. Suarez-Farinas, L. C. Zaba, K. E. Nograles, K. C. Pierson, H. Mitsui, C. A. Pensabene, J. Kzhyshkowska, J. G. Krueger and M. A. Lowes (2010). "A subpopulation of CD163-positive macrophages is classically activated in psoriasis." J Invest Dermatol 130(10): 2412-2422.

Furue, M., K. Furue, G. Tsuji and T. Nakahara (2020). "Interleukin-17A and Keratinocytes in Psoriasis." Int J Mol Sci 21(4).

Galli, S. J., N. Gaudenzio and M. Tsai (2020). "Mast Cells in Inflammation and Disease: Recent Progress and Ongoing Concerns." Annu Rev Immunol 38: 49-77.

Gangwar, R. S., J. E. Gudjonsson and N. L. Ward (2022). "Mouse Models of Psoriasis: A Comprehensive Review." J Invest Dermatol 142(3 Pt B): 884-897.

Geisse, J. K., P. Rich, A. Pandya, K. Gross, K. Andres, A. Ginkel and M. Owens (2002). "Imiquimod 5% cream for the treatment of superficial basal cell carcinoma: a double-blind, randomized, vehicle-controlled study." J Am Acad Dermatol 47(3): 390-398.

Gelfand, J. M. and H. Yeung (2012). "Metabolic syndrome in patients with psoriatic disease." J Rheumatol Suppl 89: 24-28.

Gilliet, M., C. Conrad, M. Geiges, A. Cozzio, W. Thurlimann, G. Burg, F. O. Nestle and R. Dummer (2004). "Psoriasis triggered by toll-like receptor 7 agonist imiquimod in the presence of dermal plasmacytoid dendritic cell precursors." Arch Dermatol 140(12): 1490-1495.

Golden, J. B., S. G. Groft, M. V. Squeri, S. M. Debanne, N. L. Ward, T. S. McCormick and K. D. Cooper (2015). "Chronic Psoriatic Skin Inflammation Leads to Increased Monocyte Adhesion and Aggregation." J Immunol 195(5): 2006-2018.

Goldminz, A. M., S. C. Au, N. Kim, A. B. Gottlieb and P. F. Lizzul (2013). "NF-kappaB: an essential transcription factor in psoriasis." J Dermatol Sci 69(2): 89-94.

Griffiths, C. E. and J. N. Barker (2007). "Pathogenesis and clinical features of psoriasis." Lancet 370(9583): 263-271.

Gudjonsson, J. E., A. Johnston, M. Dyson, H. Valdimarsson and J. T. Elder (2007). "Mouse models of psoriasis." J Invest Dermatol **127**(6): 1292-1308.

Guttman-Yassky, E., M. A. Lowes, J. Fuentes-Duculan, J. Whynot, I. Novitskaya, I. Cardinale, A. Haider, A. Khatcherian, J. A. Carucci, R. Bergman and J. G. Krueger (2007). "Major differences in inflammatory dendritic cells and their products distinguish atopic dermatitis from psoriasis." J Allergy Clin Immunol **119**(5): 1210-1217.

Ha, H. L., H. Wang, P. Pisitkun, J. C. Kim, I. Tassi, W. Tang, M. I. Morasso, M. C. Udey and U. Siebenlist (2014). "IL-17 drives psoriatic inflammation via distinct, target cell-specific mechanisms." Proc Natl Acad Sci U S A **111**(33): E3422-3431.

Haak, S., A. L. Croxford, K. Kreymborg, F. L. Heppner, S. Pouly, B. Becher and A. Waisman (2009). "IL-17A and IL-17F do not contribute vitally to autoimmune neuro-inflammation in mice." J Clin Invest **119**(1): 61-69.

Hafner, M., J. Wenk, A. Nenci, M. Pasparakis, K. Scharffetter-Kochanek, N. Smyth, T. Peters, D. Kess, O. Holtkotter, P. Shephard, J. E. Kudlow, H. Smola, I. Haase, A. Schippers, T. Krieg and W. Muller (2004). "Keratin 14 Cre transgenic mice authenticate keratin 14 as an oocyte-expressed protein." Genesis **38**(4): 176-181.

Haljasorg, U., R. Bichele, M. Saare, M. Guha, J. Maslovskaja, K. Kond, A. Remm, M. Pihlap, L. Tomson, K. Kisand, M. Laan and P. Peterson (2015). "A highly conserved NF-kappaB-responsive enhancer is critical for thymic expression of Aire in mice." Eur J Immunol **45**(12): 3246-3256.

Haniffa, M., M. Gunawan and L. Jardine (2015). "Human skin dendritic cells in health and disease." J Dermatol Sci **77**(2): 85-92.

Hayden, M. S. and S. Ghosh (2008). "Shared principles in NF-kappaB signaling." Cell **132**(3): 344-362.

Heitmann, J., V. G. Frings, A. Geier, M. Goebeler and A. Kerstan (2021). "Non-alcoholic fatty liver disease and psoriasis - is there a shared proinflammatory network?" J Dtsch Dermatol Ges **19**(4): 517-528.

Hijnen, D., E. F. Knol, Y. Y. Gent, B. Giovannone, S. J. Beijn, T. S. Kupper, C. A. Bruijnzeel-Koomen and R. A. Clark (2013). "CD8(+) T cells in the lesional skin of atopic dermatitis and psoriasis patients are an important source of IFN-gamma, IL-13, IL-17, and IL-22." J Invest Dermatol **133**(4): 973-979.

Hiltensperger, M., E. Beltran, R. Kant, S. Tyystjarvi, G. Lepennetier, H. Dominguez Moreno, I. J. Bauer, S. Grassmann, S. Jarosch, K. Schober, V. R. Buchholz, S. Kenet, C. Gasperi, R. Ollinger, R. Rad, A. Muschaweckh, C. Sie, L. Aly, B. Knier, G. Garg, A. M. Afzali, L. A. Gerdes, T. Kumpfel, S. Franzenburg, N. Kawakami, B. Hemmer, D. H. Busch, T. Misgeld, K. Dornmair and T. Korn (2021). "Skin and gut imprinted helper T cell subsets exhibit distinct functional phenotypes in central nervous system autoimmunity." Nat Immunol **22**(7): 880-892.

Ho, A. W. and T. S. Kupper (2019). "T cells and the skin: from protective immunity to inflammatory skin disorders." Nat Rev Immunol 19(8): 490-502.

Homey, B., H. Alenius, A. Muller, H. Soto, E. P. Bowman, W. Yuan, L. McEvoy, A. I. Lauerma, T. Assmann, E. Bunemann, M. Lehto, H. Wolff, D. Yen, H. Marxhausen, W. To, J. Sedgwick, T. Ruzicka, P. Lehmann and A. Zlotnik (2002). "CCL27-CCR10 interactions regulate T cell-mediated skin inflammation." Nat Med 8(2): 157-165.

Hot, A., V. Lenief, M. A. Cazalis and P. Miossec (2010). "Pathogenic role of IL-17 in endothelial dysfunction, a link between rheumatoid arthritis and atherosclerosis." Annals of the Rheumatic Diseases 69: A44-A45.

Hu, H., X. Wu, W. Jin, M. Chang, X. Cheng and S. C. Sun (2011). "Noncanonical NF-kappaB regulates inducible costimulator (ICOS) ligand expression and T follicular helper cell development." Proc Natl Acad Sci U S A 108(31): 12827-12832.

Hu, S. C., H. S. Yu, F. L. Yen, C. L. Lin, G. S. Chen and C. C. Lan (2016). "Neutrophil extracellular trap formation is increased in psoriasis and induces human beta-defensin-2 production in epidermal keratinocytes." Sci Rep 6: 31119.

Huang, T., Z. Gao, Y. Zhang, K. Fan, F. Wang, Y. Li, J. Zhong, H. Y. Fan, Q. Cao, J. Zhou, Y. Xiao, H. Hu and J. Jin (2018). "CRL4(DCAF2) negatively regulates IL-23 production in dendritic cells and limits the development of psoriasis." J Exp Med 215(8): 1999-2017.

Itano, A. A., S. J. McSorley, R. L. Reinhardt, B. D. Ehst, E. Ingulli, A. Y. Rudensky and M. K. Jenkins (2003). "Distinct dendritic cell populations sequentially present antigen to CD4 T cells and stimulate different aspects of cell-mediated immunity." Immunity 19(1): 47-57.

Jane-wit, D., Y. V. Surovtseva, L. Qin, G. Li, R. Liu, P. Clark, T. D. Manes, C. Wang, M. Kashgarian, N. C. Kirkiles-Smith, G. Tellides and J. S. Pober (2015). "Complement membrane attack complexes activate noncanonical NF-kappaB by forming an Akt+ NIK+ signalosome on Rab5+ endosomes." Proc Natl Acad Sci U S A 112(31): 9686-9691.

Jang, D. I., A. H. Lee, H. Y. Shin, H. R. Song, J. H. Park, T. B. Kang, S. R. Lee and S. H. Yang (2021). "The Role of Tumor Necrosis Factor Alpha (TNF-alpha) in Autoimmune Disease and Current TNF-alpha Inhibitors in Therapeutics." Int J Mol Sci 22(5).

Jiang, Z., X. Jiang, A. Chen and W. He (2023). "Platelet activation: a promoter for psoriasis and its comorbidity, cardiovascular disease." Front Immunol 14: 1238647.

Johnston, A., Y. Fritz, S. M. Dawes, D. Diaconu, P. M. Al-Attar, A. M. Guzman, C. S. Chen, W. Fu, J. E. Gudjonsson, T. S. McCormick and N. L. Ward (2013). "Keratinocyte overexpression of IL-17C promotes psoriasiform skin inflammation." J Immunol 190(5): 2252-2262.

Johnston, A., X. Xing, L. Wolterink, D. H. Barnes, Z. Yin, L. Reingold, J. M. Kahlenberg, P. W. Harms and J. E. Gudjonsson (2017). "IL-1 and IL-36 are dominant cytokines in generalized pustular psoriasis." J Allergy Clin Immunol 140(1): 109-120.

Kabashima, K., T. Honda, F. Ginhoux and G. Egawa (2019). "The immunological anatomy of the skin." Nat Rev Immunol **19**(1): 19-30.

Kagami, S., H. L. Rizzo, J. J. Lee, Y. Koguchi and A. Blauvelt (2010). "Circulating Th17, Th22, and Th1 cells are increased in psoriasis." J Invest Dermatol **130**(5): 1373-1383.

Kamata, M. and Y. Tada (2022). "Dendritic Cells and Macrophages in the Pathogenesis of Psoriasis." Front Immunol **13**: 941071.

Karbach, S., A. L. Croxford, M. Oelze, R. Schüler, D. Minwegen, J. Wegner, L. Koukes, N. Yogev, A. Nikolaev, S. Reißig, A. Ullmann, M. Knorr, M. Waldner, M. F. Neurath, H. Li, Z. Wu, C. Brochhausen, J. Scheller, S. Rose-John, C. Piotrowski, I. Bechmann, M. Radsak, P. Wild, A. Daiber, E. von Stebut, P. Wenzel, A. Waisman and T. Münzel (2014). "Interleukin 17 Drives Vascular Inflammation, Endothelial Dysfunction, and Arterial Hypertension in Psoriasis-Like Skin Disease." Arteriosclerosis, Thrombosis, and Vascular Biology **34**(12): 2658-2668.

Karbach, S., P. Wenzel, A. Waisman, T. Munzel and A. Daiber (2014). "eNOS uncoupling in cardiovascular diseases--the role of oxidative stress and inflammation." Curr Pharm Des **20**(22): 3579-3594.

Katakam, A. K., H. Brightbill, C. Franci, C. Kung, V. Nunez, C. Jones, 3rd, I. Peng, S. Jeet, L. C. Wu, I. Mellman, L. Delamarre and C. D. Austin (2015). "Dendritic cells require NIK for CD40-dependent cross-priming of CD8+ T cells." Proc Natl Acad Sci U S A **112**(47): 14664-14669.

Katayama, H. (2018). "Development of psoriasis by continuous neutrophil infiltration into the epidermis." Exp Dermatol **27**(10): 1084-1091.

Kawasaki, T. and T. Kawai (2014). "Toll-like receptor signaling pathways." Front Immunol **5**: 461.

Kayagaki, N., M. H. Yan, D. Seshasayee, H. Wang, W. Lee, D. M. French, I. S. Grewal, A. G. Cochran, N. C. Gordon, J. P. Yin, M. A. Starovasnik and V. M. Dixit (2002). "BAFF/BLyS receptor 3 binds the B cell survival factor BAFF ligand through a discrete surface loop and promotes processing of NF-κB2." Immunity **17**(4): 515-524.

Kerdel, F. and M. Zaiac (2015). "An evolution in switching therapy for psoriasis patients who fail to meet treatment goals." Dermatol Ther **28**(6): 390-403.

Kim, B. S., M. C. Siracusa, S. A. Saenz, M. Noti, L. A. Monticelli, G. F. Sonnenberg, M. R. Hepworth, A. S. Van Voorhees, M. R. Comeau and D. Artis (2013). "TSLP elicits IL-33-independent innate lymphoid cell responses to promote skin inflammation." Sci Transl Med **5**(170): 170ra116.

Kim, T. G., H. Jee, J. Fuentes-Duculan, W. H. Wu, D. Byamba, D. S. Kim, D. Y. Kim, D. H. Lew, W. I. Yang, J. G. Krueger and M. G. Lee (2014). "Dermal clusters of mature dendritic cells and T cells are associated with the CCL20/CCR6 chemokine system in chronic psoriasis." J Invest Dermatol **134**(5): 1462-1465.

Kissenpfennig, A., S. Henri, B. Dubois, C. Laplace-Builhe, P. Perrin, N. Romani, C. H. Tripp, P. Douillard, L. Leserman, D. Kaiserlian, S. Saeland, J. Davoust and B. Malissen (2005). "Dynamics and function of Langerhans cells in vivo: dermal dendritic cells colonize lymph node areas distinct from slower migrating Langerhans cells." Immunity **22**(5): 643-654.

Kobayashi, N., A. Nakagawa, T. Muramatsu, Y. Yamashina, T. Shirai, M. W. Hashimoto, Y. Ishigaki, T. Ohnishi and T. Mori (1998). "Supranuclear melanin caps reduce ultraviolet induced DNA photoproducts in human epidermis." J Invest Dermatol **110**(5): 806-810.

Kobayashi, T., R. R. Ricardo-Gonzalez and K. Moro (2020). "Skin-Resident Innate Lymphoid Cells - Cutaneous Innate Guardians and Regulators." Trends Immunol **41**(2): 100-112.

Krueger, J. G. (2002). "The immunologic basis for the treatment of psoriasis with new biologic agents." J Am Acad Dermatol **46**(1): 1-23; quiz 23-26.

Krutzik, S. R., B. Tan, H. Li, M. T. Ochoa, P. T. Liu, S. E. Sharfstein, T. G. Graeber, P. A. Sieling, Y. J. Liu, T. H. Rea, B. R. Bloom and R. L. Modlin (2005). "TLR activation triggers the rapid differentiation of monocytes into macrophages and dendritic cells." Nat Med **11**(6): 653-660.

Kurschus, F. C. and S. Moos (2017). "IL-17 for therapy." J Dermatol Sci **87**(3): 221-227.

Lacher, S. M., C. Thurm, U. Distler, A. N. Mohebiany, N. Israel, M. Kitic, A. Ebering, Y. Tang, M. Klein, G. H. Wabnitz, F. Wanke, Y. Samstag, T. Bopp, F. C. Kurschus, L. Simeoni, S. Tenzer and A. Waisman (2018). "NF-kappaB inducing kinase (NIK) is an essential post-transcriptional regulator of T-cell activation affecting F-actin dynamics and TCR signaling." J Autoimmun **94**: 110-121.

Lada, G. (2025). "Immune links in comorbid depression and psoriasis: A narrative mini-review and perspective." Brain Behav Immun Health **44**: 100949.

Laggner, U., P. Di Meglio, G. K. Perera, C. Hundhausen, K. E. Lacy, N. Ali, C. H. Smith, A. C. Hayday, B. J. Nickoloff and F. O. Nestle (2011). "Identification of a novel proinflammatory human skin-homing Vgamma9Vdelta2 T cell subset with a potential role in psoriasis." J Immunol **187**(5): 2783-2793.

Lande, R., E. Botti, C. Jandus, D. Dojcinovic, G. Fanelli, C. Conrad, G. Chamilos, L. Feldmeyer, B. Marinari, S. Chon, L. Vence, V. Riccieri, P. Guillaume, A. A. Navarini, P. Romero, A. Costanzo, E. Piccolella, M. Gilliet and L. Frasca (2014). "The antimicrobial peptide LL37 is a T-cell autoantigen in psoriasis." Nat Commun **5**: 5621.

Lande, R., J. Gregorio, V. Facchinetti, B. Chatterjee, Y. H. Wang, B. Homey, W. Cao, Y. H. Wang, B. Su, F. O. Nestle, T. Zal, I. Mellman, J. M. Schroder, Y. J. Liu and M. Gilliet (2007). "Plasmacytoid dendritic cells sense self-DNA coupled with antimicrobial peptide." Nature **449**(7162): 564-569.

Legoux, F., D. Bellet, C. Daviaud, Y. El Morr, A. Darbois, K. Niort, E. Procopio, M. Salou, J. Gilet, B. Ryffel, A. Balvay, A. Foussier, M. Sarkis, A. El Marjou, F. Schmidt, S. Rabot and O. Lantz

(2019). "Microbial metabolites control the thymic development of mucosal-associated invariant T cells." Science 366(6464): 494-499.

Liang, S. C., X. Y. Tan, D. P. Luxenberg, R. Karim, K. Dunussi-Joannopoulos, M. Collins and L. A. Fouser (2006). "Interleukin (IL)-22 and IL-17 are coexpressed by Th17 cells and cooperatively enhance expression of antimicrobial peptides." J Exp Med 203(10): 2271-2279.

Liao, G., M. Zhang, E. W. Harhaj and S. C. Sun (2004). "Regulation of the NF-kappaB-inducing kinase by tumor necrosis factor receptor-associated factor 3-induced degradation." J Biol Chem 279(25): 26243-26250.

Lin, A. M., C. J. Rubin, R. Khandpur, J. Y. Wang, M. Riblett, S. Yalavarthi, E. C. Villanueva, P. Shah, M. J. Kaplan and A. T. Bruce (2011). "Mast cells and neutrophils release IL-17 through extracellular trap formation in psoriasis." J Immunol 187(1): 490-500.

Liu, B., X. Xia, F. Zhu, E. Park, S. Carbajal, K. Kiguchi, J. DiGiovanni, S. M. Fischer and Y. Hu (2008). "IKKalpha is required to maintain skin homeostasis and prevent skin cancer." Cancer Cell 14(3): 212-225.

Liu, P., C. Peng, X. Chen, L. Wu, M. Yin, J. Li, Q. Qin, Y. Kuang and W. Zhu (2021). "Acitretin Promotes the Differentiation of Myeloid-Derived Suppressor Cells in the Treatment of Psoriasis." Front Med (Lausanne) 8: 625130.

Liu, X. T., Z. R. Shi, S. Y. Lu, D. Hong, X. N. Qiu, G. Z. Tan, H. Xiong, Q. Guo and L. Wang (2022). "Enhanced Migratory Ability of Neutrophils Toward Epidermis Contributes to the Development of Psoriasis via Crosstalk With Keratinocytes by Releasing IL-17A." Front Immunol 13: 817040.

Lolli, E., R. Saraceno, E. Calabrese, M. Ascolani, P. Scarozza, A. Chiricozzi, S. Onali, C. Petruzziello, S. Chimenti, F. Pallone and L. Biancone (2015). "Psoriasis Phenotype in Inflammatory Bowel Disease: A Case-Control Prospective Study." J Crohns Colitis 9(9): 699-707.

Lowes, M. A., C. B. Russell, D. A. Martin, J. E. Towne and J. G. Krueger (2013). "The IL-23/T17 pathogenic axis in psoriasis is amplified by keratinocyte responses." Trends Immunol 34(4): 174-181.

Lowes, M. A., M. Suarez-Farinas and J. G. Krueger (2014). "Immunology of psoriasis." Annu Rev Immunol 32: 227-255.

Ma, Z., X. Sun, Y. Lin, Z. Wang, Q. Nie, J. Yu, J. Yang and L. Zhu (2025). "The Dynamic Expression Changes of Neutrophil Extracellular Traps in Mouse Apical Periodontitis: A Potential Correlation With IL-17." J Immunol Res 2025: 8039031.

Mabuchi, T., T. Takekoshi and S. T. Hwang (2011). "Epidermal CCR6+ gammadelta T cells are major producers of IL-22 and IL-17 in a murine model of psoriasiform dermatitis." J Immunol 187(10): 5026-5031.

Madison, K. C. (2003). "Barrier function of the skin: "la raison d'etre" of the epidermis." J Invest Dermatol **121**(2): 231-241.

Maione, F., C. Cicala, E. Liverani, N. Mascolo, M. Perretti and F. D'Acquisto (2011). "IL-17A increases ADP-induced platelet aggregation." Biochem Biophys Res Commun **408**(4): 658-662.

Mair, F., S. Joller, R. Hoeppli, L. Onder, M. Hahn, B. Ludewig, A. Waisman and B. Becher (2015). "The NFkappaB-inducing kinase is essential for the developmental programming of skin-resident and IL-17-producing gammadelta T cells." Elife **4**.

Martini, E., M. Wiken, S. Cheuk, I. Gallais Serezal, F. Baharom, M. Stahle, A. Smed-Sorensen and L. Eidsmo (2017). "Dynamic Changes in Resident and Infiltrating Epidermal Dendritic Cells in Active and Resolved Psoriasis." J Invest Dermatol **137**(4): 865-873.

Mehta, N. N., R. S. Azfar, D. B. Shin, A. L. Neimann, A. B. Troxel and J. M. Gelfand (2010). "Patients with severe psoriasis are at increased risk of cardiovascular mortality: cohort study using the General Practice Research Database." Eur Heart J **31**(8): 1000-1006.

Mehta, N. N., Y. Yu, B. Saboury, N. Foroughi, P. Krishnamoorthy, A. Raper, A. Baer, J. Antigua, A. S. Van Voorhees, D. A. Torigian, A. Alavi and J. M. Gelfand (2011). "Systemic and vascular inflammation in patients with moderate to severe psoriasis as measured by [18F]-fluorodeoxyglucose positron emission tomography-computed tomography (FDG-PET/CT): a pilot study." Arch Dermatol **147**(9): 1031-1039.

Meng, F., K. Wang, T. Aoyama, S. I. Grivennikov, Y. Paik, D. Scholten, M. Cong, K. Iwaisako, X. Liu, M. Zhang, C. H. Osterreicher, F. Stickel, K. Ley, D. A. Brenner and T. Kisseleva (2012). "Interleukin-17 signaling in inflammatory, Kupffer cells, and hepatic stellate cells exacerbates liver fibrosis in mice." Gastroenterology **143**(3): 765-776 e763.

Mercurio, L., C. M. Failla, L. Capriotti, C. Scarponi, F. Facchiano, M. Morelli, S. Rossi, G. Pagnanelli, C. Albanesi, A. Cavani and S. Madonna (2020). "Interleukin (IL)-17/IL-36 axis participates to the crosstalk between endothelial cells and keratinocytes during inflammatory skin responses." PLoS One **15**(4): e0222969.

Mesin, L., J. Ersching and G. D. Victora (2016). "Germinal Center B Cell Dynamics." Immunity **45**(3): 471-482.

Metzemaekers, M., M. Gouwy and P. Proost (2020). "Neutrophil chemoattractant receptors in health and disease: double-edged swords." Cell Mol Immunol **17**(5): 433-450.

Miyawaki, S., Y. Nakamura, H. Suzuka, M. Koba, R. Yasumizu, S. Ikehara and Y. Shibata (1994). "A new mutation, aly, that induces a generalized lack of lymph nodes accompanied by immunodeficiency in mice." Eur J Immunol **24**(2): 429-434.

Mizuguchi, S., K. Gotoh, Y. Nakashima, D. Setoyama, Y. Takata, S. Ohga and D. Kang (2021). "Mitochondrial Reactive Oxygen Species Are Essential for the Development of Psoriatic Inflammation." Front Immunol **12**: 714897.

Moos, S., A. N. Mohebiany, A. Waisman and F. C. Kurschus (2019). "Imiquimod-Induced Psoriasis in Mice Depends on the IL-17 Signaling of Keratinocytes." J Invest Dermatol **139**(5): 1110-1117.

Morales, J., B. Homey, A. P. Vicari, S. Hudak, E. Oldham, J. Hedrick, R. Orozco, N. G. Copeland, N. A. Jenkins, L. M. McEvoy and A. Zlotnik (1999). "CTACK, a skin-associated chemokine that preferentially attracts skin-homing memory T cells." Proc Natl Acad Sci U S A **96**(25): 14470-14475.

Mrowietz, U., F. Lauffer, W. Sondermann, S. Gerdes and P. Sewerin (2024). "Psoriasis as a Systemic Disease." Dtsch Arztebl Int **121**(14): 467-472.

Mukaida, N., A. Harada, K. Yasumoto and K. Matsushima (1992). "Properties of pro-inflammatory cell type-specific leukocyte chemotactic cytokines, interleukin 8 (IL-8) and monocyte chemotactic and activating factor (MCAF)." Microbiol Immunol **36**(8): 773-789.

Murray, S. E. (2013). "Cell-intrinsic role for NF-kappa B-inducing kinase in peripheral maintenance but not thymic development of Foxp3+ regulatory T cells in mice." PLoS One **8**(9): e76216.

Mylonas, A. and C. Conrad (2018). "Psoriasis: Classical vs. Paradoxical. The Yin-Yang of TNF and Type I Interferon." Front Immunol **9**: 2746.

Nestle, F. O., C. Conrad, A. Tun-Kyi, B. Homey, M. Gombert, O. Boyman, G. Burg, Y. J. Liu and M. Gilliet (2005). "Plasmacytoid predendritic cells initiate psoriasis through interferon-alpha production." J Exp Med **202**(1): 135-143.

Neurath, L., M. Sticherling, G. Schett and F. Fagni (2024). "Targeting cytokines in psoriatic arthritis." Cytokine Growth Factor Rev **78**: 1-13.

Nickoloff, B. J., S. L. Kunkel, M. Burdick and R. M. Strieter (1995). "Severe combined immunodeficiency mouse and human psoriatic skin chimeras. Validation of a new animal model." Am J Pathol **146**(3): 580-588.

Nograles, K. E., L. C. Zaba, E. Guttman-Yassky, J. Fuentes-Duculan, M. Suarez-Farinas, I. Cardinale, A. Khatcherian, J. Gonzalez, K. C. Pierson, T. R. White, C. Pensabene, I. Coats, I. Novitskaya, M. A. Lowes and J. G. Krueger (2008). "Th17 cytokines interleukin (IL)-17 and IL-22 modulate distinct inflammatory and keratinocyte-response pathways." Br J Dermatol **159**(5): 1092-1102.

Olveira, A., S. Augustin, S. Benlloch, J. Ampuero, J. A. Suarez-Perez, S. Armesto, E. Vilarrasa, I. Belinchon-Romero, P. Herranz, J. Crespo, F. Guimera, L. Gomez-Labrador, V. Martin and J. M. Carrascosa (2023). "The Essential Role of IL-17 as the Pathogenetic Link between Psoriasis and Metabolic-Associated Fatty Liver Disease." Life (Basel) **13**(2).

Onder, L., V. Nindl, E. Scandella, Q. Chai, H. W. Cheng, S. Caviezel-Firner, M. Novkovic, D. Bomze, R. Maier, F. Mair, B. Ledermann, B. Becher, A. Waisman and B. Ludewig (2015).

"Alternative NF-kappaB signaling regulates mTEC differentiation from podoplanin-expressing precursors in the cortico-medullary junction." Eur J Immunol 45(8): 2218-2231.

Orlando, G., B. Molon, A. Viola, M. Alaibac, R. Angioni and S. Piaserico (2022). "Psoriasis and Cardiovascular Diseases: An Immune-Mediated Cross Talk?" Front Immunol 13: 868277.

Oyoshi, M. K., A. Elkhal, J. E. Scott, M. A. Wurbel, J. L. Hornick, J. J. Campbell and R. S. Geha (2011). "Epicutaneous challenge of orally immunized mice redirects antigen-specific gut-homing T cells to the skin." J Clin Invest 121(6): 2210-2220.

Pardasani, A. G., S. R. Feldman and A. R. Clark (2000). "Treatment of psoriasis: an algorithm-based approach for primary care physicians." Am Fam Physician 61(3): 725-733, 736.

Parisi, R., I. Y. K. Iskandar, E. Kontopantelis, M. Augustin, C. E. M. Griffiths, D. M. Ashcroft and A. Global Psoriasis (2020). "National, regional, and worldwide epidemiology of psoriasis: systematic analysis and modelling study." BMJ 369: m1590.

Pasparakis, M., I. Haase and F. O. Nestle (2014). "Mechanisms regulating skin immunity and inflammation." Nat Rev Immunol 14(5): 289-301.

Pene, J., S. Chevalier, L. Preisser, E. Venereau, M. H. Guilleux, S. Ghannam, J. P. Moles, Y. Danger, E. Ravon, S. Lesaux, H. Yssel and H. Gascan (2008). "Chronically inflamed human tissues are infiltrated by highly differentiated Th17 lymphocytes." J Immunol 180(11): 7423-7430.

Pham, A. H., J. M. McCaffery and D. C. Chan (2012). "Mouse lines with photo-activatable mitochondria to study mitochondrial dynamics." Genesis 50(11): 833-843.

Pietrowski, E., B. Bender, J. Huppert, R. White, H. J. Luhmann and C. R. Kuhlmann (2011). "Pro-inflammatory effects of interleukin-17A on vascular smooth muscle cells involve NAD(P)H-oxidase derived reactive oxygen species." J Vasc Res 48(1): 52-58.

Proksch, E., J. M. Brandner and J. M. Jensen (2008). "The skin: an indispensable barrier." Exp Dermatol 17(12): 1063-1072.

Qi, C., Y. Wang, P. Li and J. Zhao (2021). "Gamma Delta T Cells and Their Pathogenic Role in Psoriasis." Front Immunol 12: 627139.

Raharja, A., S. K. Mahil and J. N. Barker (2021). "Psoriasis: a brief overview." Clin Med (Lond) 21(3): 170-173.

Rajan, N. and J. A. Langtry (2006). "Generalized exacerbation of psoriasis associated with imiquimod cream treatment of superficial basal cell carcinomas." Clin Exp Dermatol 31(1): 140-141.

Rajesh, A., L. Wise and M. Hibma (2019). "The role of Langerhans cells in pathologies of the skin." Immunology & Cell Biology 97(8): 700-713.

Raubenheimer, P. J., M. J. Nyirenda and B. R. Walker (2006). "A choline-deficient diet exacerbates fatty liver but attenuates insulin resistance and glucose intolerance in mice fed a high-fat diet." Diabetes 55(7): 2015-2020.

Rendon, A. and K. Schakel (2019). "Psoriasis Pathogenesis and Treatment." Int J Mol Sci 20(6).

Res, P. C., G. Piskin, O. J. de Boer, C. M. van der Loos, P. Teeling, J. D. Bos and M. B. Teunissen (2010). "Overrepresentation of IL-17A and IL-22 producing CD8 T cells in lesional skin suggests their involvement in the pathogenesis of psoriasis." PLoS One 5(11): e14108.

Reynolds, G., P. Vegh, J. Fletcher, E. F. M. Poyner, E. Stephenson, I. Goh, R. A. Botting, N. Huang, B. Olabi, A. Dubois, D. Dixon, K. Green, D. Maunder, J. Engelbert, M. Efremova, K. Polanski, L. Jardine, C. Jones, T. Ness, D. Horsfall, J. McGrath, C. Carey, D. M. Popescu, S. Webb, X. N. Wang, B. Sayer, J. E. Park, V. A. Negri, D. Belokhvostova, M. D. Lynch, D. McDonald, A. Filby, T. Hagai, K. B. Meyer, A. Husain, J. Coxhead, R. Vento-Tormo, S. Behjati, S. Lisgo, A. C. Villani, J. Bacardit, P. H. Jones, E. A. O'Toole, G. S. Ogg, N. Rajan, N. J. Reynolds, S. A. Teichmann, F. M. Watt and M. Haniffa (2021). "Developmental cell programs are co-opted in inflammatory skin disease." Science 371(6527).

Ricardo-Gonzalez, R. R., S. J. Van Dyken, C. Schneider, J. Lee, J. C. Nussbaum, H. E. Liang, D. Vaka, W. L. Eckalbar, A. B. Molofsky, D. J. Erle and R. M. Locksley (2018). "Tissue signals imprint ILC2 identity with anticipatory function." Nat Immunol 19(10): 1093-1099.

Rippa, A. L., E. P. Kalabusheva and E. A. Vorotelyak (2019). "Regeneration of Dermis: Scarring and Cells Involved." Cells 8(6).

Rodriguez-Rosales, Y. A., J. D. Langereis, M. A. J. Gorris, J. van den Reek, E. Fasse, M. G. Netea, I. J. M. de Vries, L. Gomez-Munoz, B. van Cranenbroek, A. Korber, W. Sondermann, I. Joosten, E. de Jong and H. Koenen (2021). "Immunomodulatory aged neutrophils are augmented in blood and skin of psoriasis patients." J Allergy Clin Immunol 148(4): 1030-1040.

Romanovsky, A. A. (2014). "Skin temperature: its role in thermoregulation." Acta Physiol 210: 498–507.

Rowe, A. M., S. E. Murray, H. P. Raue, Y. Koguchi, M. K. Slifka and D. C. Parker (2013). "A cell-intrinsic requirement for NF-kappaB-inducing kinase in CD4 and CD8 T cell memory." J Immunol 191(7): 3663-3672.

Saiag, P., B. Coulomb, C. Lebreton, E. Bell and L. Dubertret (1985). "Psoriatic fibroblasts induce hyperproliferation of normal keratinocytes in a skin equivalent model in vitro." Science 230(4726): 669-672.

Salem, I., A. Ramser, N. Isham and M. A. Ghannoum (2018). "The Gut Microbiome as a Major Regulator of the Gut-Skin Axis." Front Microbiol 9: 1459.

Sanchez Rodriguez, R., M. L. Pauli, I. M. Neuhaus, S. S. Yu, S. T. Arron, H. W. Harris, S. H. Yang, B. A. Anthony, F. M. Sverdrup, E. Krow-Lucal, T. C. MacKenzie, D. S. Johnson, E. H. Meyer, A. Lohr, A. Hsu, J. Koo, W. Liao, R. Gupta, M. G. Debbaneh, D. Butler, M. Huynh, E. C.

Levin, A. Leon, W. Y. Hoffman, M. H. McGrath, M. D. Alvarado, C. H. Ludwig, H. A. Truong, M. M. Maurano, I. K. Gratz, A. K. Abbas and M. D. Rosenblum (2014). "Memory regulatory T cells reside in human skin." J Clin Invest **124**(3): 1027-1036.

Schaller, T., J. Ringen, B. Fischer, T. Bieler, K. Perius, T. Knopp, K. S. Kommoss, T. Korn, M. Heikenwalder, M. Oelze, A. Daiber, T. Munzel, D. Kramer, P. Wenzel, J. Wild, S. Karbach and A. Waisman (2023). "Reactive oxygen species produced by myeloid cells in psoriasis as a potential biofactor contributing to the development of vascular inflammation." Biofactors **49**(4): 861-874.

Schroder, J. M., H. Gregory, J. Young and E. Christophers (1992). "Neutrophil-activating proteins in psoriasis." J Invest Dermatol **98**(2): 241-247.

Schüler, R., A. Brand, S. Klebow, J. Wild, F. P. Veras, E. Ullmann, S. Roohani, F. Kolbinger, S. Kossmann, C. Wohn, A. Daiber, T. Münzel, P. Wenzel, A. Waisman, B. E. Clausen and S. Karbach (2019). "Antagonization of IL-17A Attenuates Skin Inflammation and Vascular Dysfunction in Mouse Models of Psoriasis." Journal of Investigative Dermatology **139**(3): 638-647.

Schüler, R., P. Efentakis, J. Wild, J. Lagrange, V. Garlapati, M. Molitor, S. Kossmann, M. Oelze, P. Stamm, H. Li, K. Schäfer, T. Münzel, A. Daiber, A. Waisman, P. Wenzel and S. H. Karbach (2019). "T Cell-Derived IL-17A Induces Vascular Dysfunction via Perivascular Fibrosis Formation and Dysregulation of ·NO/cGMP Signaling." Oxidative Medicine and Cellular Longevity **2019**: 1-15.

Senra, L., A. Mylonas, R. D. Kavanagh, P. G. Fallon, C. Conrad, J. Borowczyk-Michalowska, L. J. Wrobel, G. Kaya, N. Yawalkar, W. H. Boehncke and N. C. Brembilla (2019). "IL-17E (IL-25) Enhances Innate Immune Responses during Skin Inflammation." J Invest Dermatol **139**(8): 1732-1742 e1717.

Shao, S., H. Fang, E. Dang, K. Xue, J. Zhang, B. Li, H. Qiao, T. Cao, Y. Zhuang, S. Shen, T. Zhang, P. Qiao, C. Li, J. E. Gudjonsson and G. Wang (2019). "Neutrophil Extracellular Traps Promote Inflammatory Responses in Psoriasis via Activating Epidermal TLR4/IL-36R Crosstalk." Front Immunol **10**: 746.

Sieminska, I., M. Pieniawska and T. M. Grzywa (2024). "The Immunology of Psoriasis-Current Concepts in Pathogenesis." Clin Rev Allergy Immunol **66**(2): 164-191.

Singh, T. P., M. P. Schon, K. Wallbrecht, A. Gruber-Wackernagel, X. J. Wang and P. Wolf (2013). "Involvement of IL-9 in Th17-associated inflammation and angiogenesis of psoriasis." PLoS One **8**(1): e51752.

Skrzeczynska-Moncznik, J., K. Zabieglo, O. Osiecka, A. Morytko, P. Brzoza, L. Drozdz, M. Kapinska-Mrowiecka, B. Korkmaz, M. Pastuszczak, J. Kosalka-Wegiel, J. Musial and J. Cichy (2020). "Differences in Staining for Neutrophil Elastase and its Controlling Inhibitor SLPI Reveal Heterogeneity among Neutrophils in Psoriasis." J Invest Dermatol **140**(7): 1371-1378 e1373.

Stratis, A., M. Pasparakis, R. A. Rupec, D. Markur, K. Hartmann, K. Scharffetter-Kochanek, T. Peters, N. van Rooijen, T. Krieg and I. Haase (2006). "Pathogenic role for skin macrophages in a

mouse model of keratinocyte-induced psoriasis-like skin inflammation." J Clin Invest 116(8): 2094-2104.

Suarez-Farinas, M., K. Li, J. Fuentes-Duculan, K. Hayden, C. Brodmerkel and J. G. Krueger (2012). "Expanding the psoriasis disease profile: interrogation of the skin and serum of patients with moderate-to-severe psoriasis." J Invest Dermatol 132(11): 2552-2564.

Sultana, S. S., B. B. Monir, D. Bhowmik, H. A. Mostafa, S. Tarafder, I. Nigar and T. M. Asaduzzaman (2024). "Serum IL-23, IL-17 and TNF-α level as Psoriasis severity markers: A hospital based cross sectional study." Journal of Shaheed Suhrawardy Medical College 14(2): 25-29.

Sun, L., W. Liu and L. J. Zhang (2019). "The Role of Toll-Like Receptors in Skin Host Defense, Psoriasis, and Atopic Dermatitis." J Immunol Res 2019: 1824624.

Sun, S. C. (2011). "Non-canonical NF-kappaB signaling pathway." Cell Res 21(1): 71-85.

Sun, S. C. (2017). "The non-canonical NF-kappaB pathway in immunity and inflammation." Nat Rev Immunol 17(9): 545-558.

Sun, S. C., P. A. Ganchi, C. Beraud, D. W. Ballard and W. C. Greene (1994). "Autoregulation of the NF-kappa B transactivator RelA (p65) by multiple cytoplasmic inhibitors containing ankyrin motifs." Proc Natl Acad Sci U S A 91(4): 1346-1350.

Sun, S. C. and S. C. Ley (2008). "New insights into NF-kappaB regulation and function." Trends Immunol 29(10): 469-478.

Suzuki, T., S. Hirakawa, T. Shimauchi, T. Ito, J. Sakabe, M. Detmar and Y. Tokura (2014). "VEGF-A promotes IL-17A-producing gammadelta T cell accumulation in mouse skin and serves as a chemotactic factor for plasmacytoid dendritic cells." J Dermatol Sci 74(2): 116-124.

Swindell, W. R., K. A. Michaels, A. J. Sutter, D. Diaconu, Y. Fritz, X. Xing, M. K. Sarkar, Y. Liang, A. Tsoi, J. E. Gudjonsson and N. L. Ward (2017). "Imiquimod has strain-dependent effects in mice and does not uniquely model human psoriasis." Genome Med 9(1): 24.

Szeimies, R. M., M. J. Gerritsen, G. Gupta, J. P. Ortonne, S. Serresi, J. Bichel, J. H. Lee, T. L. Fox and A. Alomar (2004). "Imiquimod 5% cream for the treatment of actinic keratosis: results from a phase III, randomized, double-blind, vehicle-controlled, clinical trial with histology." J Am Acad Dermatol 51(4): 547-555.

Tamoutounour, S., M. Guilliams, F. Montanana Sanchis, H. Liu, D. Terhorst, C. Malosse, E. Pollet, L. Ardouin, H. Luche, C. Sanchez, M. Dalod, B. Malissen and S. Henri (2013). "Origins and functional specialization of macrophages and of conventional and monocyte-derived dendritic cells in mouse skin." Immunity 39(5): 925-938.

Tang, Y., Z. Bian, L. Zhao, Y. Liu, S. Liang, Q. Wang, X. Han, Y. Peng, X. Chen, L. Shen, D. Qiu, Z. Li and X. Ma (2011). "Interleukin-17 exacerbates hepatic steatosis and inflammation in non-alcoholic fatty liver disease." Clin Exp Immunol 166(2): 281-290.

Teijeira, A., M. C. Hunter, E. Russo, S. T. Proulx, T. Frei, G. F. Debes, M. Coles, I. Melero, M. Detmar, A. Rouzaut and C. Halin (2017). "T Cell Migration from Inflamed Skin to Draining Lymph Nodes Requires Intralymphatic Crawling Supported by ICAM-1/LFA-1 Interactions." Cell Rep **18**(4): 857-865.

Ten Bergen, L. L., A. Petrovic, A. Krogh Aarebrot and S. Appel (2020). "The TNF/IL-23/IL-17 axis-Head-to-head trials comparing different biologics in psoriasis treatment." Scand J Immunol **92**(4): e12946.

Terhorst, D., R. Chelbi, C. Wohn, C. Malosse, S. Tamoutounour, A. Jorquera, M. Bajenoff, M. Dalod, B. Malissen and S. Henri (2015). "Dynamics and Transcriptomics of Skin Dendritic Cells and Macrophages in an Imiquimod-Induced, Biphasic Mouse Model of Psoriasis." J Immunol **195**(10): 4953-4961.

Thelen, F. and D. A. Witherden (2020). "Get in Touch With Dendritic Epithelial T Cells!" Front Immunol **11**: 1656.

Tillman, D. K., Jr. and M. T. Carroll (2007). "Topical imiquimod therapy for basal and squamous cell carcinomas: a clinical experience." Cutis **79**(3): 241-248.

Tomura, M., N. Yoshida, J. Tanaka, S. Karasawa, Y. Miwa, A. Miyawaki and O. Kanagawa (2008). "Monitoring cellular movement in vivo with photoconvertible fluorescence protein "Kaede" transgenic mice." Proc Natl Acad Sci U S A **105**(31): 10871-10876.

Turkowyd, B., A. Balinovic, D. Virant, H. G. G. Carnero, F. Caldana, M. Endesfelder, D. Bourgeois and U. Endesfelder (2017). "A General Mechanism of Photoconversion of Green-to-Red Fluorescent Proteins Based on Blue and Infrared Light Reduces Phototoxicity in Live-Cell Single-Molecule Imaging." Angew Chem Int Ed Engl **56**(38): 11634-11639.

Vallabhapurapu, S. and M. Karin (2009). "Regulation and function of NF-kappaB transcription factors in the immune system." Annu Rev Immunol **27**: 693-733.

Vallabhapurapu, S., A. Matsuzawa, W. Zhang, P. Tseng, J. Keats, H. Wang, D. Vignali, P. Bergsagel and M. Karin (2008). "Nonredundant and complementary functions of TRAF2 and TRAF3 in a ubiquitination cascade that activates NIK-dependent alternative NF-kappaBsignaling." Immunol Rev **9**: 1364-1370.

van der Fits, L., S. Mourits, J. S. Voerman, M. Kant, L. Boon, J. D. Laman, F. Cornelissen, A. M. Mus, E. Florencia, E. P. Prens and E. Lubberts (2009). "Imiquimod-induced psoriasis-like skin inflammation in mice is mediated via the IL-23/IL-17 axis." J Immunol **182**(9): 5836-5845.

Van Nuffel, E., A. Schmitt, I. S. Afonina, K. Schulze-Osthoff, R. Beyaert and S. Hailfinger (2017). "CARD14-Mediated Activation of Paracaspase MALT1 in Keratinocytes: Implications for Psoriasis." J Invest Dermatol **137**(3): 569-575.

Vanbervliet, B., N. Bendriss-Vermare, C. Massacrier, B. Homey, O. de Bouteiller, F. Briere, G. Trinchieri and C. Caux (2003). "The inducible CXCR3 ligands control plasmacytoid dendritic cell

responsiveness to the constitutive chemokine stromal cell-derived factor 1 (SDF-1)/CXCL12." J Exp Med 198(5): 823-830.

Vena, G. A., M. Vestita and N. Cassano (2010). "Psoriasis and cardiovascular disease." Dermatol Ther 23(2): 144-151.

Vlachos, C., G. Gaitanis, K. H. Katsanos, D. K. Christodoulou, E. Tsianos and I. D. Bassukas (2016). "Psoriasis and inflammatory bowel disease: links and risks." Psoriasis (Auckl) 6: 73-92.

von Stebut, E., W. H. Boehncke, K. Ghoreschi, T. Gori, Z. Kaya, D. Thaci and A. Schaffler (2019). "IL-17A in Psoriasis and Beyond: Cardiovascular and Metabolic Implications." Front Immunol 10: 3096.

Waisman, A. (2012). "To be 17 again--anti-interleukin-17 treatment for psoriasis." N Engl J Med 366(13): 1251-1252.

Walter, A., M. Schafer, V. Cecconi, C. Matter, M. Urosevic-Maiwald, B. Belloni, N. Schonewolf, R. Dummer, W. Bloch, S. Werner, H. D. Beer, A. Knuth and M. van den Broek (2013). "Aldara activates TLR7-independent immune defence." Nat Commun 4: 1560.

Wang, A., A. L. Fogel, M. J. Murphy, G. Panse, M. K. McGeary, J. M. McNiff, M. Bosenberg, M. D. Vesely, J. M. Cohen, C. J. Ko, B. A. King and W. Damsky (2021). "Cytokine RNA In Situ Hybridization Permits Individualized Molecular Phenotyping in Biopsies of Psoriasis and Atopic Dermatitis." JID Innov 1(2): 100021.

Wang, H., T. Peters, D. Kess, A. Sindrilaru, T. Oreshkova, N. Van Rooijen, A. Stratis, A. C. Renkl, C. Sunderkotter, M. Wlaschek, I. Haase and K. Scharffetter-Kochanek (2006). "Activated macrophages are essential in a murine model for T cell-mediated chronic psoriasiform skin inflammation." J Clin Invest 116(8): 2105-2114.

Wang, X. and Y. Lai (2024). "Keratinocytes in the pathogenesis, phenotypic switch, and relapse of psoriasis." Eur J Immunol 54(5): e2250279.

Wang, Y., R. Edelmayer, J. Wetter, K. Salte, D. Gauvin, L. Leys, S. Paulsboe, Z. Su, I. Weinberg, M. Namovic, S. B. Gauld, P. Honore, V. E. Scott and S. McGaraughty (2019). "Monocytes/Macrophages play a pathogenic role in IL-23 mediated psoriasis-like skin inflammation." Sci Rep 9(1): 5310.

Wang, Y., J. Zang, C. Liu, Z. Yan and D. Shi (2022). "Interleukin-17 Links Inflammatory Cross-Talks Between Comorbid Psoriasis and Atherosclerosis." Front Immunol 13: 835671.

Watanabe, R., A. Gehad, C. Yang, L. L. Scott, J. E. Teague, C. Schlapbach, C. P. Elco, V. Huang, T. R. Matos, T. S. Kupper and R. A. Clark (2015). "Human skin is protected by four functionally and phenotypically discrete populations of resident and recirculating memory T cells." Sci Transl Med 7(279): 279ra239.

Weih, F. and J. Caamano (2003). "Regulation of secondary lymphoid organ development by the nuclear factor-kappaB signal transduction pathway." Immunol Rev 195: 91-105.

Wild, J., R. Jung, T. Knopp, P. Efentakis, D. Benaki, A. Grill, J. Wegner, M. Molitor, V. Garlapati, N. Rakova, L. Marko, A. Marton, E. Mikros, T. Munzel, S. Kossmann, M. Rauh, D. Nakano, K. Kitada, F. Luft, A. Waisman, P. Wenzel, J. Titze and S. Karbach (2021). "Aestivation motifs explain hypertension and muscle mass loss in mice with psoriatic skin barrier defect." Acta Physiol (Oxf) 232(1): e13628.

Wilson, N. J., K. Boniface, J. R. Chan, B. S. McKenzie, W. M. Blumenschein, J. D. Mattson, B. Basham, K. Smith, T. Chen, F. Morel, J. C. Lecron, R. A. Kastelein, D. J. Cua, T. K. McClanahan, E. P. Bowman and R. de Waal Malefyt (2007). "Development, cytokine profile and function of human interleukin 17-producing helper T cells." Nat Immunol 8(9): 950-957.

Wohn, C., J. L. Ober-Blobaum, S. Haak, S. Pantelyushin, C. Cheong, S. P. Zahner, S. Onderwater, M. Kant, H. Weighardt, B. Holzmann, B. Reizis, B. Becher, E. P. Prens and B. E. Clausen (2013). "Langerin(neg) conventional dendritic cells produce IL-23 to drive psoriatic plaque formation in mice." Proc Natl Acad Sci U S A 110(26): 10723-10728.

Wolf, M. J., A. Adili, K. Piotrowitz, Z. Abdullah, Y. Boege, K. Stemmer, M. Ringelhan, N. Simonavicius, M. Egger, D. Wohlleber, A. Lorentzen, C. Einer, S. Schulz, T. Clavel, U. Protzer, C. Thiele, H. Zischka, H. Moch, M. Tschop, A. V. Tumanov, D. Haller, K. Unger, M. Karin, M. Kopf, P. Knolle, A. Weber and M. Heikenwalder (2014). "Metabolic activation of intrahepatic CD8+ T cells and NKT cells causes nonalcoholic steatohepatitis and liver cancer via cross-talk with hepatocytes." Cancer Cell 26(4): 549-564.

Wu, J. K., G. Siller and G. Strutton (2004). "Psoriasis induced by topical imiquimod." Australas J Dermatol 45(1): 47-50.

Xia, X., L. Zhu, M. Xu, Z. Lei, H. Yu, G. Li, X. Wang, H. Jia, Z. Yin, F. Huang and Y. Gao (2024). "ANKRD22 promotes resolution of psoriasiform skin inflammation by antagonizing NIK-mediated IL-23 production." Mol Ther 32(5): 1561-1577.

Xiao, G., E. W. Harhaj and S.-C. Sun (2001). "NF-κB-Inducing Kinase Regulates the Processing of NF-κB2 p100." Molecular Cell 7(2): 401-409.

Xie, W., S. Xiao, H. Huang and Z. Zhang (2022). "Incidence of and Risk Factors for Paradoxical Psoriasis or Psoriasiform Lesions in Inflammatory Bowel Disease Patients Receiving Anti-TNF Therapy: Systematic Review With Meta-Analysis." Front Immunol 13: 847160.

Xu, X., L. Su, Y. Gao and Y. Ding (2017). "The Prevalence of Nonalcoholic Fatty Liver Disease and Related Metabolic Comorbidities Was Associated with Age at Onset of Moderate to Severe Plaque Psoriasis: A Cross-Sectional Study." PLoS One 12(1): e0169952.

Yamaguchi, Y. and V. J. Hearing (2009). "Physiological factors that regulate skin pigmentation." Biofactors 35(2): 193-199.

Yamazaki, F. (2021). "Psoriasis: Comorbidities." J Dermatol 48(6): 732-740.

Yamazaki, S., A. Nishioka, S. Kasuya, N. Ohkura, H. Hemmi, T. Kaisho, O. Taguchi, S. Sakaguchi and A. Morita (2014). "Homeostasis of thymus-derived Foxp3+ regulatory T cells is controlled by ultraviolet B exposure in the skin." J Immunol 193(11): 5488-5497.

Yilmaz, S. B., N. Cicek, M. Coskun, O. Yegin and E. Alpsoy (2012). "Serum and tissue levels of IL-17 in different clinical subtypes of psoriasis." Arch Dermatol Res 304(6): 465-469.

Yoshiki, R., K. Kabashima, T. Honda, S. Nakamizo, Y. Sawada, K. Sugita, H. Yoshioka, S. Ohmori, B. Malissen, Y. Tokura and M. Nakamura (2014). "IL-23 from Langerhans cells is required for the development of imiquimod-induced psoriasis-like dermatitis by induction of IL-17A-producing gammadelta T cells." J Invest Dermatol 134(7): 1912-1921.

Yu, J., X. Zhou, M. Nakaya, W. Jin, X. Cheng and S. C. Sun (2014). "T cell-intrinsic function of the noncanonical NF-kappaB pathway in the regulation of GM-CSF expression and experimental autoimmune encephalomyelitis pathogenesis." J Immunol 193(1): 422-430.

Zarnegar, B., Y. Wang, D. Mahoney, P. Dempsey, H. Cheung, J. He, T. Shiba, X. Yang, W. Yeh, T. Mak, R. Korneluk and G. Cheng (2008). "Activation of noncanonical NF-κB requires coordinated assembly of a regulatory complex of the adaptors cIAP1, cIAP2, TRAF2, TRAF3 and the kinase NIK." Nat Immunol. 9(12): 1371-1378.

Zhang, C., G. R. Merana, T. Harris-Tryon and T. C. Scharschmidt (2022). "Skin immunity: dissecting the complex biology of our body's outer barrier." Mucosal Immunol 15(4): 551-561.

Zhang, L. J., S. X. Chen, C. F. Guerrero-Juarez, F. Li, Y. Tong, Y. Liang, M. Liggins, X. Chen, H. Chen, M. Li, T. Hata, Y. Zheng, M. V. Plikus and R. L. Gallo (2019). "Age-Related Loss of Innate Immune Antimicrobial Function of Dermal Fat Is Mediated by Transforming Growth Factor Beta." Immunity 50(1): 121-136 e125.

Zhang, L. J., G. L. Sen, N. L. Ward, A. Johnston, K. Chun, Y. Chen, C. Adase, J. A. Sanford, N. Gao, M. Chensee, E. Sato, Y. Fritz, J. Baliwag, M. R. Williams, T. Hata and R. L. Gallo (2016). "Antimicrobial Peptide LL37 and MAVS Signaling Drive Interferon-beta Production by Epidermal Keratinocytes during Skin Injury." Immunity 45(1): 119-130.

Zheng, T., W. Zhao, H. Li, S. Xiao, R. Hu, M. Han, H. Liu, Y. Liu, K. Otsu, X. Liu and G. Huang (2018). "p38alpha signaling in Langerhans cells promotes the development of IL-17-producing T cells and psoriasiform skin inflammation." Sci Signal 11(521).

Zhu, B., M. Jing, Q. Yu, X. Ge, F. Yuan and L. Shi (2022). "Treatments in psoriasis: from standard pharmacotherapy to nanotechnology therapy." Postepy Dermatol Alergol 39(3): 460-471.

Zhu, R., X. Yao and W. Li (2024). "Langerhans cells and skin immune diseases." Eur J Immunol 54(10): e2250280.

Zhu, Y., Y. Ma, W. Zu, J. Song, H. Wang, Y. Zhong, H. Li, Y. Zhang, Q. Gao, B. Kong, J. Xu, F. Jiang, X. Wang, S. Li, C. Liu, H. Liu, T. Lu and Y. Chen (2020). "Identification of N-Phenyl-7H-

pyrrolo[2,3-d]pyrimidin-4-amine Derivatives as Novel, Potent, and Selective NF-kappaB Inducing Kinase (NIK) Inhibitors for the Treatment of Psoriasis." J Med Chem 63(13): 6748-6773.

Zindanci, I., O. Albayrak, M. Kavala, E. Kocaturk, B. Can, S. Sudogan and M. Koc (2012). "Prevalence of metabolic syndrome in patients with psoriasis." ScientificWorldJournal 2012: 312463.

8 EIDESSTATTLICHE VERSICHERUNG

Hiermit versichere ich, dass ich die von mir vorgelegte Dissertation angefertigt, die benutzten Quellen und Hilfsmittel vollständig angegeben und die Stellen der Arbeit, einschließlich Tabellen und Abbildungen, die andere Werke im Wortlaut oder dem Sinn nach entnommen sind, in jedem Einzelfall als Entlehnung kenntlich gemacht habe; dass diese Dissertation noch keiner anderen Fakultät oder Universität zur Prüfung vorgelegen hat, dass sie noch nicht veröffentlicht worden ist, sowie dass ich eine solche Veröffentlichung vor Abschluss des Promotionsverfahrens nicht vornehmen werde. Die Bestimmungen dieser Promotionsordnung sind mir bekannt.

Mainz, Januar 2026

Theresa Schaller

9 CURRICULUM VITAE

10 PUBLICATION

Schaller, T., J. Ringen, B. Fischer, T. Bieler, K. Perius, T. Knopp, K. S. Kommoss, T. Korn, M. Heikenwalder, M. Oelze, A. Daiber, T. Munzel, D. Kramer, P. Wenzel, J. Wild, S. Karbach and A. Waisman (2023). "Reactive oxygen species produced by myeloid cells in psoriasis as a potential biofactor contributing to the development of vascular inflammation." Biofactors **49**(4): 861-874.

11 ACKNOWLEDGMENTS